Itemized Response to Anonymous Referee #1's Comments

Ms. Ref. No.: acp-2019-916

Title: Characteristics, sources, and reactions of nitrous acid during winter at an urban site in the Central Plains Economic Region in China

Response to Anonymous Referee #1:

We have carefully addressed your comments on our manuscript and made necessary revisions of the previous manuscript. We sincerely thank you for valuable and constructive inputs. We believe that we have adequately addressed all of your comments and thus the current version has been greatly improved with those valuable comments and further English editing. The revised phrases/sentences/paragraphs are shown in the line number of the revised text.

The followings are our itemized replies to your comments.

General comments:

1. In general, the text can be followed. However, there are many awkward, unclear, redundant, unnecessary, ambiguous, and confusing phrases/statements (see the following tech/English comments). A professional expert must edit the text for clarity and for better flow before resubmission.

> Response: We sent the manuscript to a professional expert to enhance the readability of the manuscript. The revised portion has been highlighted with yellow color in the revised version (see the response of the following tech/English comments).

2. The rationale for your study is weak – need more elaboration. The fact that no study has been performed in Zhengzhou (L 129) does not justify the novelty of your study. You should have covered the setbacks of previous studies and state those tasks (including tables/figures) currently evaluated have not been properly addressed in previous studies. Unfortunately, I have found none. Anyway, pls emphasize the

uniqueness of your study.

Response: For your comment, we add the sentences in the revised text.

L 134-147: Many papers (Huang et al., 2017; Tong et al., 2016) took $PM_{2.5}$ as the main control factor of HONO, and studied the differences of HONO sources and characteristics between clean and polluted periods. Homogeneous reaction, direct emission, heterogeneous reaction, and daytime budget analysis were conducted during the period of worsening pollution (namely HD period in this paper). Total NO_X emissions in cities with different leading factors of emissions have been declining year by year due to Chinese government emission control measures, but some Chinese cities are still in high-NO_X areas (e.g. Beijing, Shanghai, Guangzhou, and Zhengzhou.) (Kim et al., 2015; Liu et al., 2017). Under high-NO_X conditions, some papers (Cui et al., 2018; Hou et al., 2016) suggested that heterogeneous reaction was the main source of HONO and did not conduct a quantitative analysis of homogeneous reaction, especially in winter. So, we explore relevant studies of homogeneous reactions. In addition, the source contributions of HONO at night varied with the degree of pollution level were not explained.

3. I have a hard time figuring out that the results from one single sampling site located on the rooftop of a building in Zhengzhou university (L 134) can represent the air quality in general and HONO in particular in the entire Zhengzhou city (180 million population, L 106). This is why there are so many monitoring stations (traffic, urban and background) within a given large city to reflect the air quality within the city. Pls modify your title as well those in the text.

Response: Thank you for your comment. As you say, one single sampling site cannot represent the air quality in general and HONO in the entire Zhengzhou city. We have revised the title, “Characteristics, sources, and reactions of nitrous acid during winter at an urban site in the Central Plains Economic Region in China”.

4. Need to clearly cover HONO sources and sinks as well as homogeneous (NO+ •OH) and heterogenous (NO_2 + H_2O) in the text (introduction and discussion). For example, the role of ground surface at night for HONO deposit (sink) and the reemission (source) from HONO reservoirs (e.g., soil nitrite), etc. The other sink source, albeit insignificant, is that HONO may react with others to form new compounds, as in the case of reactions with amines in forming nitrosamines. How about transport of HONO? – what is the lifetime in atmosphere (hours under in-door conditions).

Response: OK. We added the sentence in the introduction in the revised text.

L 51-54: Therefore, the changes in the contribution of the homogeneous reaction, heterogeneous conversion, and direct emission during pollution can be observed by studying the formation mechanism of HONO.

In the discussion, we thought that the contribution of soot surface to HONO production is usually much lower than expected because the uptake efficiency of NO_2 decreases with the prolonged reaction time caused by surface deactivation. The aerosol surface is an important medium for the heterogeneous transformation from NO_2 to HONO (Liu et al., 2014). So, we added the sentences in the revised text.

L 364-368: the contribution of soot surface to HONO production is usually much lower than expected because the uptake efficiency of NO_2 decreases with the prolonged reaction time caused by surface deactivation. The aerosol surface is an important medium for the heterogeneous transformation from NO_2 to HONO (Liu et al., 2014).

We have clearly known that other HONO sources are not the main HONO sources and sinks: 1. HONO is formed by NO_2 through the photolysis of sooty surface and adsorbed nitric acid and nitrate at UV wavelengths (Kleffmann et al., 1999). 2. The homogeneous nucleation of NO_2, H_2O, and NH_3 is the HONO formation pathway (Zhang and Tao, 2010). 3. HONO can deposit and react with amines in forming nitrosamines (Li et al., 2012). So, we added the sentences in the revised

text.

L 98-102: The unknown sources of HONO may include the NO_2 photolysis of sooty surface and adsorbed nitric acid and nitrate at UV wavelengths (Kleffmann et al., 1999). The homogeneous nucleation of NO_2, H_2O, and NH_3 is the HONO formation pathway (Zhang and Tao, 2010). In the meanwhile, HONO can deposit and react with amines in forming nitrosamines (Li et al., 2012) for sinking.

We knew that the lifetime of HONO was 10–20 min at daytime (Lu et al., 2018) and the estimated lifetime was about 3.3 h in the nighttime (Nie et al., 2015).

5. Need to discuss the uncertainty in your results due to variations of many parameters (e.g., rate constants and OH radical values, L 250-253). This leads to the following comments about the use of significant figures.

Response: Measured species and performance of the instruments are counted in **Table S1**. The rate constants are learned from the study (Atkinson et al., 2004). We don't know the uncertainty of rate constants.

Table S1.
Measured species and performance of the instruments.

Species	Measurement technique	Detection limit	Accuracy
$PM_{2.5}$	Tapered Element Oscillating Microbalance	1.5 μg m^{-3}	± 5%
HONO	Ion Chromatography	4 pptv	± 20%
CO	Absorbs Infrared Radiation	40 ppbv	± 5%
NO	Chemiluminescence	60 pptv	± 20%
NO_2	Chemiluminescence	300 pptv	± 20%
O_3	UV Photometry	0.5 ppbv	± 5%

The results came from instrument manufacturers.

Hence, we assumed ± 50% ·OH values to estimate the uncertainty of P_{OH+NO}^{net}. The ·OH values of 1.25×10^5 and 3.75×10^5 molecule cm^{-3} were calculated the P_{OH+NO}^{net} values of 0.16 and 0.49 ppbv h^{-1}.

L 295-297: We assumed ± 50% ·OH values to estimate the uncertainty of P_{OH+NO}^{net}. The ·OH values of 1.25×10^5 and 3.75×10^5 molecule cm^{-3} were calculated the P_{OH+NO}^{net} values of 0.16 and 0.49 ppbv h^{-1}.

6. Be careful about use of significant figures. Delete decimal points for RH (L 182, 185, 187, 194, Table 2, etc.), for NO2 level (L 197-198; also, you compare with standard of 80), for PM2.5 (Table 2), for level in µg m-3 (L 198, etc.), for ratio (L 34, 304, etc.).

Response: Thank you for the comment. We modified the problem in **Table 1** and revised the text. We have learned how to use significant figures.

Table 1.

Data statistics of HONO, $PM_{2.5}$, NO_2, NO, NO_X, $HONO/NO_2$, $HONO/NO_X$, O_3, CO, T, RH, and WS during the measurement period, mean value ± standard deviation.

Trace gases	CD			PD			SPD			Total days
	Day	Night	All	Day	Night	All	Day	Night	All	
$PM_{2.5}$ ($\mu g\ m^{-3}$)	37 ± 15	41 ± 17	39 ± 16	80 ± 32	93 ± 46	87 ± 40	148 ± 29	147 ± 33	147 ± 31	91 ± 54
HONO (ppbv)	0.9 ± 0.7	1.4 ± 0.7	1.1 ± 0.7	1.9 ± 1.7	2.7 ± 1.3	2.3 ± 1.5	3.5 ± 2.7	4.0 ± 1.1	3.7 ± 2.1	2.5 ± 1.9
CO (ppmv)	1 ± 0.3	1 ± 0.3	1 ± 0.3	1± 0.4	1 ± 0.6	1 ± 0.5	2 ± 0.6	2 ± 0.4	2 ± 0.5	1 ± 0.6
NO (ppbv)	18.4 ± 39.3	15 ± 34.3	16.7 ± 36.8	20.3 ± 26.2	30.7 ± 33.6	25.5 ± 30.4	40.8 ± 50.8	64.3 ± 82.1	52.5 ± 68.9	31.8 ± 51.4
NO_2 (ppbv)	23 ± 13	26 ± 13	25 ± 13	29 ± 9	38 ± 10	33 ± 11	40 ± 11	43 ± 10	42 ± 11	33 ± 14
O_3 (ppbv)	21.4 ± 11.5	13.8 ± 10.0	17.6 ± 11.4	17.4 ± 11.9	8.9 ± 8.1	13.1 ± 10.9	15.6 ± 14.2	7.9 ± 7.1	11.8 ± 11.8	14.2 ± 11.7
$HONO/NO_2$ (%)	4.2 ± 3.6	5.3 ± 2.2	4.7 ± 3.1	6.8 ± 5.8	7.4 ± 3.9	7.1 ± 4.9	9.0 ± 7.7	9.8 ± 5.8	9.4 ± 6.8	7.6 ± 6.4
$HONO/NO_X$ (%)	3.3 ± 2.7	6.0 ± 5.6	4.5 ± 4.5	4.4 ± 2.5	4.6 ± 1.7	4.5 ± 2.1	5.3 ± 3.4	5.8 ± 4.7	5.6 ± 4.1	4.9 ± 3.8
RH (%)	30 ± 21	36 ± 20	33 ± 21	44 ± 17	54 ± 18	49 ± 18	64 ± 18	73 ± 13	68 ± 16	50 ± 24
WS ($m\ s^{-1}$)	0.8 ± 1.0	0.5 ± 0.7	0.7 ± 0.9	1.1 ± 1.4	0.6 ± 0.9	0.9 ± 1.2	0.4 ± 0.7	0.3 ± 0.6	0.4 ± 0.7	0.6 ± 0.9
T (°C)	4.3 ± 4.6	2.7 ± 3.6	3.5 ± 4.2	3.7 ± 3.3	2.6 ± 3.1	3.1 ± 3.2	4.6 ± 3.2	2.9 ± 2.1	3.8 ± 2.8	3.5 ± 3.5

Delete decimal points for RH (L182, 185, 187, 194, Table 2, etc.),

Response:

L 205: …with RH ranging from 5 to 79%...

L 207: …RH ranging from 17 to 86%...

L 210: …RH ranging from 30 to 96%...

L 217: …RH in CD, PD, and SPD periods was 33, 49, and 68%...

level in μg m-3 (L 198,etc.),

Response:

L 221: …values of NO_2 were 25, 33, and 42 ppbv (46, 63, and 78 μg m^{-3} lower than…

for ratio (L 34, 304, etc.).

Response:

L 34: …HONO ratio (less than 20%) was approximately 77%...

L 343: …$HONO_{emission}$/HONO ratio less than 20% was approximately 77%...

7. Be consistent with the format of unit. You use m s-1 (or μg m-3), yet m/s and μg·m-3 are in Table 2 (delete centered dot). Use ppbv throughout the text, but ppbV in Tables 1 and 2 and Fig. 8 (some ppbv and one uses ppbV).

Response: Sorry for the careless. The problems have been revised. And we checked the full text to avoid the problems.

Table 1.

Data statistics of HONO, $PM_{2.5}$, NO_2, NO, NO_X, $HONO/NO_2$, $HONO/NO_X$, O_3, CO, T, RH, and WS during the measurement period, mean value ± standard deviation.

Trace gases	CD			PD			SPD			Total days
	Day	Night	All	Day	Night	All	Day	Night	All	
$PM_{2.5}$ ($\mu g\ m^{-3}$)	37 ± 15	41 ± 17	39 ± 16	80 ± 32	93 ± 46	87 ± 40	148 ± 29	147 ± 33	147 ± 31	91 ± 54
HONO (ppbv)	0.9 ± 0.7	1.4 ± 0.7	1.1 ± 0.7	1.9 ± 1.7	2.7 ± 1.3	2.3 ± 1.5	3.5 ± 2.7	4.0 ± 1.1	3.7 ± 2.1	2.5 ± 1.9
CO (ppmv)	1 ± 0.3	1 ± 0.3	1 ± 0.3	1 ± 0.4	1 ± 0.6	1 ± 0.5	2 ± 0.6	2 ± 0.4	2 ± 0.5	1 ± 0.6
NO (ppbv)	18.4 ± 39.3	15 ± 34.3	16.7 ± 36.8	20.3 ± 26.2	30.7 ± 33.6	25.5 ± 30.4	40.8 ± 50.8	64.3 ± 82.1	52.5 ± 68.9	31.8 ± 51.4
NO_2 (ppbv)	23 ± 13	26 ± 13	25 ± 13	29 ± 9	38 ± 10	33 ± 11	40 ± 11	43 ± 10	42 ± 11	33 ± 14
O_3 (ppbv)	21.4 ± 11.5	13.8 ± 10.0	17.6 ± 11.4	17.4 ± 11.9	8.9 ± 8.1	13.1 ± 10.9	15.6 ± 14.2	7.9 ± 7.1	11.8 ± 11.8	14.2 ± 11.7
$HONO/NO_2$ (%)	4.2 ± 3.6	5.3 ± 2.2	4.7 ± 3.1	6.8 ± 5.8	7.4 ± 3.9	7.1 ± 4.9	9.0 ± 7.7	9.8 ± 5.8	9.4 ± 6.8	7.6 ± 6.4
$HONO/NO_X$ (%)	3.3 ± 2.7	6.0 ± 5.6	4.5 ± 4.5	4.4 ± 2.5	4.6 ± 1.7	4.5 ± 2.1	5.3 ± 3.4	5.8 ± 4.7	5.6 ± 4.1	4.9 ± 3.8
RH (%)	30 ± 21	36 ± 20	33 ± 21	44 ± 17	54 ± 18	49 ± 18	64 ± 18	73 ± 13	68 ± 16	50 ± 24
WS ($m\ s^{-1}$)	0.8 ± 1.0	0.5 ± 0.7	0.7 ± 0.9	1.1 ± 1.4	0.6 ± 0.9	0.9 ± 1.2	0.4 ± 0.7	0.3 ± 0.6	0.4 ± 0.7	0.6 ± 0.9
T (℃)	4.3 ± 4.6	2.7 ± 3.6	3.5 ± 4.2	3.7 ± 3.3	2.6 ± 3.1	3.1 ± 3.2	4.6 ± 3.2	2.9 ± 2.1	3.8 ± 2.8	3.5 ± 3.5

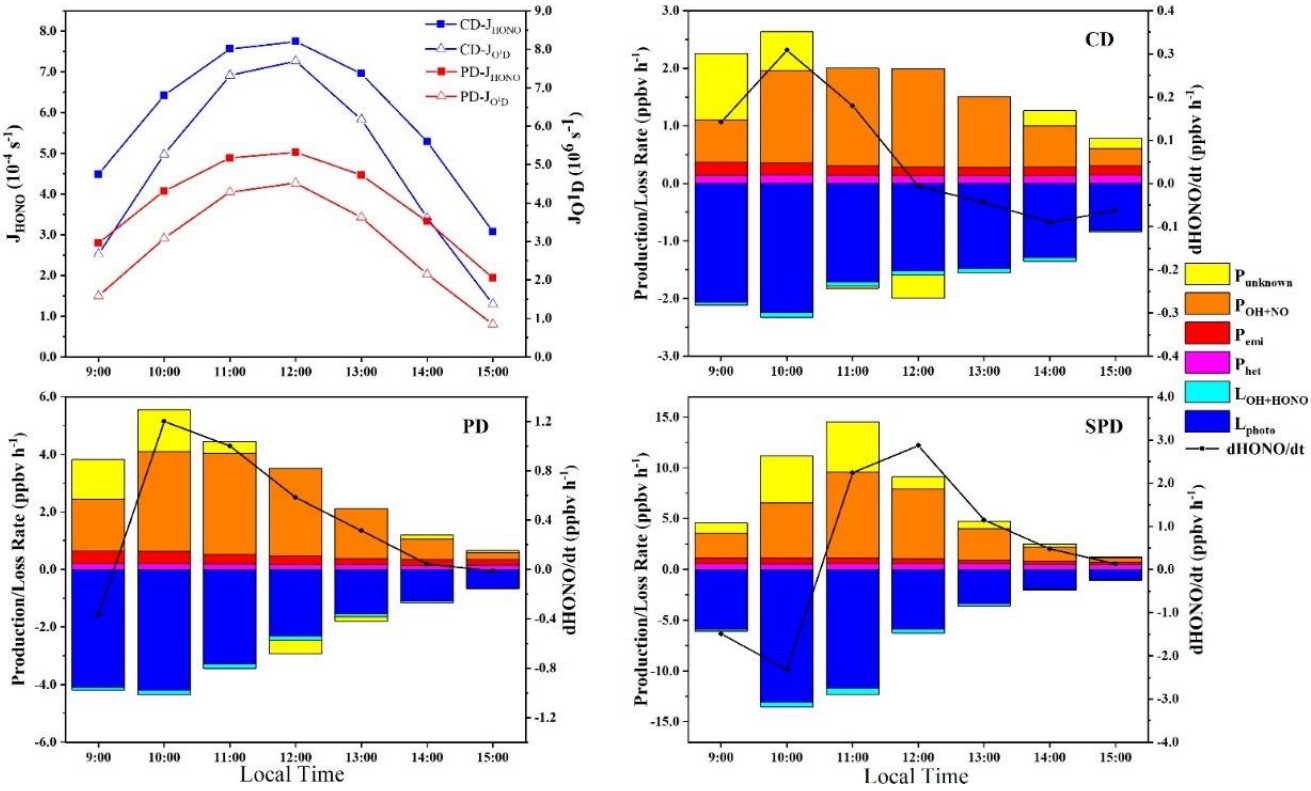

Fig. 9. The average profiles of J_{HONO} and J_{O^1D} concentrations during the daytime, and production and loss rate of the daytime HONO in CD, PD and SPD periods.

8. Data need show the variation; use Box plots or error bars in figures and add standard deviation in tables.

Response: OK. With too many error bars in figures, it will make the figures look unclear. So the error bars of **Fig. 4**, **Fig. 5**, and **Fig. 8** were placed separately in the tables of the supplement (**Table S2**, **Table S3**, and **Table S4**).

9. Need proper citations for equations and rate constants, e.g., in L 247, 250

Response: Sorry, it was our error of citations. Proper citations have been added.

L 278: At T = 298 K and P = 101 kPa… respectively (Atkinson et al., 2004; Sander et al., 2003).

10. The comparison with others (Table 1) may not be useful and must be made with care since the studied year is different (some in 2012 – may not have adequate end-of-the pipe treatment), nature of sampling sites is different (some in urban, suburban and even rural sites) and atmospheric dynamics in these regions are far different.

Response: You're right. The comparison with others must be made with care since the studied year is different. Therefore, only the observation data of HONO in the last ten years were used for comparative analysis of HONO concentration changes in urban. We removed the HONO level (Jun.-Jul. 2005 in Germany) in the revised text (**Table 2**). We analyzed the effect of the site on HONO concentration in urban. So, we added sampling sites in **Table 2**.

Table 2.

Comparisons of the daytime and nighttime HONO level, $HONO/NO_2$, and $HONO/NO_X$ mean values in Zhengzhou and other sites around the world.

Date (Site)	Instrument	HONO (ppbv)			$HONO/NO_2$ (%)		$HONO/NO_X$ (%)		Reference
		Day	Night	N/D	Day	Night	Day	Night	
Oct.–Nov. 2014 (Beijing, urban)	LOPAP (long path absorption photometer)	0.9	1.8	2.0	2.6	4.6	1.7	2.2	Tong et al., 2015
Feb.–Mar. 2014 (Beijing, urban)	LOPAP	1.8	2.1	1.2	3.8 (Severe haze)	4.3	2.5	2.5	Hou et al., 2016
		0.5	0.9	1.8	7.8 (Clean)	3.0	5.1	2.4	
Jul. 2006 (Guangzhou, rural)	LOPAP	0.2	0.9	4.5	1.0	2.5	4.3	4.5	Li et al., 2012
Jul. 2014–Aug. 2015 (Xi'an, urban)	LOPAP	0.5	1.6	3.2	3.3	6.2			Huang et al., 2017
Aug. 2010–Jun. 2012 (Shanghai, urban)	Active DOAS	0.8	1.1	1.4	4.2	4.5			Wang et al., 2013
Jul. 2009 (Paris, urban)	wet chemical derivatization technique-HPLC/UV-VIS detection	0.1	0.2	2.0	3.3	2.5			Michoud et al., 2014
Jan. 2019	AIM	2.2	2.8	1.3	6.8	8.5	4.4	5.5	This study

Jul. 2006 (Guangzhou, urban): This paper is a relatively early study on the HONO concentration level in China. We thought this paper still had a certain level of high

quality, so we put it in the table for comparison.

For avoiding this problem of atmospheric dynamics, we used observed values of HONO in Chinese cities mostly.

11. Why no discussion of OH production rate as a function of O_3 levels?? In other words, is any HONO information related to O_3 pollution level?? It is relevant since •OH radical generated from HONO is in turn used for O_3 production.

Response: Thank you for the comment. We hold the opinion that the discussion of OH production rate as a function of O_3 levels can be written as an article on account of complexity. At the same time, we found that the negative correlation between HONO and O_3 was lower in the entire period, and it was known from **Fig 4d** that the heavier the pollution level, the lower the O_3 concentration.

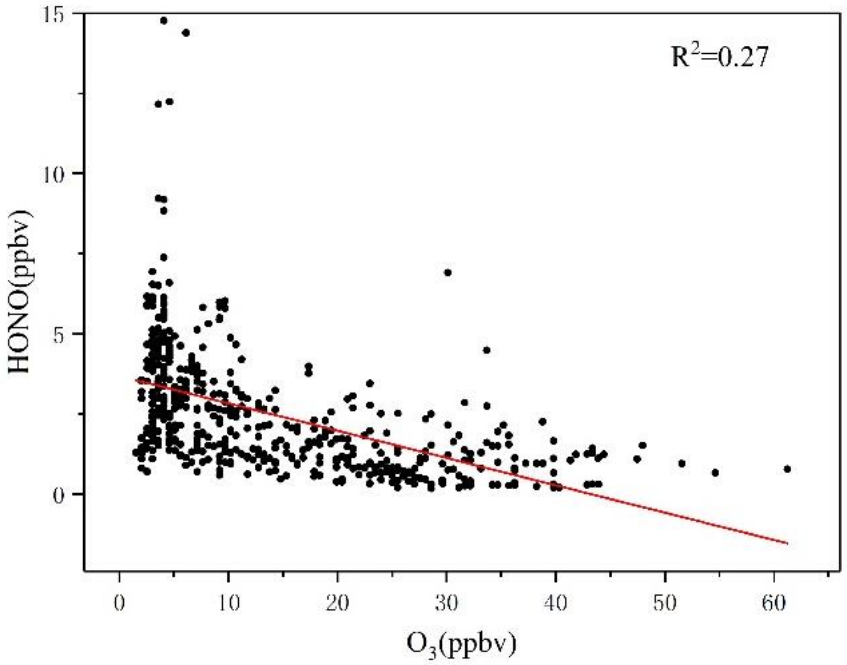

Figure The correlation between HONO and O_3.

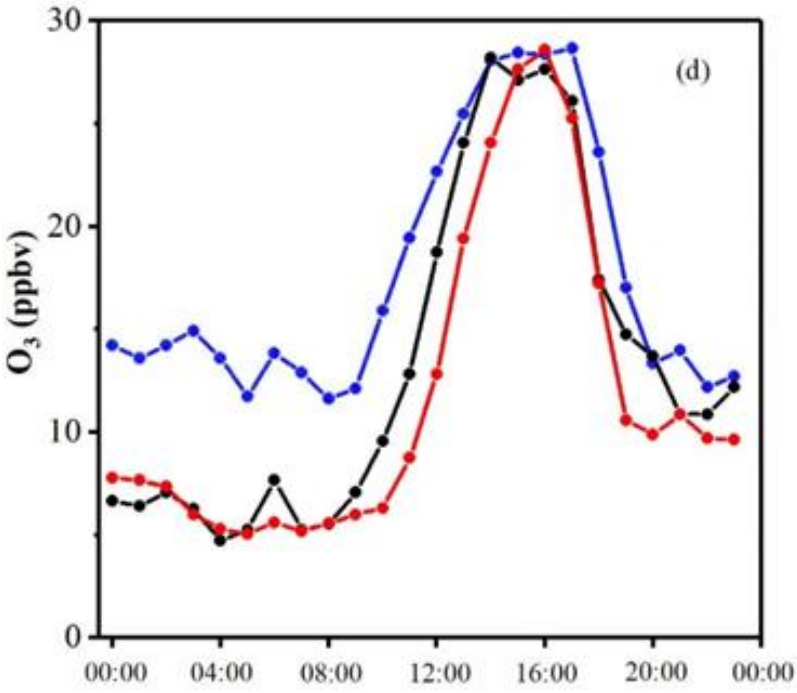

Fig. 4d. Diurnal variations of O_3. The blue points and lines represented the CD period; the black points and lines represented the PD period; the red points and lines represented the SPD period.

Specific comments:

1. “Title is misleading”

Response: OK. We have added “at an urban site” in the title. The title is “Characteristics, sources, and reactions of nitrous acid during winter at an urban site in the Central Plains Economic Region in China.”

2. L 15: All of a sudden, the phrase “three sources” pops up. Need to clearly state what they are.

Response: According to your comment, the sentence was modified in the revised text.

L 14-15: The contribution of the homogeneous reaction, heterogeneous conversion, and direct emission to HONO sources varied under different pollution levels.

3. Why not place centered dot symbol for OH radical? or •OH

Response: OK. We have changed ·OH for ·OH in the revised text.

L 44: …HONO to ·OH concentration…

L 47: …most important primary source of ·OH…

L 77: …react with the ·OH…

L 96: …the importance of the ·OH…

L 280: …concentration of ·OH…

L 282: …the average concentration of ·OH…

L 283: …the same ·OH…

L 471: …·OH and NO were formed…

L 495: …values of J_{HONO} and ·OH concentration…

4. Use a proper term in lieu of rate which refers to time

Response: Sorry for the careless. We have removed the word “rate”.

L 44: …the contribution of HONO to ·OH concentration can reach 25−50%…”

5. L 45: Why only these two? What about others including HONO itself and acetone?

Response: We have modified the sentence in the revised text.

L 43-46: …the contribution of HONO to ·OH concentration can reach 25%−50%, especially when the concentration of OH radicals produced by the photolysis of ozone, acetone, and formaldehyde…

6. L 49: what reaction? Should be more than one reaction.

Response: Sorry for my confusion. We have changed “reaction” for “the changes in the contribution of the homogeneous reaction, heterogeneous conversion, and direct emission” in the revised text.

L 51-54: …the changes in the contribution of the homogeneous reaction, heterogeneous conversion, and direct emission during pollution can be observed…

7. Citation:

Response: Sorry for my carelessness. All modifications have been made, and we have checked the full text.

a. Provide adequate spacing between citations, or Hou et al., 2016; Michoud et…. (need a spacing before the 2nd citation).

L 57: …(Elshorbany et al., 2012; Winer and Biermann, 1994)…

L 60: …(Duan et al., 2018; Min et al., 2016)…

L 61: …(Hirokawa et al., 2009; Roberts et al., 2010).

L 68: …(Hou et al., 2016; Michoud et al., 2014).

L 70: …(Acker et al., 2005; Grassian, 2001; Kurtenbach et al., 2001).

b. Make sure all cited references are listed and vice versa. For example, citations in L 55 (L 60) and Table 1 (Elshorbany et al., 2012) are not listed.

L 785: VandenBoer, T. C., Markovic…

L 606: Elshorbany, Y. F., Steil, B., Brühl, C…

c. Delete redundant citations. No need to cite twice in the beginning and at the end of the sentence. Pls change throughout the text (L 75, 82, 88, 93, 156, 157, 246, etc.) by delete the second citation.

L 72: Kurtenbach et al. (2001)…

L 77: Tong et al. (2015)…

L 90: Hao et al. (2006)…

L 96: Su et al. (2008a)…

L 105: Spataro et al. (2013)…

L 108: Tong et al. (2015)…

d. L 95; et al. (2013); delete the extra comma.

L 105: Spataro et al. (2013)…

e. Avid excessive self-citations (one is enough, e.g., L 115, 116, etc.)

f. For the same last name, use the format of Jiang et al., 2018c, 2018e; Liu…. (L 115). Pls change throughout the text.

L 123-127: As the core city of CPER, Zhengzhou characterized by severe PM (particulate matters) pollution (Jiang et al., 2018b), is selected in the study. In recent years, comprehensive PM research has been conducted on the chemical characteristics of PM in Zhengzhou. (Li et al., 2019), source apportionment (Liu et al., 2019), health risks (Jiang et al., 2019), and emission source profiles (Jiang et al., 2018a).

g. L 140: why cite this? Need year for this reference.

L 163-164: …(7:00–18:00 local time)…

h. L 181: why cite this one? Delete

L 204: …Air Quality Standards (CNAAQS) (75 μg m^{-3})…

i. L 313: Acker et al. (2005) reported...

L 352: …Acker et al. (2005)…

8. L 60: what is 1:1??

Response: Sorry for my confusion. Through the comparison of measurement results, the correlation between SC-AP deployed onsite and AIM tended to 1. For avoiding the confusion, we have removed the words "; the results exhibited a consistency of nearly 1:1" in the revised text.

L 64-66: Compared with HONO measured by SC-AP deployed onsite, HONO measured by AIM has a small error and is within the acceptable analytical uncertainty (VandenBoer et al., 2014).

9. L 79: There is no connection between these two sentences. Need a sentence(such as revised R3 reaction) leading to the following sentence.

Response: OK. We have added the sentence between these two sentences in the revised text.

L 82-87: Such calculations have been applied in studies on homogeneous reactions and daytime budgets (Hou et al., 2016; Huang et al., 2017). These are studies of homogeneous reactions, and some researchers have begun to explore the mechanism of NO_2 heterogeneous reactions. Finlayson-Pitts et al. (2003) studied the mechanism of chemical adsorption of NO_2 and H ions on the adsorbed surface…

10. L 123: These two measurements ($PM_{2.5}$ and HONO) cannot clarify the sources, sinks and reactions. Pls reword.

Response: Sorry, we have modified the sentence in the revised text.

L 133-134: The levels of $PM_{2.5}$ were divided into three periods to analyze the HONO sources, sinks, and reactions in different periods.

11. L 173: what is uncertainty of AIM? How about MDL for other gases??

Response: Thank you for your comment. Measurement technique, detection limit, and accuracy of measured species are shown in Table S1 in the supplement.

Table S1.

Measured species and performance of the instruments.

Species	Measurement technique	Detection limit	Accuracy
$PM_{2.5}$	Tapered Element Oscillating Microbalance	1.5 μg m^{-3}	± 5%
HONO	Ion Chromatography	4 pptv	± 20%
CO	Absorbs Infrared Radiation	40 ppbv	± 5%
NO	Chemiluminescence	60 pptv	± 20%
NO_2	Chemiluminescence	300 pptv	± 20%
O_3	UV Photometry	0.5 ppbv	± 5%

The results came from instrument manufacturers.

12. L 190: Table 1 must come before Table 2. Rearrange the table number.

Response: OK. We have rearranged the table number.

L 213: **Table 1** lists the data statistics…

L 265: …listed in **Table 2.**

13. Interesting. You cover all these parameters (L 199-204) shown in Fig. 2, yet Fig. 2 is mentioned several sentences later (L205). The same illogical sequence is found in L 403 which mentions $P_{unknown}$ and $P_{emi,}$ but the equation for these is shown much later (L 436). Also need to cover these rates for estimating daytime HONO budget.

Response: Sorry for my confusion. The illogical sequence had been changed. We have modified the sentences in the revised text.

L 223-226: **Fig. 2** shows the concentration changes in HONO…The variations of the average HONO, $PM_{2.5}$, NO_2…

L 456-465: …d HONO / d t = sources − sinks

$$= (P_{unknown} + P_{OH+NO} + P_{emi} + P_{het}) - (L_{OH+HONO} + L_{photo}) \quad (4),$$

$$P_{OH+NO} = k_{OH+NO}\,[OH]\,[NO] \quad (5),$$

$L_{OH+HONO} = k_{OH+HONO}$ [OH] [HONO] (6).

The d HONO / d t calculated from…

14. L 240: why??

Response: Sorry for my carelessness. Although observations of HONO levels in Zhengzhou were different from other cities because of periods, seasons, and meteorological conditions, a higher concentration of HONO was found in Zhengzhou. This situation attracted our attention. We thought the environmental impact of the increase in pollutant emissions and the number of vehicles exceeds the efforts of Zhengzhou to protect the atmospheric environment. Total NO_X emissions in cities have been declining year by year due to Chinese government emission control measures, but some Chinese cities are still in high-NO_X areas (e.g. Beijing, Shanghai, Guangzhou, and Zhengzhou.) (Kim et al., 2015; Liu et al., 2017). Therefore, we have added the sentence in the full text.

L 267-269: The reason for this phenomenon is that Zhengzhou is a high-NO_X area which provides HONO with abundant precursors (NO_2 and NO) in winter (Kim et al., 2015).

15. L 252: why in reference to Beijing?

Response: We revisit and determine the OH concentration. The OH concentration previously used is 1×10^6 molecule cm^{-3} is obtained by the simulation (Lelieveld et al., 2016). So, we have modified the sentences in the revised text.

L 280-285: [OH] is the concentration of ·OH that was not measured during the campaign. Therefore, Tan et al. (2018) found that by the field measurement, the average concentration of ·OH in Beijing at nighttime was about 2.5×10^5 molecule cm^{-3}. Moreover, the same ·OH concentration was also used to calculate the

homogeneous reaction of HONO in the recent researches of Beijing (Zhang et al., 2019), Shanghai (Cui et al., 2018), and Xi'an (Huang et al., 2017).

Finally, we chose the average concentration of ·OH in Beijing was about 2.5×10^5 molecule cm^{-3} as the nighttime ·OH concentration in Zhengzhou.

16. L 253: Can you calculate OH radical concentration from those discussed later in L 418?

Response: OK. The concentration of ·OH during the daytime was calculated by the TUV model. But there is no sunlight at night, so it cannot be counted.

17. L 287: You are talking about night and mentioned no pollution source near the site. Why all these calculations related to traffic?? Unclear.

Response: Sorry for your comment. The sentence is not clear enough. So, we have changed "because no pollution source was near the measurement site" for "because the site is close to the western Fourth-Ring Expressway of Zhengzhou City and about Lian Huo Expressway to the north." in the revised text.

L 324-326: In the current study, directly emitted HONO could have been generated by vehicle exhaust and biomass combustion because the site is close to the western Fourth-Ring Expressway of Zhengzhou City and about Lian Huo Expressway to the north.

18. Pls explain the contradictory statements: important pathway (L 321) and unimportant pathway (L 20) for heterogeneous reaction for HONO formation.

Response: Sorry for my carelessness. With respect to direct emissions, heterogeneous reactions may be a more important pathway for HONO production.

The HONO/NO_2 ratio calculated in this work is much larger than that calculated for direct emission (< 1%) (Kurtenbach et al., 2001), suggesting that heterogeneous reactions may be a more important pathway for HONO production than direct emissions.

However, the average conversions of NO_2 (C_{HONO}) in CD, PD, and SPD periods were 0.72×10^{-2}, 0.64×10^{-2}, and 1.54×10^{-2} h^{-1}, respectively, indicating that the heterogeneous conversion of NO_2 was unimportant than the homogeneous reaction. So, in order to prevent confusion, we have modified the sentence in the revised text.

L 17-20: The average conversions of NO_2 (C_{HONO}) in CD, PD, and SPD periods were 0.72×10^{-2}, 0.64×10^{-2}, and 1.54×10^{-2} h^{-1}, respectively, indicating that the heterogeneous conversion of NO_2 was unimportant than the homogeneous reaction.

19. Use the stack format for equations in a separate line (L 389); use the solidus format for those within the line (L 402).

Response: Thank you. The equations had been changed.

L 438: $C_{HONO} = \frac{([HONO_{correct}]_{t2} - [HONO_{correct}]_{t1}}{(t2 - t1)\,[NO_2]}$

L 456: d HONO / d t = sources − sinks

20. L 431: Why the same values for both PD and SPD? That means you treat PD and SPD the same.

Response: OK. These are the averages per hour of J_{HONO} and J_{O^1D} for PD and SPD. We treated PD and SPD the same. The reason is that the main input parameters of TUV cannot be obtained directly, so we quoted the input parameters in the literature. However, the input parameters of PD and SPD are not

distinguished in the papers. We wanted to study that under the same output conditions from the TUV model, the impact of different pollution levels changed on the daytime budget. We have added the sentence in the revised text.

L 491-493: We wanted to study that under the same output conditions from the TUV model in the PD and SPD periods, the impact of different pollution levels changed on the daytime budget.

21. Fig. 1: How could one tell the wind direction?? There is no shade area of black and red color (caption says so). Change in Fig. 2 too.

Response: Sorry. We have removed the word, "WD" in **Fig. 1** in the revised text. The colors of the shaded area were redefined in **Fig. 1** and **Fig. 2**. The shaded areas: white for the CD period; gray for the PD period; red for the SPD period.

22. Fig. 6d and RH effect: Was the phenomenon also observed by others?? Who is to say that 77% is the inflection point? Just say "reach a certain high level,HONO…."

Response: Thank you for your comment. The phenomenon also observed by other studies (Cui et al., 2018; Huang et al., 2017; Tong et al., 2015). "52% and 77%" was removed in the revised text.

L 400-402: When RH was increased, the $HONO/NO_2$ ratio began to increase rapidly with RH. The $HONO/NO_2$ ratio decreased when RH reached a certain high level.

L 409-410: However, the surface reached saturation when RH reached a certain high level.

23. References:

Response: Sorry for my carelessness. The problems had been changed in the

revised text.

- Be consistent! Use lowercases for journals (e.g., L 502, 515, etc.)
- Need periods after all journal abbreviations (e.g., L 502, 515, etc.)

L 565: …Atmos. Res., 74, 507-524…

L 569: …J. Geophys. Res.,…

- Adequate subscript/superscript (e.g., L 535)

L 582: …gas phase reactions of O_x, HO_x, NO_x, and SO_x…

- Use correct journal, or Phy. Chem. Chem Phy., (L 536)

L 583: …Atmos. Chem. Phys.,...

- Use lowercases for articles (e.g., L 505)

L 563: …Concentrations of nitrous acid, nitric acid, nitrite and nitrate in the gas and aerosol…

- L 546 ref is not cited.

The reference has been removed in the revised text.

Tech/English comments:

Response: Thank you for your carefulness. The problems have been modified and modified issues have been marked in yellow throughout the revised text. The parts that need explanation have been listed.

1. L 13, 178, 179: Use polluted (not pollution)

L 12: …polluted days (PD), and severely polluted days…

L 200-201: …clean days [CD], polluted days [PD], and severely polluted…

2. L 33: Use was (not should be)

L 33: …OH + HONO, was at least 0.22 ppbv h^{-1}…

3. Be consistent about the use of verb tense; some use past tense in the first part of the sentence with present tense used in the latter part.

L 34-35: …(less than 20%) was approximately 77%, which suggested…

4. L 32, 279: Delete the redundant abatement (first one)

L 32-33: …hourly level of HONO abatement pathways…

5. L 44: delete rate

L 43-44: …the contribution of HONO to ·OH…

6. L 54: UV/Vis

L 58-59: …stripping coil-UV/Vis…

7. L 56: result comparison

L 62: A result comparison of different instruments…

8. L 67: have discovered

L 72: …have discovered that motor vehicles…

9. L 68-69: How does ratio “account for”? Use “is” 0.1-0.8%

L 74: …(aside from NO_X and other pollutants) is 0.1–0.8%.

10. Reword awkward L 81, word “radiation” (L 93), confusing (L 108-110).

L 85-87: Finlayson-Pitts et al. (2003) studied the mechanism of chemical adsorption of NO_2 and H ions on the adsorbed surface was revealed by using isotope-labeled water.

L 95-98: Su et al. (2008) revealed the importance of the ·OH from HONO during daytime (9:00–15:00 local time) and found that many unknown sources which are closely related to the solar radiation leading to HONO formation.

L 119-123: The file described the different factors which affect atmospheric pollution, including the level of economic development, energy structure, industrial structure and geographical location (solar radiation) with the Yangtze River Delta, Pearl River Delta, and Jing-Jin-Ji region.

11. L 99: Use pathway of…: mechanism is the same, but pathway is different.

L 109: …the pathway of HONO formation mechanism, namely…

12. L 107: “Food Production and Modern Agriculture” specified by (not published)

This website can not be found because of the update. We have changed

"http://www.ndrc.gov.cn/zcfb/zcfbtz/201212/P020121203614181974825.pdf" for "http://www.gov.cn/zhengce/content/2011-10/07/content_8208.htm", in the revised text (L 119).

13. L 112: delete "is" and insert "is" ahead of selected

L 124: …is selected in the study.

14. L 114: Not Zhengzhou chemical characteristics. Should have written as: chemical characteristics of PM in Zhengzhou.

L 125-126: …on the chemical characteristics of PM in Zhengzhou…

15. L 121: $PM_{2.5}$ is not chemical

We have changed "chemical" for "factors" in the revised text (L 124).

L 131: …between HONO and other factors, such as $PM_{2.5}$…

16. L 124: How systematic?

We have removed "This investigation of $PM_{2.5}$ and HONO is expected to clarify the sources, sinks, and reactions in fine PM pollution and the importance of systematic research." We have added the sentences in the revised text.

L 133-147: The levels of $PM_{2.5}$ were divided into three periods to analyze the HONO sources, sinks, and reactions in different periods. Many papers (Huang et al., 2017; Tong et al., 2016) took $PM_{2.5}$ as the main control factor of HONO, and studied the differences of HONO sources and characteristics between clean and polluted periods. No homogeneous reaction, direct emission, heterogeneous

reaction, and daytime budget analysis were conducted during the period of worsening pollution (namely HD period in this paper). Total NO_X emissions in cities with different leading factors of emissions have been declining year by year due to Chinese government emission control measures, but some Chinese cities are still in high-NO_X areas (e.g. Beijing, Shanghai, Guangzhou and Zhengzhou.) (Kim et al., 2015; Liu et al., 2017). Under high-NO_X conditions, some papers (Cui et al., 2018; Hou et al., 2016) suggested that heterogeneous reaction was the main source of HONO and did not conduct a quantitative analysis of homogeneous reaction, especially in winter. So, we explore relevant studies of homogeneous reactions. In addition, the source contributions of HONO at night varied with the degree of pollution level were not explained.

17. L 137: western Fourth-Ring Expressway

L 161: …from the western Fourth-Ring Expressway of Zhengzhou City…

18. L 151: Use chemicals (in lieu of substances)

L 173: The chemicals that could be oxidized…

19. L 153: O_2 and N_2 (not O and N)

L 174: …several gases (e.g., O_2 and N_2)…

20. L 160-161: Clearly state which instrument is for which compound, e.g., 48i for CO measurement.

We have modified the sentence in the revised text.

L 181-184: A temporal resolution of the model analyzer (TE [used for measuring O_3], 48i [used for measuring CO], 42i [used for measuring NO, NO_X, and NO_2], and TEOM 1405 $PM_{2.5}$ monitor [used for measuring $PM_{2.5}$], Thermo Electron, USA) is 1 h.

21. L 167-168: The manual uses the term "should be". But in your statement, you should use "was changed" …."was calibrated".

L 193: The standard curve should be…
L 190-191: …were changed before the observation process, and the sampling flow was calibrated…

There are no serial **Numbers 22 and 23**. In order to prevent the confusion, the serial number used is consistent with the serial number in your comment.

24. L 171: A space after "≥" sign

L 194: …the correlation coefficient (≥ 0.999)…

25. L 181: specify that it is daily average

L 203: …the daily average of second grade…

26. Delete the first unit (L 182, 185, 188, 206, 301, 317, 360, etc.), first two units (L 301, 449, etc.)

L 205: …0 to 4.2 m s^{-1}…
L 208: …0 to 4.6 m s^{-1}…

L 210: …0 to 3.5 m s^{-1}…

L 230: …0.2 to 14.8 ppbv…

L 340: …2–52%, 6–34%, and 2–41%…

L 356: …1.3 and 59.0%…

L 401: …when RH reached a certain high level.

L 511: …15, 14, and 28%...

27. L 189: .. north with high WS … Also, how high is high? > 3 m/s, or > 4 m/s? Be specific!

L 212: …the maximum WS reached 4 m/s…

28. L 190: effect of pollutant removal

L 213: …the effect of pollutant removal…

29. L 202: mean values of what? of all pollutant concentrations?

L 226: The mean values of all pollutant concentrations except O_3…

30. L 209: Is your sampling site in urban area? You mentioned on the university campus. If so, the comparison is not valid.

OK. We have added the sampling site in Table 2. The university campus is urban in Zhengzhou. So, we compared the difference of the daytime and nighttime HONO level, HONO/NO_2, and HONO/NO_X mean values in urban in other cities.

Table 2.

Comparisons of the daytime and nighttime HONO level, $HONO/NO_2$, and $HONO/NO_X$ mean values in Zhengzhou and other sites around the world.

Date (Site)	Instrument	HONO (ppbv)			$HONO/NO_2$ (%)		$HONO/NO_X$ (%)		Reference
		Day	Night	N/D	Day	Night	Day	Night	
Oct.–Nov. 2014 (Beijing, urban)	LOPAP (long path absorption photometer)	0.9	1.8	2.0	2.6	4.6	1.7	2.2	Tong et al., 2015
Feb.–Mar. 2014 (Beijing, urban)	LOPAP	1.8	2.1	1.2	3.8 (Severe haze)	4.3	2.5	2.5	Hou et al., 2016
		0.5	0.9	1.8	7.8 (Clean)	3.0	5.1	2.4	
Jul. 2006 (Guangzhou, rural)	LOPAP	0.2	0.9	4.5	1.0	2.5	4.3	4.5	Li et al., 2012
Jul. 2014–Aug. 2015 (Xi'an, urban)	LOPAP	0.5	1.6	3.2	3.3	6.2			Huang et al., 2017
Aug. 2010–Jun. 2012 (Shanghai, urban)	Active DOAS	0.8	1.1	1.4	4.2	4.5			Wang et al., 2013
Jul. 2009 (Paris, urban)	wet chemical derivatization technique-HPLC/UV-VIS detection	0.1	0.2	2.0	3.3	2.5			Michoud et al., 2014
Jan. 2019	AIM	2.2	2.8	1.3	6.8	8.5	4.4	5.5	This study

31. L 214: No logic about sunrise – previous max HONO values (8-10 am) are way past sunrise. Should have written after 10 am…..

L 240: After 10:00 LT, the HONO concentration…

32. L 215: reword the incomplete phrase

We have reworded the sentence in the revised text.

L 240-242: After 10:00 LT, the HONO concentration decreased because of the increased solubility and rapid photolysis, remaining at a low level before sunset (14:00–16:00 LT).

33. L 219: delete again

L 243-244: After sunset, the concentrations of NO and NO_2 began to increase and remained at a higher level than the daytime.

34. L 220: and the concentration remained the same (Is it true??) until sunrise

It was not the same. The concentrations of NO and NO_2 began to increase and remained at a higher level than the daytime. We have modified the sentence in the revised text.

L 243-244: After sunset, the concentrations of NO and NO_2 began to increase and remained at a higher level than the daytime.

35. L 222: you meant NO_2 diffusion?

Sorry for my confusion. The concentrations of NO and NO_2 decreased after the peak values. On the one hand, NO and NO_2 can be involved in the reactions. On the other hand, NO and NO_2 diffused because of the boundary layer height increased in the daytime.

36. L 228: How is atmospheric migration? Should be "migration of atmospheric airmass".

L 253: …less affected by the migration of atmospheric airmass…

37. L 248: should be Eq. (1); Eq. (2) is in L 296.

L 277: …$P_{OH+NO}^{net} = k_{OH+NO}[OH][NO] - k_{OH+HONO}[OH][HONO]$ (1).

38. L 249, 337, 338, 349, 389, etc.: A space b/a the = sign

L 278: At T = 298 K and P = 101 kPa…

L 377-378: …$PM_{2.5}$ (R^2 = 0.23) was weaker than that between HONO and $PM_{2.5}$ (R^2 = 0.55)…

L 390-392: …CO was relatively moderate (R^2 = 0.43)…

L 438: …$C_{HONO} = \frac{([HONO_{correct}]_{t2} - [HONO_{correct}]_{t1}}{(t2 - t1)\,[NO_2]}$ (3)…

39. L 254: Adequate subscript in k_{OH+bar}

L 289: … the reaction rates of k_{OH+NO}…

40. L 274: reword

L 311-312: With the increase in pollution level, the HONO accumulation period at nighttime increased.

41. L 279: Use rate (not level)

L 316: …the hourly rate of HONO…

42. L 280: delete the extra spacing b/a the "/" sign

L 317-318: …3.36 – 1.59 ppbv)/8 h).

43. L 307: on the campus

L 346: …from the highway on the campus…

44. L 324: medium of what??

Sorry for my confusion. We have modified the sentence in the revised text.

L 361-364: With regard to the heterogeneous conversion of NO_2, several studies (An et al., 2012; Shen and Zhang, 2013) have reported that the surface of soot particles is the medium of NO_2 conversion.

45. L 349-350: wording? cannot see “indicating ...of what most cases”? Why?

Sorry for my confusion. The correlation coefficient between HONO and CO was relatively moderate (R^2 = 0.43), indicating that HONO and CO could come from the same source of emissions. Generally speaking, CO and NO are mainly related to combustion processes such as vehicle emissions, fossil fuel and biomass combustion (Tong et al., 2016). We have modified the sentence in the revised text.

L 390-396: The correlation coefficient between HONO and CO was relatively moderate (R^2 = 0.43), indicating that HONO and CO could come from the same source of emissions. Generally speaking, CO and NO are mainly related to combustion processes such as vehicle emissions, fossil fuel and biomass combustion (Tong et al., 2016). Thus, fossil fuel and biomass combustion may contribute to HONO production, but they can not be measured directly.

46. L 361: sedimentation of what? Do you mean deposit?

Right. We have modified the sentence in the revised text.

L 406-408: When RH ranged at the middle level, the heterogeneous

conversion of NO_2 to HONO was more significant than that of deposition.

47. L 367: Delete “study of the”

L 414: The correlation between $HONO_{correct}$ and NO_2…

48. L 374: decreases after…

L 421: …heterogeneous reaction (R4), and NO_2 decreased after midnight.

49. L 383: in the (not then)

L 432: …calculated in the current study…

50. L 396: How is rate improvement? Use increase

OK.

L 445: The increase in the conversion rate demonstrates…

51. L 402: The expression of …. represents

L 454: The expression of d HONO / d t represents…

52. L 411: delete an

L 471: …·OH and NO were formed as R1.

53. Table 1: A space before (%), or HONO/NOX (%); before year, or Jun. 2012, Also add SD

Table 2.

Comparisons of the daytime and nighttime HONO level, $HONO/NO_2$, and $HONO/NO_X$ mean values in Zhengzhou and other sites around the world.

Date (Site)	Instrument	HONO (ppbv)			$HONO/NO_2$ (%)		$HONO/NO_X$ (%)		Reference
		Day	Night	N/D	Day	Night	Day	Night	
Oct.–Nov. 2014 (Beijing, urban)	LOPAP (long path absorption photometer)	0.9	1.8	2.0	2.6	4.6	1.7	2.2	Tong et al., 2015
Feb.–Mar. 2014 (Beijing, urban)	LOPAP	1.8	2.1	1.2	3.8 (Severe haze)	4.3	2.5	2.5	Hou et al., 2016
		0.5	0.9	1.8	7.8 (Clean)	3.0	5.1	2.4	
Jul. 2006 (Guangzhou, rural)	LOPAP	0.2	0.9	4.5	1.0	2.5	4.3	4.5	Li et al., 2012
Jul. 2014–Aug. 2015 (Xi'an, urban)	LOPAP	0.5	1.6	3.2	3.3	6.2			Huang et al., 2017
Aug. 2010–Jun. 2012 (Shanghai, urban)	Active DOAS	0.8	1.1	1.4	4.2	4.5			Wang et al., 2013
Jul. 2009 (Paris, urban)	wet chemical derivatization technique-HPLC/UV-VIS detection	0.1	0.2	2.0	3.3	2.5			Michoud et al., 2014
Jan. 2019	AIM	2.2	2.8	1.3	6.8	8.5	4.4	5.5	This study

The values of SD were shown in the references.

54. Fig. 3: Need errors bars. Use the present tense, “represent”. Show one example in Box plots so one has an idea about the magnitude of variation.

55. Fig. 4: Need error bars

With too many error bars in figures, it will make the figures look unclear. So the error bars of **Fig. 4**, **Fig. 5**, and **Fig. 8** were placed separately in the tables of the supplement (**Table S2**, **Table S3**, and **Table S4**).

56. Fig. 6: A space after HONO

We have modified the figure in the revised text **Fig. 7**.

Fig. 7. Nighttime correlation studies between $PM_{2.5}$ and $HONO/NO_2$, $PM_{2.5}$ and HONO, CO and HONO, RH and $HONO/NO_2$ during the entire measurement period, CD, PD, and SPD periods. The blue represented the full measurement period; the light blue represented CD period; the black represented PD period; the red represented SPD period.

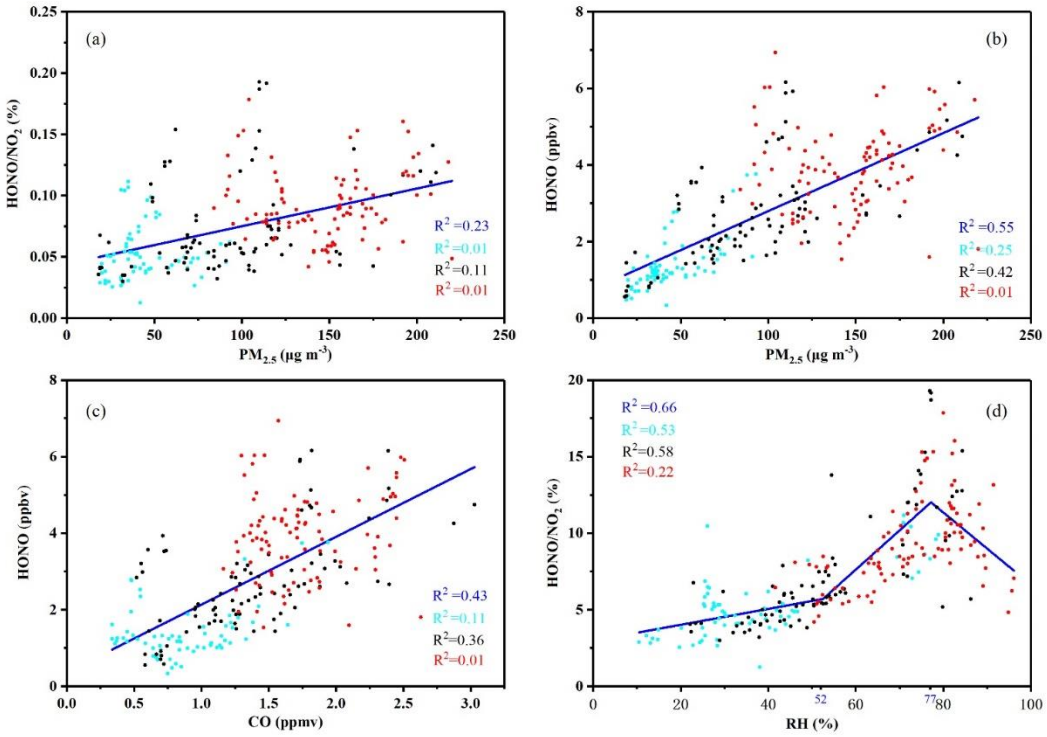

Characteristics, sources, and reactions of nitrous acid during winter at an urban site in the Central Plains Economic Region in China

Qi Hao, Nan Jiang*, Ruiqin Zhang, Liuming Yang, and Shengli Li
Key Laboratory of Environmental Chemistry and Low Carbon Technologies of Henan Province, Research Institute of Environmental Science, College of Chemistry, School of Ecology and Environment, Zhengzhou University, Zhengzhou 450001, China

Supplement:

1. This AIM method and its details.

HONO was hygroscopically grown in the parallel plate denuder and collected as an aqueous solution in a cyclone assembly. The aqueous sample aliquots from both channels were transported to the ion chromatographic systems housed inside a ground container for hourly semicontinuous online analysis of HONO. The ion chromatographic system was calibrated for NO_2^- using mixed anion standard solutions of NO_2^-.

2. The concentration of OH radicals was calculated with the formulas of NO_2, O_3, and J_{O^1D}.

$$[\mathrm{OH}] = \frac{k_{HO_2+NO}\tau_{HC}[NO_2]F_J}{k_{NO+O_3}} \times \sqrt{\frac{\alpha}{k_{HO_2+HO_2}[O_3]}} \times J(O^1D),$$

where [OH] represents the concentration of OH radicals, $k_{HO_2+NO} = 8.56 \times 10^{-12}$ cm^3 s^{-1}, $\tau_{HC} = 0.3$ s, [NO_2] represents the NO_2 concentration, $F_J = 2$ s$^{-0.5}$, $k_{NO+O_3} = 1.82 \times 10^{-14}$ cm^3 s^{-1}, $\alpha = 0.075$, $k_{HO_2+HO_2} = 8.56 \times 10^{-12}$ cm^3 s^{-1}, [O_3] represents the O_3 concentration, and $J(O^1D)$ represents the O^1D efficiency of photolysis.

Figure Captions:

Fig. S1. The correlation study between $HONO_{correct}$ and NO_2 in the nighttime.

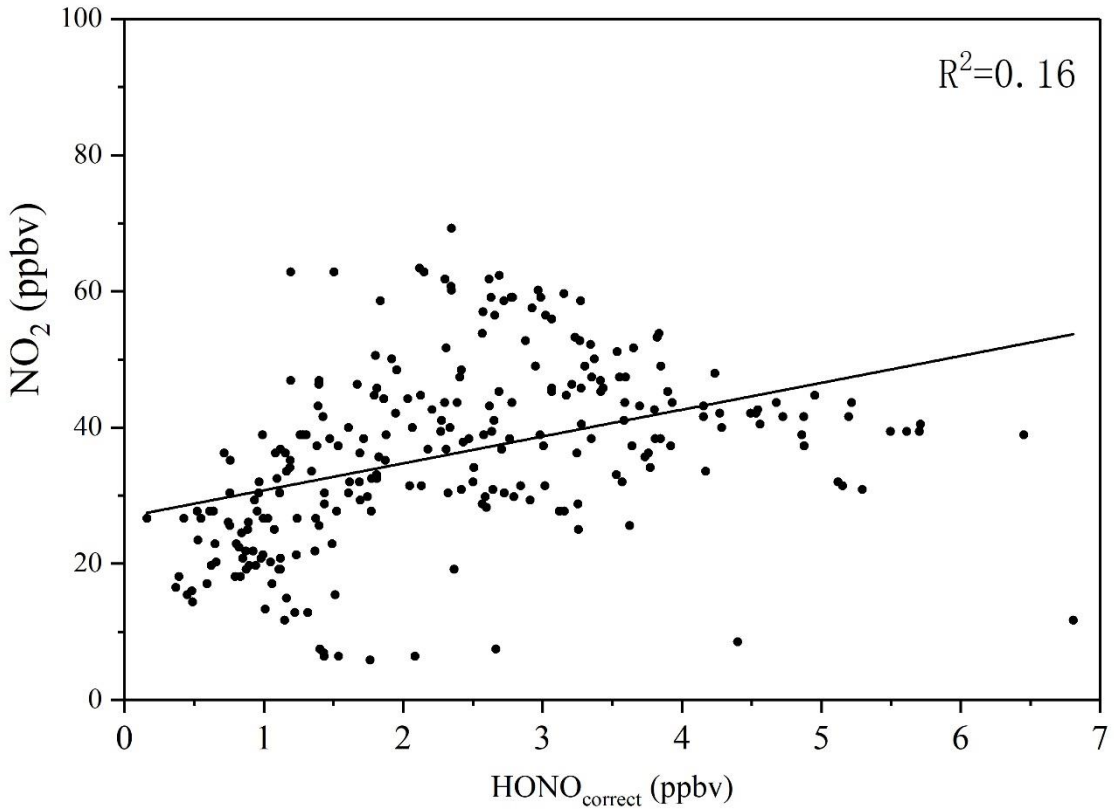

Fig. S1. The correlation study between $HONO_{correct}$ and NO_2 in the nighttime.

Table Captions:

Table S1. Measured species and performance of the instruments.

Table S2 The error bars of Fig. 4. (The units of all species except $HONO/NO_2$ and $HONO/NO_x$ are ppbv. The units of $HONO/NO_2$ and $HONO/NO_x$ are %.)

Table S3 The error bars of Fig. 5. (The units of all species except P_{OH+NO}^{net} are ppbv. The unit of P_{OH+NO}^{net} is ppbv/h.)

Table S4 The error bars of Fig. 8. (The units of all species except $HONO_{correct}/NO_2$ are ppbv. The unit of $HONO_{correct}/NO_2$ is %.)

Table S1. Measured species and performance of the instruments.

Species	Measurement technique	Detection limit	Accuracy
$PM_{2.5}$	Tapered Element Oscillating Microbalance	1.5 μg m^{-3}	± 5%
HONO	Ion Chromatography	4 pptv	± 20%
CO	Absorbs Infrared Radiation	40 ppbv	± 5%
NO	Chemiluminescence	60 pptv	± 20%
NO_2	Chemiluminescence	300 pptv	± 20%
O_3	UV Photometry	0.5 ppbv	± 5%

The results came from instrument manufacturers.

Table S2-1 The error bars of Fig. 4. (The units of all species except $HONO/NO_2$ and $HONO/NO_x$ are ppbv. The units of $HONO/NO_2$ and $HONO/NO_x$ are %.)

	Local Time (hh:mm)									
Species-period	00:00	01:00	02:00	03:00	04:00	05:00	06:00	07:00	08:00	09:00
HONO-CD	1.7 ± 1.3	1.4 ± 0.6	1.3 ± 0.4	1.2 ± 0.3	1.2 ± 0.2	1.2 ± 0.2	1.4 ± 0.3	1.5 ± 0.6	1.7 ± 0.9	1.6 ± 0.9
HONO-PD	3.2 ± 1.5	3.1 ± 1.3	3 ± 1.1	3.3 ± 1.2	3.5 ± 1.3	3.5 ± 1.2	3.6 ± 1.1	3.3 ± 0.9	3.7 ± 1.6	4.1 ± 2.8
HONO-SPD	3.7 ± 0.9	4 ± 0.8	4.2 ± 0.6	4.4 ± 0.8	4.6 ± 1	4.6 ± 1.2	4.6 ± 1.5	4.4 ± 1.3	4.4 ± 1.1	5.7 ± 3
NO-CD	14.3 ± 17	9 ± 9.7	8.5 ± 12.7	10.1 ± 22.4	10.6 ± 21.1	21.9 ± 29	27.8 ± 33	40.1 ± 51	52.6 ± 79	55.5 ± 84
NO-PD	57.3 ± 48	62.7 ± 55.9	49.6 ± 49	44 ± 47.8	47 ± 48.7	46.6 ± 30	41.4 ± 34	44.7 ± 33	48.9 ± 35	53.7 ± 44
NO-SPD	79.4 ± 103	100.1 ± 118	128.3 ±133	129 ± 134	111 ± 119	117 ± 95	100 ± 94	88.4 ± 85	82.3 ± 70	85.4 ± 71
NO_2-CD	25.4 ± 8.2	25.6 ± 9.9	24.7 ± 10.5	22.9 ± 10.4	24 ± 11.4	20.7 ± 11	20.2 ± 9	23.6 ± 11	28.6 ± 18	28.6 ± 18
NO_2-PD	41.1 ± 10	40.8 ± 11.2	39.7 ± 10.7	37.9 ± 7.1	36.6 ± 5.4	35.9 ± 5	33.8 ± 6	34.4 ± 6	33.2 ± 5	30.7 ± 6
NO_2-SPD	45.3 ± 9.5	43.5 ± 9.2	42.8 ± 8.8	42.1 ± 8.2	42.2 ± 8.1	41 ± 7.1	40.6 ± 6.9	40.7 ± 6	40.1 ± 6	39.2 ± 7
O_3-CD	14.2 ± 10	13.6 ± 10.4	14.2 ± 10.1	14.9 ± 9.4	13.6 ± 9.1	11.7 ± 10	13.8 ± 10	12.9 ± 9	11.6 ± 8	12.1 ± 7
O_3-PD	6.6 ± 6.1	6.4 ± 5.2	7.1 ± 5.2	6.3 ± 3.3	4.7 ± 2.2	5.3 ± 3	7.7 ± 6.9	5.3 ± 2.8	5.5 ± 3	7.1 ± 4
O_3-SPD	7.8 ± 6.4	7.7 ± 6.2	7.3 ± 5	6 ± 2.9	5.3 ± 2.3	5 ± 2.1	5.6 ± 2.5	5.2 ± 2.2	5.6 ± 2.6	6 ± 2.6
$HONO/NO_2$-CD	3.8 ± 1.5	4.4 ± 1	4.4 ± 1.1	4.9 ± 1	5.1 ± 0.8	8.3 ± 6	6.9 ± 2.1	6.2 ± 1.4	5.1 ± 0.8	4.3 ± 1.1
$HONO/NO_2$-PD	8 ± 3.6	7.8 ± 3.4	8 ± 3.3	9 ± 3.7	10 ± 4.5	10.1 ± 4	11.2 ± 4.6	10.3 ± 4	12.1 ± 7	14.3 ± 11
$HONO/NO_2$-SPD	8.3 ± 1.9	9.3 ± 1.4	10 ± 1.5	10.7 ± 1.9	11 ± 2.2	11.3 ± 3	11.5 ± 3.9	10.9 ± 3	11.1 ± 2	15 ± 8.3
$HONO/NO_x$-CD	2.7 ± 1.4	3.7 ± 1.5	4.2 ± 1.4	4.9 ± 1.1	4.9 ± 1	5.3 ± 2.5	5.1 ± 2.9	4.5 ± 2.4	3.6 ± 1.5	2.8 ± 1.4
$HONO/NO_x$-PD	4.4 ± 1.4	4.3 ± 1.7	4.6 ± 1.5	5.3 ± 1.3	5.3 ± 1	5.3 ± 1.1	6.6 ± 2.7	5.9 ± 2.3	6.5 ± 3.8	6.6 ± 4.3
$HONO/NO_x$-SPD	5.1 ± 2	5.3 ± 2.4	5.4 ± 3.4	5.8 ± 3.9	6.1 ± 3.9	5.7 ± 3.7	5.9 ± 3.6	5.7 ± 3	5.8 ± 2.9	6.7 ± 3.1

Table S2-2 The error bars of Fig. 4. (The units of all species except $HONO/NO_2$ and $HONO/NO_x$ are ppbv. The units of $HONO/NO_2$ and $HONO/NO_x$ are %.)

	Local Time (hh:mm)									
Species-period	10:00	11:00	12:00	13:00	14:00	15:00	16:00	17:00	18:00	19:00
HONO-CD	1.1 ± 0.6	0.6 ± 0.3	0.5 ± 0.3	0.6 ± 0.4	0.6 ± 0.5	0.7 ± 0.5	0.6 ± 0.5	0.7 ± 0.4	1 ± 0.5	1.2 ± 0.5
HONO-PD	2.9 ± 1.9	1.9 ± 1.3	1.3 ± 0.7	1 ± 0.3	0.9 ± 0.3	0.9 ± 0.3	0.9 ± 0.3	1.1 ± 0.4	1.4 ± 0.3	1.7 ± 0.3
HONO-SPD	6.9 ± 4.3	5.2 ± 3.8	3 ± 1.3	2.1 ± 0.7	1.8 ± 0.7	1.7 ± 0.6	1.8 ± 0.7	2 ± 0.5	2.7 ± 0.7	2.8 ± 0.8
NO-CD	43.9 ± 69.8	27.9 ± 40.8	14.9 ± 17.1	10.3 ± 7.8	7.3 ± 3	6 ± 4.5	6.4 ± 5.6	3.6 ± 3.4	2.6 ± 3.2	5.9 ± 7.7
NO-PD	49.3 ± 45.2	30 ± 26.2	21 ± 20.7	12.7 ± 14.7	9.4 ± 12.3	8.4 ± 9.5	5.7 ± 4.7	6.3 ± 6.8	9 ± 9	10 ± 10.3
NO-SPD	90.8 ± 73.4	79.3 ± 69.3	57.1 ± 52.3	34.8 ± 36.4	24.5 ± 28.7	19 ± 24.7	15 ± 18.8	11.8 ± 11	11.8 ± 7.9	22.4 ± 21
NO_2-CD	26.8 ± 15.7	22.7 ± 9.2	17.6 ± 7.1	17.1 ± 9	19.6 ± 9.6	21 ± 10.7	20.5 ± 9	21.4 ± 9	26 ± 12.5	30 ± 13.7
NO_2-PD	30 ± 6.9	28.8 ± 7.7	27.4 ± 9.6	24.8 ± 9.4	22.5 ± 10.6	25 ± 9.9	25.7 ± 9.3	27.1 ± 9	35 ± 8.7	36.2 ± 9.2
NO_2-SPD	39.8 ± 7.8	41.5 ± 8.3	42.3 ± 10.1	39.5 ± 12.6	38.5 ± 14.3	38 ± 14.7	38 ± 13.9	42 ± 15.4	45 ± 11.5	47 ± 10.8
O_3-CD	15.9 ± 8.8	19.5 ± 9.7	22.6 ± 8.3	25.5 ± 8.5	28.1 ± 9.1	29 ± 10.8	28 ± 10.8	29 ± 10.2	23.6 ± 10	17 ± 8.9
O_3-PD	9.6 ± 6.1	12.8 ± 6.2	18.7 ± 8.3	24.1 ± 8.4	28.2 ± 9.7	27 ± 10.8	28 ± 10.4	26 ± 10.5	17.4 ± 8.6	15 ± 11.6
O_3-SPD	6.3 ± 2.4	8.7 ± 4.5	12.8 ± 8.5	19.4 ± 12.9	24.1 ± 14.7	28 ± 16.6	29 ± 17.6	25 ± 16.1	17 ± 11.1	10.6 ± 9.7
$HONO/NO_2$-CD	4.1 ± 2.3	3.1 ± 1.9	3.3 ± 1.9	3.3 ± 1.3	3.1 ± 1.3	3.1 ± 1.3	2.9 ± 1.4	3.1 ± 1.4	3.9 ± 1.4	4.5 ± 2.2
$HONO/NO_2$-PD	9.4 ± 5.6	6.2 ± 3	4.7 ± 1.5	4.2 ± 1.2	4.7 ± 2.2	3.9 ± 0.7	3.7 ± 0.4	4.1 ± 1.2	4.3 ± 0.9	5 ± 1.5
$HONO/NO_2$-SPD	18.9 ± 13.7	13.7 ± 12	7.3 ± 3.5	5.6 ± 2.6	4.9 ± 2.1	4.8 ± 2.4	4.9 ± 1.6	5 ± 1	6.3 ± 1.8	6.2 ± 1.5
$HONO/NO_x$-CD	2.9 ± 2.1	2.2 ± 1.5	2.4 ± 1.5	2.5 ± 1.1	2.5 ± 1	2.6 ± 0.9	2.5 ± 0.9	2.8 ± 1	3.7 ± 1.1	4.1 ± 1.9
$HONO/NO_x$-PD	4.8 ± 2.4	3.8 ± 1.3	3.5 ± 1.2	3.5 ± 1.5	4 ± 2.1	3.4 ± 0.9	3.3 ± 0.5	3.7 ± 1.2	3.8 ± 0.7	4.3 ± 1.5
$HONO/NO_x$-SPD	8.2 ± 5.8	6.9 ± 5.7	4.3 ± 2	4 ± 2	3.8 ± 1.6	3.9 ± 1.9	4.3 ± 1.6	4.5 ± 1.2	5.5 ± 1.5	4.9 ± 1.3

Table S2-3 The error bars of Fig. 4. (The units of all species except $HONO/NO_2$ and $HONO/NO_x$ are ppbv. The units of $HONO/NO_2$ and $HONO/NO_x$ are %.)

	Local Time (hh:mm)			
Species-period	20:00	21:00	22:00	23:00
HONO-CD	1.3 ± 0.6	1.6 ± 0.9	2 ± 0.9	2.1 ± 0.9
HONO-PD	1.7 ± 0.7	1.8 ± 0.8	2 ± 0.9	2.1 ± 0.9
HONO-SPD	3.1 ± 0.9	3.2 ± 0.9	3.7 ± 0.8	4.6 ± 1.2
NO-CD	11.1 ± 16.9	14.5 ± 22.5	35.5 ± 68.9	50.8 ± 99.2
NO-PD	15 ± 14.1	15.3 ± 14.7	27.4 ± 28.5	33.9 ± 28.9
NO-SPD	29.4 ± 24.2	37.3 ± 26.6	38.5 ± 23.1	51.4 ± 31.4
NO_2-CD	31 ± 13.8	30.3 ± 14.5	31.6 ± 13.6	31 ± 14.3
NO_2-PD	37.3 ± 10.5	38.5 ± 13.9	38.3 ± 13.5	37.1 ± 13.2
NO_2-SPD	44.5 ± 11	43.5 ± 11.5	43.5 ± 11.1	42.1 ± 13.1
O_3-CD	13.3 ± 10.1	14 ± 11	12.2 ± 8.7	12.7 ± 8.8
O_3-PD	13.7 ± 10.3	10.9 ± 8.5	10.9 ± 7.7	12.2 ± 10.4
O_3-SPD	9.9 ± 8.6	10.8 ± 9.2	9.7 ± 8.7	9.6 ± 9.6
$HONO/NO_2$-CD	4.6 ± 2.2	5.7 ± 2.6	6.5 ± 2.6	6.8 ± 2.7
$HONO/NO_2$-PD	4.7 ± 1.9	4.6 ± 1.2	4.9 ± 0.8	5.3 ± 0.8
$HONO/NO_2$-SPD	7 ± 1.5	7.5 ± 1.4	8.9 ± 2.3	9.4 ± 2.4
$HONO/NO_x$-CD	4 ± 1.9	4.8 ± 2.2	4.9 ± 2.8	5 ± 3
$HONO/NO_x$-PD	3.9 ± 2.1	3.9 ± 1.3	3.8 ± 1	3.8 ± 0.9
$HONO/NO_x$-SPD	5.1 ± 1.5	5.2 ± 2	5.8 ± 2	5 ± 1.4

Table S3-1 The error bars of Fig. 5. (The units of all species except P_{OH+NO}^{net} are ppbv. The unit of P_{OH+NO}^{net} is ppbv/h.)

	Local Time (hh:mm)									
Species-period	19:00	20:00	21:00	22:00	23:00	00:00	01:00	02:00	03:00	04:00
P_{OH+NO}^{net}-CD	0.04 ± 0.06	0.08 ± 0.12	0.11 ± 0.17	0.33 ± 0.54	0.47 ± 0.79	0.12 ± 0.13	0.07 ± 0.08	0.03 ± 0.03	0.01 ± 0.1	0.02 ± 0.1
HONO-CD	1.18 ± 0.48	1.32 ± 0.62	1.62 ± 0.9	2.02 ± 0.94	2.09 ± 0.9	1.67 ± 1.34	1.43 ± 0.63	1.26 ± 0.44	1.2 ± 0.3	1.2 ± 0.22
NO-CD	5.4 ± 6.5	10.2 ± 14.4	13.3 ± 19.2	38.2 ± 62.2	54.9 ± 89.7	15 ± 14.8	8.8 ± 8.6	3.7 ± 4.2	1.5 ± 2.3	2.5 ± 2.6
P_{OH+NO}^{net}-HD	0.07 ± 0.07	0.1 ± 0.1	0.1 ± 0.1	0.19 ± 0.2	0.23 ± 0.2	0.4 ± 0.34	0.44 ± 0.4	0.34 ± 0.35	0.3 ± 0.34	0.3 ± 0.34
HONO-HD	1.7 ± 0.27	1.71 ± 0.68	1.82 ± 0.78	1.98 ± 0.89	2.06 ± 0.93	3.21 ± 1.54	3.05 ± 1.27	3.01 ± 1.08	3.3 ± 1.17	3.5 ± 1.34
NO-HD	8.5 ± 8.4	12.2 ± 11.5	12.5 ± 12	22.4 ± 23.3	27.7 ± 23.6	46.8 ± 39.5	51.2 ± 45.6	40.5 ± 40	35.9 ± 39	38 ± 39.7
P_{OH+NO}^{net}-SHD	0.15 ± 0.15	0.2 ± 0.17	0.25 ± 0.18	0.26 ± 0.16	0.35 ± 0.23	0.55 ± 0.75	0.7 ± 0.85	0.9 ± 0.96	0.9 ± 1.0	0.8 ± 0.86
HONO-SHD	2.8 ± 0.8	3.1 ± 0.9	3.2 ± 0.9	3.7 ± 0.8	4.6 ± 1.2	3.7 ± 0.9	4 ± 0.8	4.2 ± 0.6	4.4 ± 0.8	4.6 ± 1
NO-SHD	18 ± 17	24 ± 20	30 ± 21	31 ± 19	42 ± 25	64 ± 84	81 ± 96	104 ± 108	105 ± 110	90 ± 97

Table S3-2 The error bars of Fig. 5. (The units of all species except P_{OH+NO}^{net} are ppbv. The unit of P_{OH+NO}^{net} is ppbv/h.)

	Local Time (hh:mm)	
Species-period	05:00	06:00
P_{OH+NO}^{net}-CD	0.12 ± 0.18	0.17 ± 0.22
HONO-CD	1.25 ± 0.21	1.36 ± 0.35
NO-CD	13.7 ± 20.9	19.5 ± 25.1
P_{OH+NO}^{net}-HD	0.32 ± 0.22	0.28 ± 0.25
HONO-HD	3.5 ± 1.16	3.56 ± 1.09
NO-HD	38 ± 25.2	33.8 ± 28.5
P_{OH+NO}^{net}-SHD	0.82 ± 0.87	0.7 ± 0.68
HONO-SHD	4.6 ± 1.2	4.6 ± 1.5
NO-SHD	95.6 ± 99	81.8 ± 77.1

Table S4-1 The error bars of Fig. 8. (The units of all species except $HONO_{correct}/NO_2$ are ppbv. The unit of $HONO_{correct}/NO_2$ is %.)

	Local Time (hh:mm)									
Species-period	19:00	20:00	21:00	22:00	23:00	00:00	01:00	02:00	03:00	04:00
$HONO_{correct}$-CD	1.0 ± 0.4	1.1 ± 0.6	1.4 ± 0.8	1.6 ± 0.7	1.6 ± 0.6	1.4 ± 1.4	1.2 ± 0.7	1.1 ± 0.5	1.1 ± 0.4	1.1 ± 0.2
NO_2-CD	30 ± 15	31 ± 15	30 ± 15	34 ± 15	34 ± 15	25 ± 9	24 ± 8	22 ± 8	20 ± 8	20 ± 8
$HONO_{correct}/NO_2$-CD	3.7 ± 2.2	3.9 ± 2.2	4.9 ± 2.6	5.5 ± 2.7	5.7 ± 2.9	11 ± 18.2	8.9 ± 12	8.6 ± 10.8	8.5 ± 9.7	7.7 ± 7.4
$HONO_{correct}$-HD	1.4 ± 0.3	1.4 ± 0.7	1.5 ± 0.7	1.6 ± 0.8	1.7 ± 0.8	2.7 ± 1.3	2.5 ± 1	2.5 ± 0.8	2.9 ± 0.9	3.1 ± 1.1
NO2-HD	36 ± 9	37 ± 10	39 ± 14	38 ± 13	37 ± 13	41 ± 10	41 ± 11	40 ± 11	38 ± 7	37 ± 5
$HONO_{correct}/NO_2$-HD	4.2 ± 1.5	3.8 ± 2	3.8 ± 1.2	4 ± 0.8	4.4 ± 0.7	6.7 ± 3.1	6.5 ± 2.8	6.7 ± 2.8	7.8 ± 3.1	8.7 ± 3.8
$HONO_{correct}$-SHD	2.4 ± 0.6	2.6 ± 0.7	2.7 ± 0.7	3.2 ± 0.7	4.1 ± 1.3	3.1 ± 0.8	3.3 ± 0.6	3.4 ± 0.7	3.6 ± 1	3.9 ± 1.1
NO_2-SHD	47 ± 11	44 ± 11	43 ± 11	44 ± 11	42 ± 13	45 ± 9	43 ± 9	43 ± 9	42 ± 8	42 ± 8
$HONO_{correct}/NO_2$-SHD	5.4 ± 1.4	6.1 ± 1.4	6.5 ± 1.4	7.8 ± 2.2	14.4 ± 16.7	7 ± 1.9	7.8 ± 1.6	8.1 ± 2.2	8.8 ± 2.8	9.3 ± 2.9

Table S4-2 The error bars of Fig. 8. (The units of all species except $HONO_{correct}/NO_2$ are ppbv. The unit of $HONO_{correct}/NO_2$ is %.)

	Local Time (hh:mm)	
Species-period	05:00	06:00
$HONO_{correct}$-CD	1.0 ± 0.4	1.1 ± 0.6
NO_2-CD	30 ± 15	31 ± 15
$HONO_{correct}/NO_2$-CD	3.7 ± 2.2	3.9 ± 2.2
$HONO_{correct}$-HD	1.4 ± 0.3	1.4 ± 0.7
NO_2-HD	36 ± 9	37 ± 10
$HONO_{correct}/NO_2$-HD	4.2 ± 1.5	3.8 ± 2
$HONO_{correct}$-SHD	2.4 ± 0.6	2.6 ± 0.7
NO_2-SHD	47 ± 11	44 ± 11
$HONO_{correct}/NO_2$-SHD	5.4 ± 1.4	6.1 ± 1.4

Reference

An, J., Li, Y., Chen, Y., Li, J., Qu, Y., and Tang, Y.: Enhancements of major aerosol components due to additional HONO sources in the North China Plain and implications for visibility and haze, Adv. Atoms. Sci., 30, 57-66, https://doi.org/10.1007/s00376-012-2016-9, 2012.

Atkinson, R., Baulch, D. L., Cox, R. A., Crowley, J. N., Hampson, R. F., Hynes, R. G., Jenkin, M. E., Rossi, M. J., and Troe, J.: Evaluated kinetic and photochemical data for atmospheric chemistry: Volume I - gas phase reactions of O_x, HO_x, NO_x and SO_x species, Atmos. Chem. Phys., 4, 1461-1738, https://doi.org/10.5194/acp-4-1461-2004, 2004.

Cui, L., Li, R., Zhang, Y., Meng, Y., Fu, H., and Chen, J.: An observational study of nitrous acid (HONO) in Shanghai, China: The aerosol impact on HONO formation during the haze episodes, Sci. Total Environ., 630, 1057-1070, https://doi.org/10.1016/j.scitotenv.2018.02.063, 2018.

Finlayson-Pitts, B. J., Wingen, L. M., Sumner, A. L., Syomin, D., and Ramazan, K. A.: The heterogeneous hydrolysis of NO2 in laboratory systems and in outdoor and indoor atmospheres: An integrated mechanism, PCCP, 5, 223-242, https://doi.org/10.1039/b208564j, 2003.

Hou, S., Tong, S., Ge, M., and An, J.: Comparison of atmospheric nitrous acid during severe haze and clean periods in Beijing, China, Atmos. Environ., 124, 199-206, https://doi.org/10.1016/j.atmosenv.2015.06.023, 2016.

Huang, R. J., Yang, L., Cao, J., Wang, Q., Tie, X., Ho, K. F., Shen, Z., Zhang, R., Li, G., Zhu, C., Zhang, N., Dai, W., Zhou, J., Liu, S., Chen, Y., Chen, J., and O'Dowd, C. D.: Concentration and sources of atmospheric nitrous acid (HONO) at an urban site in Western China, Sci. Total Environ., 593-594, 165-172, https://doi.org/10.1016/j.scitotenv.2017.02.166, 2017.

Jiang, N., Dong, Z., Xu, Y., Yu, F., Yin, S., Zhang, R., and Tang, X.: Characterization of PM_{10} and $PM_{2.5}$ Source Profiles of Fugitive Dust in Zhengzhou, China, Aerosol Air Qual. Res., 18, 314-329, https://doi.org/10.4209/aaqr.2017.04.0132, 2018a.

Jiang, N., Wang, K., Yu, X., Su, F., Yin, S., Li, Q., and Zhang, R.: Chemical characteristics and source apportionment by two receptor models of size-segregated aerosols in an emerging megacity in China, Aerosol Air Qual. Res., 18, 1375–1390, https://doi.org/10.4209/aaqr.2017.10.0413, 2018b.

Jiang, N., Liu, X., Wang, S., Yu, X., Yin, S., Duan, S., Shenbo, W., Zhang, R., and Li, S.: Pollution characterization, source identification, and health risks of atmospheric-particle-bound heavy metals in PM_{10} and $PM_{2.5}$ at multiple sites in an emerging megacity in the Central Region of China, Aerosol Air Qual. Res., 19, 247-271, https://doi.org/10.4209/aaqr.2018.07.0275, 2019.

Kim, D.-R., Lee, J.-B., Keun Song, C., Kim, S.-Y., Ma, Y.-l., Lee, K.-M., Cha, J.-S., and Lee, S.-D.: Temporal and spatial distribution of tropospheric NO_2 over Northeast Asia using OMI data during the years 2005–2010, Atmos. Pollut. Res.,

6, 768-776, https://doi.org/10.5094/apr.2015.085, 2015.
Kleffmann, J., Becker, K. H., Lackhoff, M., and Wiesen, P.: Heterogeneous conversion of NO2 on carbonaceous surfaces, PCCP, 1, 5443-5450, https://doi.org/10.1039/a905545b, 1999.
Kurtenbach, R., Becker, K. H., Gomes, J. A. G., Kleffmann, J., Lorzer, J. C., Spittler, M., Wiesen, P., Ackermann, R., Geyer, A., and Platt, U.: Investigations of emissions and heterogeneous formation of HONO in a road traffic tunnel, Atmos. Environ., 35, 3385-3394, https://doi.org/10.1016/s1352-2310(01)00138-8, 2001.
Lelieveld, J., Gromov, S., Pozzer, A., and Taraborrelli, D.: Global tropospheric hydroxyl distribution, budget and reactivity, Atmos. Chem. Phys., 16, 12477-12493, https://doi.org/10.5194/acp-16-12477-2016, 2016.
Li, Q., Jiang, N., Yu, X., Dong, Z., Duan, S., Zhang, L., and Zhang, R.: Sources and spatial distribution of PM2.5-bound polycyclic aromatic hydrocarbons in Zhengzhou in 2016, Atmos. Res., 216, 65–75, https://doi.org/10.1016/j.atmosres.2018.09.011, 2019.
Li, X., Brauers, T., Häseler, R., Bohn, B., Fuchs, H., Hofzumahaus, A., Holland, F., Lou, S., Lu, K. D., Rohrer, F., Hu, M., Zeng, L. M., Zhang, Y. H., Garland, R. M., Su, H., Nowak, A., Wiedensohler, A., Takegawa, N., Shao, M., and Wahner, A.: Exploring the atmospheric chemistry of nitrous acid (HONO) at a rural site in Southern China, Atmos. Chem. Phys., 12, 1497-1513, https://doi.org/10.5194/acp-12-1497-2012, 2012.
Liu, F., Beirle, S., Zhang, Q., van der, A. R., Zheng, B., Tong, D., and He, K.: NOx emission trends over Chinese cities estimated from OMI observations during 2005 to 2015, Atmos Chem Phys, 17, 9261-9275, https://doi.org/10.5194/acp-17-9261-2017, 2017.
Liu, X., Jiang, N., Yu, X., Zhang, R., Li, S., Li, Q., and Kang, P.: Chemical characteristics, sources apportionment, and risk assessment of PM2.5 in different functional areas of an emerging megacity in China, Aerosol Air Qual. Res., 19, 2222-2238, https://doi.org/10.4209/aaqr.2019.02.0076, 2019.
Liu, Z., Wang, Y., Costabile, F., Amoroso, A., Zhao, C., Huey, L. G., Stickel, R., Liao, J., and Zhu, T.: Evidence of aerosols as a media for rapid daytime HONO production over China, Environ. Sci. Technol., 48, 14386-14391, https://doi.org/10.1021/es504163z, 2014.
Lu, X., Wang, Y., Li, J., Shen, L., and Fung, J. C. H.: Evidence of heterogeneous HONO formation from aerosols and the regional photochemical impact of this HONO source, Environ. Res. Lett., 13, https://doi.org/10.1088/1748-9326/aae492, 2018.
Nie, W., Ding, A. J., Xie, Y. N., Xu, Z., Mao, H., Kerminen, V. M., Zheng, L. F., Qi, X. M., Huang, X., Yang, X. Q., Sun, J. N., Herrmann, E., Petäjä, T., Kulmala, M., and Fu, C. B.: Influence of biomass burning plumes on HONO chemistry in eastern China, Atmos. Chem. Phys., 15, 1147-1159, https://doi.org/10.5194/acp-

15-1147-2015, 2015.

Sander, S., Friedl, R., Golden, D., Kurylo, M., Huie, R., Orkin, V., Moortgat, G., Ravishankara, A. R., Kolb, C., Molina, M., and Finlayson-Pitts, B.: Chemical Kinetics and Photochemical Data for Use in Atmospheric Studies; JPL Publication 02-25, 2003.

Shen, L. J., and Zhang, Z. F.: Heterogeneous reactions of NO_2 on the surface of black carbon, Prog. Chem., 25, 28-35, 2013.

Su, H., Cheng, Y. F., Cheng, P., Zhang, Y. H., Dong, S., Zeng, L. M., Wang, X., Slanina, J., Shao, M., and Wiedensohler, A.: Observation of nighttime nitrous acid (HONO) formation at a non-urban site during PRIDE-PRD2004 in China, Atmos. Environ., 42, 6219-6232, https://doi.org/10.1016/j.atmosenv.2008.04.006, 2008.

Tan, Z., Rohrer, F., Lu, K., Ma, X., Bohn, B., Broch, S., Dong, H., Fuchs, H., Gkatzelis, G. I., Hofzumahaus, A., Holland, F., Li, X., Liu, Y., Liu, Y., Novelli, A., Shao, M., Wang, H., Wu, Y., Zeng, L., Hu, M., Kiendler-Scharr, A., Wahner, A., and Zhang, Y.: Wintertime photochemistry in Beijing: observations of RO_x radical concentrations in the North China Plain during the BEST-ONE campaign, Atmos. Chem. Phys., 18, 12391-12411, https://doi.org/10.5194/acp-18-12391-2018, 2018.

Tong, S., Hou, S., Zhang, Y., Chu, B., Liu, Y., He, H., Zhao, P., and Ge, M.: Comparisons of measured nitrous acid (HONO) concentrations in a pollution period at urban and suburban Beijing, in autumn of 2014, Sci. China Chem., 58, 1393-1402, https://doi.org/10.1007/s11426-015-5454-2, 2015.

Tong, S., Hou, S., Zhang, Y., Chu, B., Liu, Y., He, H., Zhao, P., and Ge, M.: Exploring the nitrous acid (HONO) formation mechanism in winter Beijing: direct emissions and heterogeneous production in urban and suburban areas, Faraday Discuss., 189, 213-230, https://doi.org/10.1039/c5fd00163c, 2016.

VandenBoer, T. C., Markovic, M. Z., Sanders, J. E., Ren, X., Pusede, S. E., Browne, E. C., Cohen, R. C., Zhang, L., Thomas, J., Brune, W. H., and Murphy, J. G.: Evidence for a nitrous acid (HONO) reservoir at the ground surface in Bakersfield, CA, during CalNex 2010, J. Geophys. Res.-Atmos., 119, 9093-9106, https://doi.org/10.1002/2013jd020971, 2014.

Zhang, B., and Tao, F.-M.: Direct homogeneous nucleation of NO2, H2O, and NH3 for the production of ammonium nitrate particles and HONO gas, Chem. Phys. Lett., 489, 143-147, https://doi.org/10.1016/j.cplett.2010.02.059, 2010.

Zhang, W., Tong, S., Ge, M., An, J., Shi, Z., Hou, S., Xia, K., Qu, Y., Zhang, H., Chu, B., Sun, Y., and He, H.: Variations and sources of nitrous acid (HONO) during a severe pollution episode in Beijing in winter 2016, Sci. Total Environ., 648, 253-262, https://doi.org/10.1016/j.scitotenv.2018.08.133, 2019.

Itemized Response to Anonymous Referee #2's Comments

Ms. Ref. No.: acp-2019-916

Title: Characteristics, sources, and reactions of nitrous acid during winter at an urban site in the Central Plains Economic Region in China

Response to Anonymous Referee #2:

We have carefully addressed your comments on our manuscript and made necessary revisions of the previous manuscript. We sincerely thank you for valuable and constructive inputs. We believe that we have adequately addressed all of your comments and thus the current version has been greatly improved with those valuable comments and further English editing. The revised phrases/sentences/paragraphs are shown in the line number of the revised text.

The followings are our itemized replies to your comments.

Main comments:

1) The description of HONO measurements is too brief and insufficient while all the study rely on it. A detailed and self-sufficient description of the measurement technique for HONO is therefore needed even if it has been described in another study. Estimation of instrumental uncertainties are also lacking.

Furthermore, description of the measurement techniques used for ancillary species should also be given (at least the measurement principle and not only the model and brand of the analyzers).

On the contrary Fig. S1 and S2 does not bring valuable information and should be completed to describe more precisely the measurement principle or should be removed.

Response: Thank you for your comment. A detailed description of this inlet design and the performance characteristics of the AIM system can be found in Markovic et al. (2012). HONO was hygroscopically grown in the parallel plate denuder and collected as an aqueous solution in a cyclone assembly. The aqueous sample

aliquots from both channels were transported to the ion chromatographic systems housed inside a ground container for hourly semicontinuous online analysis of HONO. The ion chromatographic system was calibrated for NO_2^- using mixed anion standard solutions of NO_2^-, which was concentrated and analyzed as described by Markovic et al. (2012).

So, we have modified the sentence in the revised text.

L 176-179: This measurement method and its details have been successfully evaluated in many field studies (Markovic et al., 2012; Tian et al., 2018; Wang et al., 2019), and shown in the supplement.

In the supplement, we have added, this part in the supplement.

1. This AIM method and its details.

HONO was hygroscopically grown in the parallel plate denuder and collected as an aqueous solution in a cyclone assembly. The aqueous sample aliquots from both channels were transported to the ion chromatographic systems housed inside a ground container for hourly semicontinuous online analysis of HONO. The ion chromatographic system was calibrated for NO_2^- using mixed anion standard solutions of NO_2^-.

The description of the measurement techniques and instrumental uncertainties was shown in **Table S1.**

Table S1. Measured species and performance of the instruments.

Species	Measurement technique	Detection limit	Accuracy
$PM_{2.5}$	Tapered Element Oscillating Microbalance	1.5 μg m^{-3}	± 5%
HONO	Ion Chromatography	4 pptv	± 20%
CO	Absorbs Infrared Radiation	40 ppbv	± 5%
NO	Chemiluminescence	60 pptv	± 20%
NO_2	Chemiluminescence	300 pptv	± 20%
O_3	UV photometry	0.5 ppbv	± 5%

The results came from instrument manufacturers.

At last, Fig. S1 and S2 have been removed.

2) P10, line 253: 1.0x10$_6$ molecules cm$_{-3}$ is very high for nighttime concentrations of OH especially in January. Lelieveld et al. (2016) report nocturnal concentrations of OH between 1.5x10$_4$ and 3x10$_4$ molecules cm$_{-3}$ for January in the region concerned by the present study and not 1.0x10$_6$ molecules cm$_{-3}$ as stated by the authors. Tan et al. (2018) also found nighttime OH concentrations below 1x10$_5$ in Beijing during winter (February).

Response: Thank you. Your comment is critical and important. We revisit and determine the OH concentration. You are right. 2.5×10^5 cm^3 $molecule^{-1}$ is very high for nighttime concentrations of OH, especially in January.

And, nighttime OH concentration increased as the latitude decreases ranged 3 to 6×10^5 cm^3 $molecule^{-1}$ (Lelieveld et al., 2016) (On the first figure) by the general circulation model EMAC (ECHAM/MESSy Atmospheric Chemistry).

Tan et al. (2018) found that by the field measurement, the average concentration of ·OH in Beijing at nighttime was about 2.5×10^5 cm^3 $molecule^{-1}$ (On the second figure). There is no specific concentration of ·OH at nighttime in winter in the study (Tan et al., 2018).

Moreover, the same ·OH concentration (2.5×10^5 cm^3 $molecule^{-1}$) was also used to calculate the homogeneous reaction of HONO in the recent research (Zhang et al., 2019). And, nighttime OH concentration increased as the latitude decreases ranged 3 to 6×10^5 molecule cm^{-3} (Lelieveld et al., 2016). Zhengzhou has a lower latitude than Beijing, so the concentration of OH used in this study is 2.5×10^5 cm^3 $molecule^{-1}$.

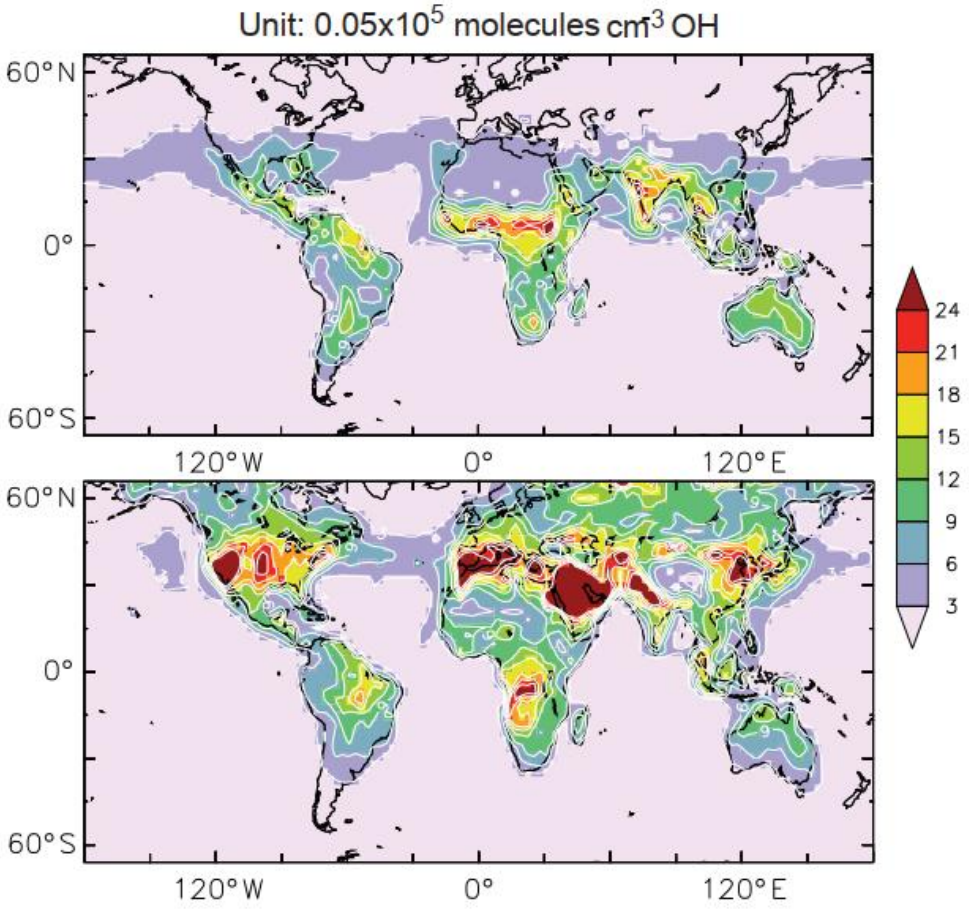

Figure 2. Nighttime OH in the boundary layer in January (top) and July (bottom). Color coding is the same as Fig. 1, but concentrations are scaled by a factor of 20 ($\times 0.05 \times 10^5$ molecules cm^{-3}).

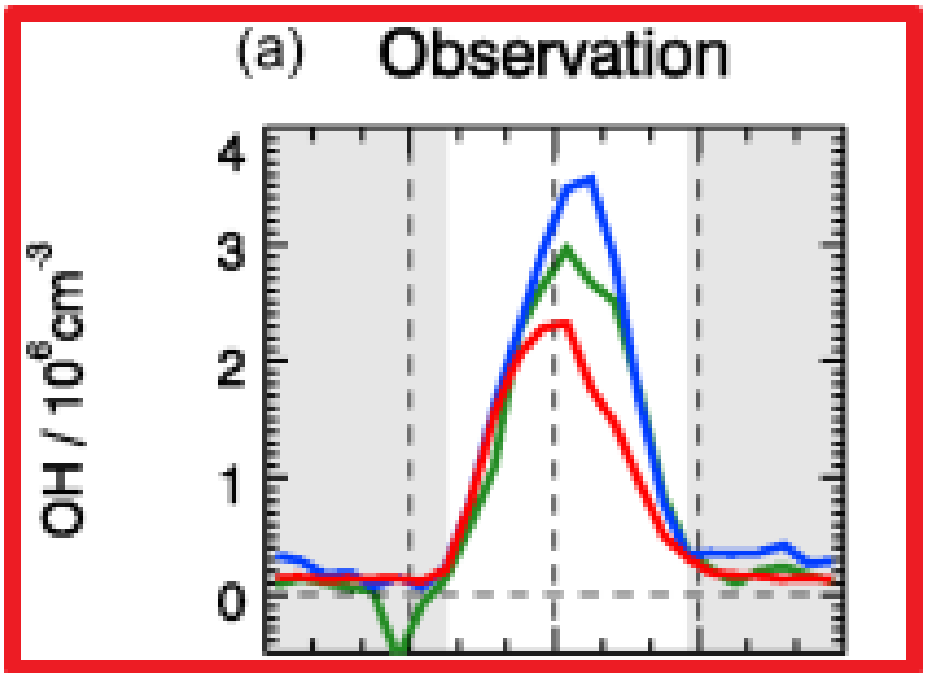

Figure 7. Mean diurnal profiles of observed **(a)** and modeled **(b)** OH, HO_2, RO_2, and k_{OH} for three different chemical and meteorological conditions. The categories for background, clean, and polluted episodes are the same as in Table 2, and similar to those applied to Figs. 9 and 12. The grey areas denote nighttime.

So, we have modified the sentences in the revised text.

L 281-288: Therefore, Tan et al. (2018) found that by the field measurement, the average concentration of ·OH in Beijing at nighttime was about 2.5×10^5 molecule cm^{-3}. Moreover, the same ·OH was also used to calculate the homogeneous reaction of HONO in the recent research (Zhang et al., 2019). And, nighttime OH concentration increased as the latitude decreases ranged 3 to 6×10^5 molecule cm^{-3} (Lelieveld et al., 2016). Zhengzhou has a lower latitude than Beijing, so the concentration of OH used in this study is 2.5×10^5 molecule cm^{-3}.

The calculation of $P_{netOH+NO}$ should therefore be corrected using a more realistic OH concentrations. This may change the quantitative and relative contribution of homogeneous reaction to accumulated HONO formation at night. In this case, discussion and conclusion of the article on this point should also be revised consequently.

The calculation of P^{net}_{OH+NO} has therefore been corrected using the OH concentration (2.5×10^5 cm^3 $molecule^{-1}$). We have modified the sentence in the revised text.

L 293-295: The mean value of P^{net}_{OH+NO} was 0.33 ppbv h^{-1}, and the specific values in CD, PD, and SPD periods were 0.13, 0.26, and 0.56 ppbv h^{-1}, respectively.

Finally, the discussion and conclusion of the article on this point were also revised consequently.

L 316-318: …Second, the hourly rate of HONO abatement pathways, except OH + HONO, should be at least 0.22 ppbv h^{-1} (i.e., 3.36 – 1.59 ppbv)/8 h)…

L 549-550: The mean value of P_{OH+NO}^{net} in the CD, PD, and SPD periods were 0.13, 0.26, and 0.56 ppbv h^{-1}, respectively.

3) A restructuration of section 3.3 is needed. Indeed all the paragraphs between the beginning of this section and the introductive paragraph for equations 4 to 6 (i.e. from P15, line 402 to P16, line 432) should be moved after these equations (i.e. eq. 4 to 6). Indeed, these paragraphs described the different terms used in the equation 4, 5 and 6 while they do not have been presented yet and this make the reading of this section very confusing.

Response: Sorry for my confusion. The equations 4 to 6 have been moved before all the paragraphs. We have modified the sentences in the revised text.

L 454-465: The expression of d HONO / d t represents the observed variations of hourly HONO concentrations, for which we can use Δ HONO/Δ d t instead:

$$\text{d HONO / d t} = \text{sources} - \text{sinks}$$

$$= (P_{unknown} + P_{OH+NO} + P_{emi} + P_{het}) - (L_{OH+HONO} + L_{photo}) \quad (4),$$

$$P_{OH+NO} = k_{OH+NO}\,[OH]\,[NO] \quad (5),$$

$$L_{OH+HONO} = k_{OH+HONO}\,[OH]\,[HONO] \quad (6).$$

The d HONO / d t calculated from the measurements was small and evenly distributed around zero (Li et al., 2012). $P_{unknown}$ is the production rate by an unknown daytime HONO source. P_{OH+NO} is the rate of reaction of NO and OH. P_{emi} represents the direct emission rate of HONO from combustion processes. By studying the source and reduction, the daytime HONO budget was analyzed with Eq. (4) (Su et al., 2008).

4) P15, lines 403-404: "$P_{unknown}$ is the production rate by an unknown daytime HONO source". Please explain how $P_{unknown}$ is calculated. Do you assume that dHONO/dt is

equal to zero to do so? If it is the case, it should be indicated somewhere.

P17, lines 459-460: “However, further research is needed to analyze the unknown sources of daytime HONO”. Why didn’t you do it in this study? A deeper analysis of the processes that may be responsible for the observed unknown HONO production would have been valuable in this study. This further analysis is missing to strengthen the interest of this study for publication.

Response: Sorry for my careless. $P_{unknown}$ is calculated by:

$d\,HONO / d\,t = (P_{unknown} + P_{OH+NO} + P_{emi} + P_{het}) - (L_{OH+HONO} + L_{photo})$;

$P_{unknown} = L_{OH+HONO} + L_{photo} - P_{OH+NO} - P_{emi} - P_{het}$.

The sentence has been added in the revised text.

L 460-461: The $d\,HONO / d\,t$ calculated from the measurements was small and evenly distributed around zero (Li et al., 2012).

We have studied the correlation between the unknown source of HONO and the $PM_{2.5}$ mass concentrations was lower. So, we can not probably use the $P_{unknown}$ calculated to perform this correlation for explaining the unknown source. The unknown sources of HONO may include the NO_2 photolysis of sooty surface and adsorbed nitric acid and nitrate at UV wavelengths (Kleffmann et al., 1999). The homogeneous nucleation of NO_2, H_2O, and NH_3 is the HONO formation pathway (Zhang and Tao, 2010). In the meanwhile, HONO can deposit and react with amines in forming nitrosamines (Li et al., 2012) for sinking.

This further analysis and method are not found yet.

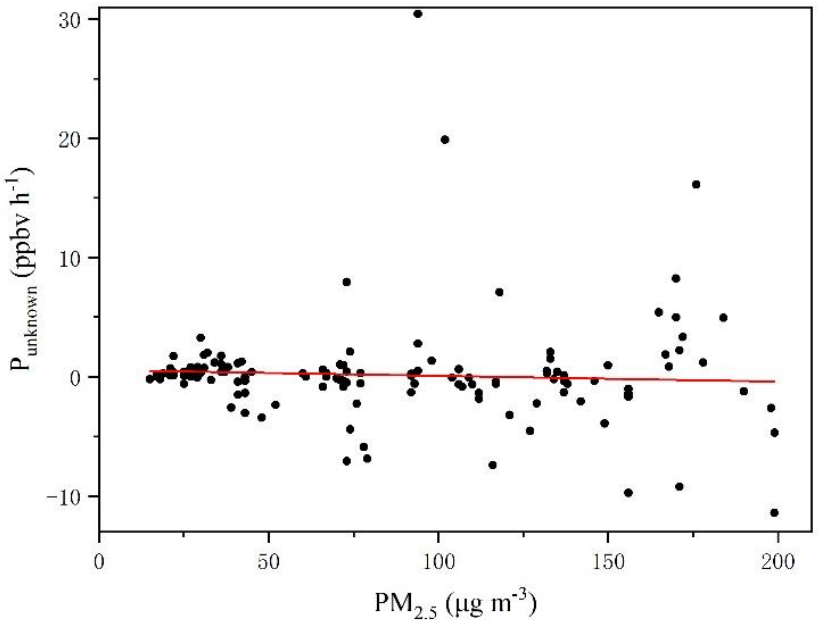

Figure The correlation between $PM_{2.5}$ and $P_{unknown}$.

Minor comments:

1. -P1, line 22: Change "(i.e., the concentration of NO…" for "(i.e., when the concentration of NO…".

Response: OK. We have added the word, "When", in the revised text.

L 21-23: …under high-NO_X conditions (i.e., when the concentration of NO was higher than…

2. -P2, line 32: Change "The hourly abatement level of HONO abatement" for "The hourly level of HONO abatement".

Response: Thank you. We have removed the word, "abatement", in the revised text.

L 32-33: The hourly level of HONO abatement pathways, except for…

3. -P2, line 46: Change “OH radical is also an important oxidant” for “OH radical is an important oxidant”.

Response: OK. We have removed the word, “also”, in the revised text.

L 48-49:·OH is an important oxidant in the atmosphere, and it can react with organic substances…

4. -P2, lines 49-50: “Therefore, reaction changes during pollution can be observed by studying the formation mechanism of HONO”. This sentence is not clear to me. Please clarify it or remove it.

Response: Sorry for the confusion. We explored the sources and characteristics of HONO at different pollution levels, as well as the reaction mechanism. We have not explained the reaction mechanism and pathways, so we have changed “reaction” for “the changes in the contribution of the homogeneous reaction, heterogeneous conversion, and direct emission”. This sentence has been changed in the revised text.

L 51-54: Therefore, the changes in the contribution of the homogeneous reaction, heterogeneous conversion, and direct emission during pollution can be observed by studying the formation mechanism of HONO.

5. -P2, lines 53-54: “Nitro-Mac” is the name of the instrument but it does not described the technique of measurement. Please replace it by “wet chemical derivatization technique-HPLC/UV-VIS detection”.

Response: Thank you for your comment. We have changed “Nitro-Mac” for “wet chemical derivatization technique-HPLC/UV-VIS detection”. We have modified the sentence in the revised text.

L 58-69: …wet chemical derivatization technique-HPLC/UV-VIS detection…

6. -P3, line 55: The description of instruments existing for HONO measurements is not exhaustive. Important techniques such as IBBCEAS (e.g. Min et al., 2016; Duan et al., 2018) or CIMS (e.g. Hirokawa et al., 2009 ; Roberts et al., 2010) are missing. Please add them to your list.

Response: Sorry for my carelessness. We have analyzed and explored these techniques, and the important techniques have been added in the same sentence in the revised text.

L 55-62: Several instruments have been used to determine ambient HONO concentrations, and these include differential optical absorption spectrophotometer (DOAS) (Elshorbany et al., 2012; Winer and Biermann, 1994), long path absorption photometer (LOPAP) (Heland et al., 2001), wet chemical derivatization technique-HPLC/UV-VIS detection (Michoud et al., 2014), stripping coil-UV/Vis absorption photometer (SC-AP) (Pinto et al., 2014), IBBCEAS (Duan et al., 2018; Min et al., 2016), CIMS (Hirokawa et al., 2009; Roberts et al., 2010), and ambient ion monitor (AIM) (VandenBoer et al., 2014).

7. -P3, line 72: Change “be absorbed by” for “react with”.

Response: OK. We have modified the sentence in the revised text.

L 76-77: …HONO can react with the ·OH…

8. -P5, lines 137-138: “The site is close to the West Fourth Ring Road”. How far is it? Please be more precise.

Response: Sorry for my carelessness. We will be more precise in the full text and

examine the logic problems. The sentence has been changed in the revised text.

L 160-162: The site is about 500 m from the western Fourth-Ring Expressway of Zhengzhou City and about 2 km from Lian Huo Expressway to the north.

9. -P6, line 142: “High-Time-resolution instrument”. A temporal resolution of 1h is not what is usually called high time resolution. Please change the title of this section.

Response: OK， we have changed “High-Time-resolution instrument” for “Instruments”. And, the title has been modified, “Characteristics, sources, and reactions of nitrous acid during winter at an urban site in the Central Plains Economic Region in China”, in the revised text.

10. -P6, line 153: Change “(e.g., O and N)” for “(e.g., O2 and N2)”

Response: Sorry for my carelessness. The sentence has been modified in the revised text.

L 74: …several gases (e.g., O_2 and N_2) were expelled…

11. -P7, lines 166-168: “The instrument parts and consumables should be changed regularly during the observation process, and the sampling flow should be calibrated to reduce the negative effect of accessories on sampling”.

Could you be more specific? How often these maintenances have been made during the measurement period? What consumables exactly have been changed?

How is it compatible with the frequency of replacement given here and the frequency of calibration? Please clarify.

Response: OK. This is my omission. During the measurement, we have replaced the filter once a week and ensured enough hydrogen peroxide for absorbing

HONO by the denuder. The instrument parts and consumables should be changed before the observation process, and the sampling flow should be calibrated to reduce the negative effect of accessories. The sentence has been modified in the revised text.

L 189-191: The instrument parts and consumables should be changed before the observation process, and the sampling flow should be calibrated to reduce the negative effect of accessories.

And we have added the sentence in the revised text.

L 185-187: Before this measurement period, the membrane of the denuder has been replaced and standard anion and cation solutions have been prepared on Jan. 3rd.

The standard curve has been drawn to ensure the appropriateness of the correlation coefficient (≥ 0.999) and the accuracy of the sample retention time and response value. There is no need to stop the instrument during the replacement of the parts, and the calibration has been completed before the measurement period. The calibration can be used for one to two months at a time.

12. -P7, line 192: Wind direction is not presented in table 2. Please remove it from the list of parameters presented in table 2.

Response: Sorry. We have modified the table heading in the revised text.

Table 1 Data statistics of HONO, $PM_{2.5}$, NO_2, NO, NO_X, HONO/NO_2, HONO/NO_X, O_3, CO, T, RH, and WS during the measurement period, mean value ± standard deviation.

13. -P8, line 217: Change “Fig. S3” for “Fig. 3”.

The comparison of diurnal variation of HONO during the three period is given in Fig. 3 and not in Fig. S3. Fig. S3 concerns the whole measurement period. Once the

modification will bemade, there will be no reference in the article to Fig. S3. So please comment this figure in the text or remove it from the supplement.

Response: OK. We have put the diurnal variation of HONO during the entire period in **Fig. 3** and analyzed the diurnal variation of HONO in the three periods in **Fig. 4**(a) in the revised text. And, we have modified the sentence in the revised text.

L 232-234: The diurnal variations of HONO during the measurement were similar in the three periods, as shown in **Fig. 3** and **Fig. 4**.

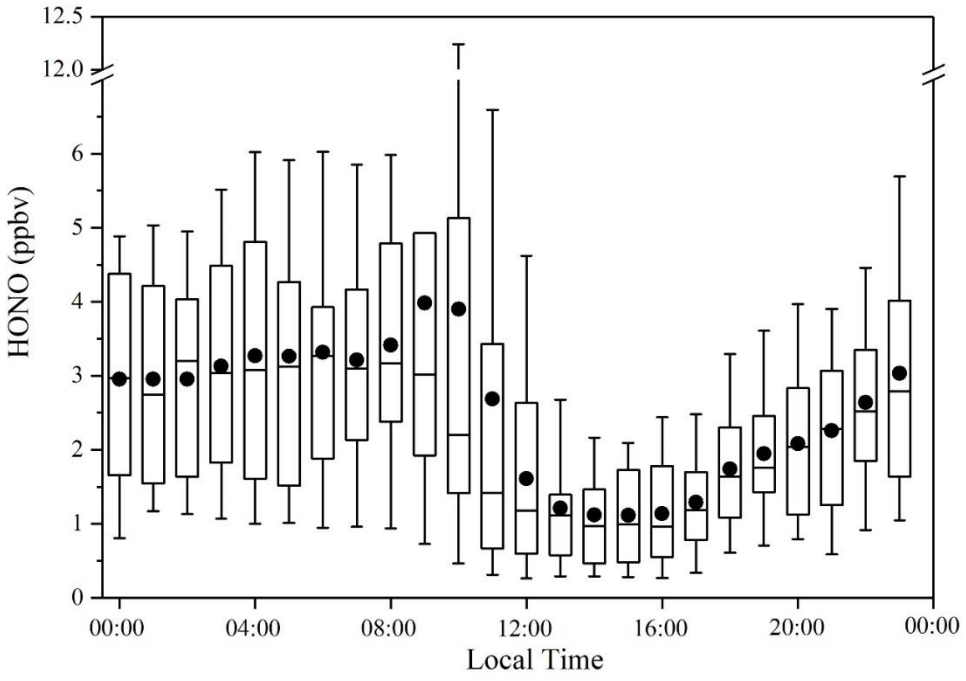

Fig. 3. Diurnal variations of HONO during the measurement.

14. -P8, lines 217-218: "The NO and NO_2 concentration increased in the morning rush hours, decreased rapidly afterward, and remained low in the afternoon." This statement is not true for NO_2 and only right for NO during the CD period but not for the PD and SPD period. Please modify this statement consequently.

Response: Thank you for your comment. The sentence has been modified in the revised text.

L 242-243: The NO concentration decreased rapidly in the forenoon, and remained low in the afternoon.

15. -P10, line 251: Change “that cannot be obtained in the measurement” for “that was not measured during the campaign”.

Response: OK. We have modified the sentence in the revised text.

L 275-276: [OH] is the concentration of ·OH that was not measured during the campaign.

16. -P10, line 253: Wrong unit: please change “cm^3 $molecule^{-1}$” for “molecule cm^{-3}”.

Response: Sorry for my carelessness. The units have been modified in the full text.

L 282: …2.5×10^5 molecule cm^{-3}.

L 286:…3 to 6×10^5 molecule cm^{-3}…

L 493-498: The mean values of J_{HONO} and ·OH concentration in the CD, PD, and SPD periods were 5.93×10^{-4}, 3.79×10^{-4}, and 3.79×10^{-4} molecule cm^{-3} and 4.10×10^6, 2.93×10^6, and 3.76×10^6 molecule cm^{-3}, respectively. The results of the calculated OH radicals ranged from $(0.58-11.49)\times10^6$ molecule cm^{-3}, and the mean value was 3.57×10^6 molecule cm^{-3} at noon in Zhengzhou.

17. -P11, line 279: Change “the hourly abatement level of HONO abatement” for “the hourly level of HONO abatement”.

Response: Thank you. We have removed the word, “abatement”, in the revised

text.

L 316-317: Second, the hourly level of HONO abatement pathways, except OH + HONO, should be at least 0.22 ppbv h^{-1} (i.e., 3.36 – 1.59 ppbv)/8 h).

18. -P11, lines 278-282: "Second, the hourly abatement level of HONO abatement pathways, except OH + HONO, should be at least 1.47 ppbv h-1 (i.e., 13.41 – 1.59 ppbv) / 8 h). The contributions of other HONO abatement pathways in the current work even exceeded the formation of heterogeneous reactions, similar to a previous study (Spataro et al., 2013)."If this statement is maintained after the recalculation of $P_{netOH+NO}$ using a more realistic nocturnal OH concentrations, authors should comment on which other losses of HONO can be significant at night (e.g. deposition, heterogeneous losses…). At least, a raw estimation of loss by deposition could be performed to estimate whether it can explain the lacking abatement processes.

Response: Thank you for your comment. At night, in addition to reaction with HONO to OH, there were two HONO removal pathways: heterogeneous loss on aerosols and deposition (Li et al., 2012). The heterogeneous loss of aerosols can not be calculated directly. And, the main factor of the dry deposition on ground surfaces is the deposition velocity of HONO. The reported value of deposition velocity ranged from 0.092 or 2 cm s^{-1} (Harrison et al., 1996; Stutz, 2002). Sorry, we can not give a raw estimation of loss by deposition, but what we can be sure of is that the phenomenon may arise because the dry deposition on ground surfaces can be the main HONO removal pathway at night.

So this is my confusion. This statement is maintained after the recalculation of P_{OH+NO}^{net} using a more realistic nocturnal OH concentrations, the dry deposition on ground surfaces can be the HONO removal pathway at night. We have changed "The contributions of other HONO abatement pathways in the current work even exceeded the formation of heterogeneous reactions, similar to a previous study

(Spataro et al., 2013).” for “This phenomenon may arise because the dry deposition on ground surfaces can be the main HONO removal pathway at night, similar to a previous study (Li et al., 2012).” in the revised text (L 318-320).

19. -P13, lines 342-344: “The increased HONO in ambient air during the pollution period could have been caused by the comparatively high loading and large particle surface”. The fair correlation between HONO concentrations and $PM_{2.5}$ mass concentrations may also just pinpoint the mainly anthropogenic origins of these two pollutants with high direct or indirect contribution of combustion sources for both of them and not the importance of HONO heterogeneous formation pathways on aerosol surfaces.

Response: Thank you. This is my carelessness. The fair correlation between HONO concentrations and $PM_{2.5}$ mass concentrations did not explain the importance of HONO heterogeneous formation pathways on aerosol surfaces. What we want to explain is whether there is a change in the intensity of NO_2 heterogeneous reactions during the increase in heavy pollution levels, so we found a relevant explanation (Cui et al., 2018). Cui et al. (2018) studied the more intense heterogeneous conversion of NO_2 to HONO on particle surfaces during the pollution episodes at a single particle scale. We have modified the sentences in the revised text.

L 382-386: The fair correlation between HONO and $PM_{2.5}$ may pinpoint the mainly anthropogenic origins of these two pollutants with the high direct or indirect contribution of combustion sources. The reason for the increased HONO during the heavy pollution period could be by the comparatively high loading and large particle surface (Cui et al., 2018).

A correlation between the calculated unknown source of HONO and the $PM_{2.5}$ mass

concentrations (as a proxy for aerosol surface even if it is not perfect) would have been more convincing. Authors can probably use the $P_{unknown}$ calculated in section 3.3 to perform this correlation.

We have studied the correlation between the unknown source of HONO and the $PM_{2.5}$ mass concentrations was lower. So, we can not probably use the $P_{unknown}$ calculated in section 3.3 to perform this correlation for explaining the unknown source.

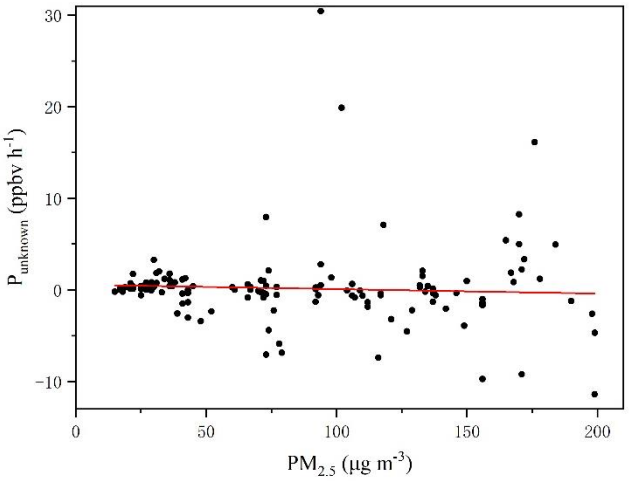

20. -P14, line 383: Change “in then current study” for “in the current study”.

Response: Sorry for my carelessness. The sentence has been modified in the revised text.

L 432: …HONO was calculated in the current study…

21. -P15, line 393: Change “the conversion rates” for “the averaged conversion rates”.

Response: OK. The sentence has been modified in the revised text.

L 442-443: The averaged conversion rates…

22. -P15, lines 395-396: Change “The improvement” for “the increase”.

Response: OK. The sentence has been modified in the revised text.

L 445: The increase in the conversion rate…

23. -P15, lines 398-399: “the high utilization efficiency of the aerosol surface due to good particle surface properties”. I do not understand this statement. Please clarify and rephrase.

Response: Sorry for my confusion. The exact uptake coefficients of NO_2 on ground and aerosol surfaces are variable and should be different (Harrison and Collins, 1998). The present analysis simplified this process by treating the ground and aerosol surfaces the same. The uptake coefficient is mainly dependent on the surface characteristics, e.g. surface area, surface type (Lu et al., 2018). We have added the sentences in the revised text.

L 448-452: The exact uptake coefficients of NO_2 on ground and aerosol surfaces are variable and should be different (Harrison and Collins, 1998). The present analysis simplified this process by treating the ground and aerosol surfaces the same. The uptake coefficient is mainly dependent on the surface characteristics, e.g. surface type and moisture (Lu et al., 2018).

24. -P15-16, lines 415-418: “the tropospheric ultraviolet and visible (TUV) transfer model of the National Center for Atmospheric Research (http://cprm.acom.ucar.edu/Models/TUV/Interactive_TUV/) (Hou et al.,2016) was used to calculate the J_{HONO} value”. It should be addressed that the J_{HONO} values obtained this way are only suitable for clear sky days without clouds, unless the presence of clouds have been taken into account. If so, the method used should be described. Furthermore, the values for O_3 column as well as for the surface albedo used in TUV

model should be indicated and justification about the choice of these values should be given.

Response: OK. Sorry for my carelessness. The problem you pointed out is correct. TUV is an interactive model for calculation of photodissociation coefficients (J values) over the visible and ultraviolet spectral range in the atmosphere under clear sky conditions. The J_{HONO} values obtained this way were assumed in clear sky days without clouds. We would add a description of O_3 column and the surface albedo. O_3 column density measured by the Ozone Monitoring Instrument (OMI, data available at https://ozonewatch.gsfc.nasa.gov/data/omi/Y2019/). The O_3 column density ranges from 292 to 306 DU during the entire period. The experimental site being situated in an urban region, the surface albedo is considered as 0.13 (Sailor, 1995). The ground elevation and the measurement altitude are 168 and 188 m respectively.

So we have added the sentences in the revised text.

L 478-484: The J_{HONO} values obtained this way were assumed in clear sky days without clouds. O_3 column and the surface albedo. O_3 column density measured by the Ozone Monitoring Instrument (OMI, data available at https://ozonewatch.gsfc.nasa.gov/data/omi/Y2019/). The O_3 column density ranges from 292 to 306 DU during the entire period. The experimental site being situated in an urban region, the surface albedo is considered as 0.13 (Sailor, 1995). The ground elevation and the measurement altitude are 168 and 188 m respectively.

25. -P16, lines 418-419: “The concentration of OH radicals was calculated with the formulas of NO_2, O_3, and JO_1D”.Please specify the equation used for OH calculation.

Response: Thank you for your comment. This part of the formulas of NO_2, O_3, and J_{O^1D} has been described a lot in the paper (Rohrer and Berresheim, 2006). Sorry

for my carelessness. We have placed this part in the revised supplement.

2. The concentration of OH radicals was calculated with the formulas of NO_2, O_3, and J_{O^1D}.

$$[OH] = \frac{k_{HO_2+NO}\tau_{HC}[NO_2]F_J}{k_{NO+O_3}} \times \sqrt{\frac{\alpha}{k_{HO_2+HO_2}[O_3]}} \times J(O^1D),$$

where [OH] represents the concentration of OH radicals, $k_{HO_2+NO} = 8.56 \times 10^{-12}$ $cm^3\ s^{-1}$, $\tau_{HC} = 0.3$ s, $[NO_2]$ represents the NO_2 concentration, $F_J = 2\ s^{-0.5}$, $k_{NO+O_3} = 1.82 \times 10^{-14}$ $cm^3\ s^{-1}$, $\alpha = 0.075$, $k_{HO_2+HO_2} = 8.56 \times 10^{-12}$ $cm^3\ s^{-1}$, $[O_3]$ represents the O_3 concentration, and $J(O^1D)$ represents the O^1D efficiency of photolysis.

We have modified the sentence in the revised text.

L 484-485: The concentration of OH radicals was calculated with the formulas of NO_2, O_3, and J_{O^1D} in the supplement.

26. -P16, line 427: "The mean values of JHONO and OH radical concentration". Is it daily mean or mean values at noon? Please specify this.

Response: OK. TUV can only calculate the photolysis efficiency under daylight conditions. So, J_{HONO} and ·OH concentration are the mean values at noon. To prevent this confusion, we have modified the sentence in the revised text.

L 495-500: The mean values of J_{HONO} and ·OH concentration at noon in the CD, PD, and SPD periods were 5.93×10^{-4}, 3.79×10^{-4}, and 3.79×10^{-4} molecule cm^{-3} and 4.10×10^{6}, 2.93×10^{6}, and 3.76×10^{6} molecule cm^{-3}, respectively."

27. -P17, lines 454-455: "Although the values of P_{OH+NO} had high uncertainty because of the NO concentrations".How NO concentrations can affect largely the uncertainties of P_{OH+NO} calculations? Does NO measurements suffer from high uncertainties? Why? If this is the case this point should be also addressed in the section 2.2. Please clarify

this statement.

Response: Sorry. This sentence is my expression problem. What I mean is that the concentration of NO has a great influence on it, but the homogeneous reaction is still an important pathway. The uncertainty of NO measurements was shown in **Table S1.**

So we have changed "Although the values of P_{OH+NO} had high uncertainty because of the NO concentrations, P_{OH+NO} contributed the most to HONO production during daytime." for "The concentration of NO has a great influence on P_{OH+NO}, so the homogeneous reaction is still an important pathway of HONO production during the daytime." in the revised text (L 516-518).

28. -Fig. 8: Please modify the legend of the figure to be consistent with the title and the manuscript (use PD and SPD instead of HD and SHD). Furthermore, J_{HONO} and J_{O1D} are shown only for two periods and not for all three. Why? Please include the values for the third period (SPD) or explain why it is not shown.

Response: OK. We have modified the problem in **Fig. 9**.

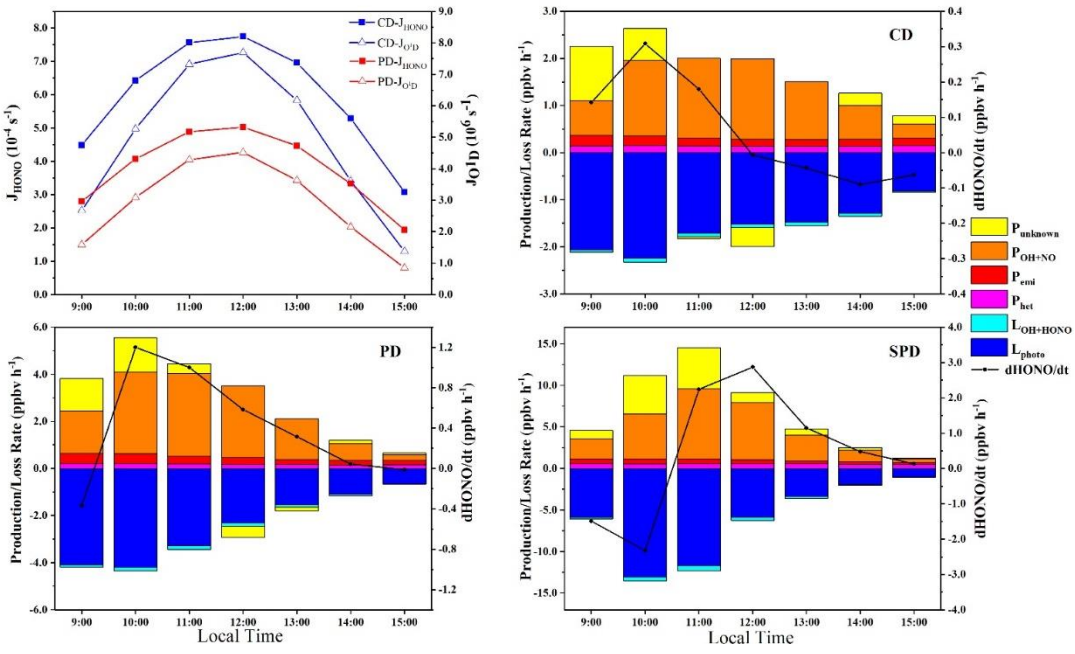

Fig. 9. The average profiles of J_{HONO} and J_{O^1D} concentrations during the daytime, and production and loss rate of the daytime HONO in CD, PD and SPD periods.

We treated PD and SPD the same. The reason is that the main input parameters of TUV cannot be obtained directly, so we quoted the input parameters in the literature. However, the input parameters of PD and SPD are not distinguished in the papers. We wanted to study that under the same output conditions from the TUV model, the impact of different pollution levels changed on the daytime budget. We have added the sentence in the revised text.

L 491-493: We wanted to study that under the same output conditions from the TUV model in the PD and SPD periods, the impact of different pollution levels changed on the daytime budget.

29. -Table 2: Please remove WD from the title of the table since no data of wind direction is shown in it.

Response: Sorry. We have removed the word, “WD”, in the revised text.

Table 1. Data statistics of HONO, $PM_{2.5}$, NO_2, NO, NO_X, HONO/NO_2, HONO/NO_X, O_3, CO, T, RH, and WS during the measurement period, mean value ± standard deviation.

Characteristics, sources, and reactions of nitrous acid during winter at an urban site in the Central Plains Economic Region in China

Qi Hao, Nan Jiang*, Ruiqin Zhang, Liuming Yang, and Shengli Li
Key Laboratory of Environmental Chemistry and Low Carbon Technologies of Henan Province, Research Institute of Environmental Science, College of Chemistry, School of Ecology and Environment, Zhengzhou University, Zhengzhou 450001, China

Supplement:

1. This AIM method and its details.

HONO was hygroscopically grown in the parallel plate denuder and collected as an aqueous solution in a cyclone assembly. The aqueous sample aliquots from both channels were transported to the ion chromatographic systems housed inside a ground container for hourly semicontinuous online analysis of HONO. The ion chromatographic system was calibrated for NO_2^- using mixed anion standard solutions of NO_2^-.

2. The concentration of OH radicals was calculated with the formulas of NO_2, O_3, and J_{O^1D}.

$$[\mathrm{OH}] = \frac{k_{HO_2+NO}\tau_{HC}[NO_2]F_J}{k_{NO+O_3}} \times \sqrt{\frac{\alpha}{k_{HO_2+HO_2}[O_3]}} \times J(O^1D),$$

where [OH] represents the concentration of OH radicals, $k_{HO_2+NO} = 8.56 \times 10^{-12}$ cm^3 s^{-1}, $\tau_{HC} = 0.3$ s, [NO_2] represents the NO_2 concentration, $F_J = 2$ s$^{-0.5}$, $k_{NO+O_3} = 1.82 \times 10^{-14}$ cm^3 s^{-1}, $\alpha = 0.075$, $k_{HO_2+HO_2} = 8.56 \times 10^{-12}$ cm^3 s^{-1}, [O_3] represents the O_3 concentration, and $J(O^1D)$ represents the O^1D efficiency of photolysis.

Figure Captions:

Fig. S1. The correlation study between $HONO_{correct}$ and NO_2 in the nighttime.

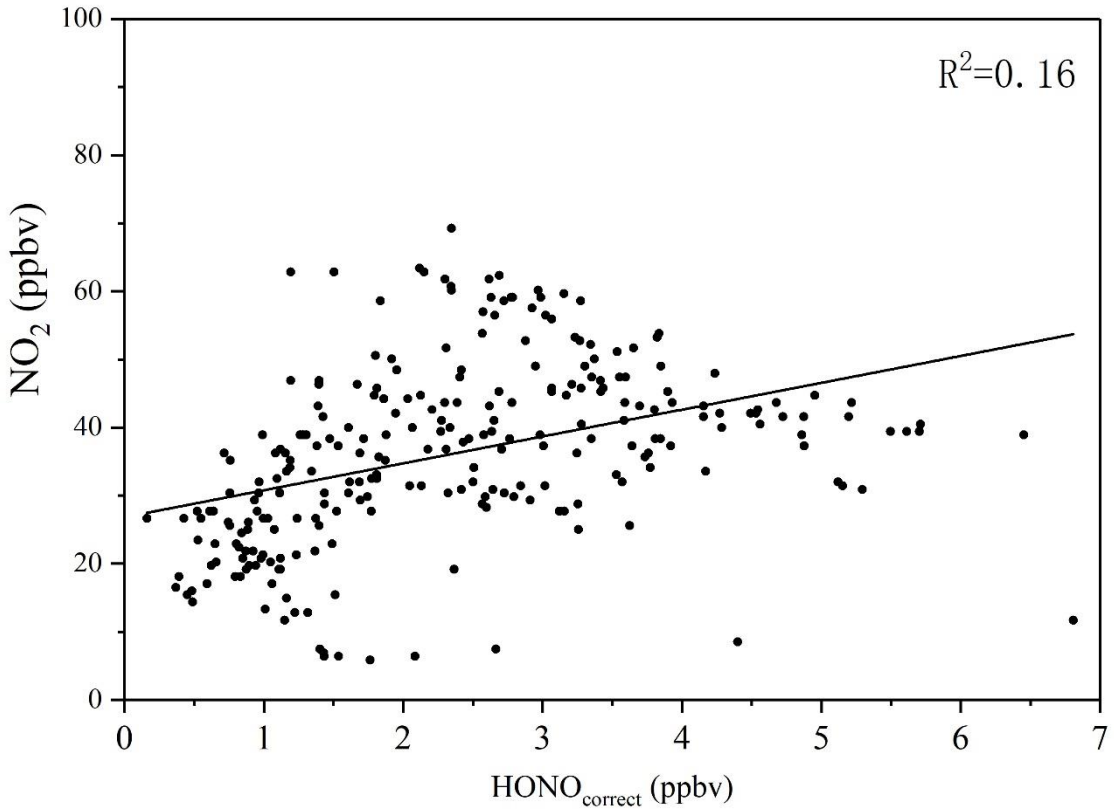

Fig. S1. The correlation study between $HONO_{correct}$ and NO_2 in the nighttime.

Table Captions:

Table S1. Measured species and performance of the instruments.

Table S2 The error bars of Fig. 4. (The units of all species except $HONO/NO_2$ and $HONO/NO_x$ are ppbv. The units of $HONO/NO_2$ and $HONO/NO_x$ are %.)

Table S3 The error bars of Fig. 5. (The units of all species except P_{OH+NO}^{net} are ppbv. The unit of P_{OH+NO}^{net} is ppbv/h.)

Table S4 The error bars of Fig. 8. (The units of all species except $HONO_{correct}/NO_2$ are ppbv. The unit of $HONO_{correct}/NO_2$ is %.)

Table S1. Measured species and performance of the instruments.

Species	Measurement technique	Detection limit	Accuracy
$PM_{2.5}$	Tapered Element Oscillating Microbalance	1.5 μg m^{-3}	± 5%
HONO	Ion Chromatography	4 pptv	± 20%
CO	Absorbs Infrared Radiation	40 ppbv	± 5%
NO	Chemiluminescence	60 pptv	± 20%
NO_2	Chemiluminescence	300 pptv	± 20%
O_3	UV Photometry	0.5 ppbv	± 5%

The results came from instrument manufacturers.

Table S2-1 The error bars of Fig. 4. (The units of all species except $HONO/NO_2$ and $HONO/NO_x$ are ppbv. The units of $HONO/NO_2$ and $HONO/NO_x$ are %.)

	Local Time (hh:mm)									
Species-period	00:00	01:00	02:00	03:00	04:00	05:00	06:00	07:00	08:00	09:00
HONO-CD	1.7 ± 1.3	1.4 ± 0.6	1.3 ± 0.4	1.2 ± 0.3	1.2 ± 0.2	1.2 ± 0.2	1.4 ± 0.3	1.5 ± 0.6	1.7 ± 0.9	1.6 ± 0.9
HONO-PD	3.2 ± 1.5	3.1 ± 1.3	3 ± 1.1	3.3 ± 1.2	3.5 ± 1.3	3.5 ± 1.2	3.6 ± 1.1	3.3 ± 0.9	3.7 ± 1.6	4.1 ± 2.8
HONO-SPD	3.7 ± 0.9	4 ± 0.8	4.2 ± 0.6	4.4 ± 0.8	4.6 ± 1	4.6 ± 1.2	4.6 ± 1.5	4.4 ± 1.3	4.4 ± 1.1	5.7 ± 3
NO-CD	14.3 ± 17	9 ± 9.7	8.5 ± 12.7	10.1 ± 22.4	10.6 ± 21.1	21.9 ± 29	27.8 ± 33	40.1 ± 51	52.6 ± 79	55.5 ± 84
NO-PD	57.3 ± 48	62.7 ± 55.9	49.6 ± 49	44 ± 47.8	47 ± 48.7	46.6 ± 30	41.4 ± 34	44.7 ± 33	48.9 ± 35	53.7 ± 44
NO-SPD	79.4 ± 103	100.1 ± 118	128.3 ±133	129 ± 134	111 ± 119	117 ± 95	100 ± 94	88.4 ± 85	82.3 ± 70	85.4 ± 71
NO_2-CD	25.4 ± 8.2	25.6 ± 9.9	24.7 ± 10.5	22.9 ± 10.4	24 ± 11.4	20.7 ± 11	20.2 ± 9	23.6 ± 11	28.6 ± 18	28.6 ± 18
NO_2-PD	41.1 ± 10	40.8 ± 11.2	39.7 ± 10.7	37.9 ± 7.1	36.6 ± 5.4	35.9 ± 5	33.8 ± 6	34.4 ± 6	33.2 ± 5	30.7 ± 6
NO_2-SPD	45.3 ± 9.5	43.5 ± 9.2	42.8 ± 8.8	42.1 ± 8.2	42.2 ± 8.1	41 ± 7.1	40.6 ± 6.9	40.7 ± 6	40.1 ± 6	39.2 ± 7
O_3-CD	14.2 ± 10	13.6 ± 10.4	14.2 ± 10.1	14.9 ± 9.4	13.6 ± 9.1	11.7 ± 10	13.8 ± 10	12.9 ± 9	11.6 ± 8	12.1 ± 7
O_3-PD	6.6 ± 6.1	6.4 ± 5.2	7.1 ± 5.2	6.3 ± 3.3	4.7 ± 2.2	5.3 ± 3	7.7 ± 6.9	5.3 ± 2.8	5.5 ± 3	7.1 ± 4
O_3-SPD	7.8 ± 6.4	7.7 ± 6.2	7.3 ± 5	6 ± 2.9	5.3 ± 2.3	5 ± 2.1	5.6 ± 2.5	5.2 ± 2.2	5.6 ± 2.6	6 ± 2.6
$HONO/NO_2$-CD	3.8 ± 1.5	4.4 ± 1	4.4 ± 1.1	4.9 ± 1	5.1 ± 0.8	8.3 ± 6	6.9 ± 2.1	6.2 ± 1.4	5.1 ± 0.8	4.3 ± 1.1
$HONO/NO_2$-PD	8 ± 3.6	7.8 ± 3.4	8 ± 3.3	9 ± 3.7	10 ± 4.5	10.1 ± 4	11.2 ± 4.6	10.3 ± 4	12.1 ± 7	14.3 ± 11
$HONO/NO_2$-SPD	8.3 ± 1.9	9.3 ± 1.4	10 ± 1.5	10.7 ± 1.9	11 ± 2.2	11.3 ± 3	11.5 ± 3.9	10.9 ± 3	11.1 ± 2	15 ± 8.3
$HONO/NO_x$-CD	2.7 ± 1.4	3.7 ± 1.5	4.2 ± 1.4	4.9 ± 1.1	4.9 ± 1	5.3 ± 2.5	5.1 ± 2.9	4.5 ± 2.4	3.6 ± 1.5	2.8 ± 1.4
$HONO/NO_x$-PD	4.4 ± 1.4	4.3 ± 1.7	4.6 ± 1.5	5.3 ± 1.3	5.3 ± 1	5.3 ± 1.1	6.6 ± 2.7	5.9 ± 2.3	6.5 ± 3.8	6.6 ± 4.3
$HONO/NO_x$-SPD	5.1 ± 2	5.3 ± 2.4	5.4 ± 3.4	5.8 ± 3.9	6.1 ± 3.9	5.7 ± 3.7	5.9 ± 3.6	5.7 ± 3	5.8 ± 2.9	6.7 ± 3.1

Table S2-2 The error bars of Fig. 4. (The units of all species except $HONO/NO_2$ and $HONO/NO_x$ are ppbv. The units of $HONO/NO_2$ and $HONO/NO_x$ are %.)

	Local Time (hh:mm)									
Species-period	10:00	11:00	12:00	13:00	14:00	15:00	16:00	17:00	18:00	19:00
HONO-CD	1.1 ± 0.6	0.6 ± 0.3	0.5 ± 0.3	0.6 ± 0.4	0.6 ± 0.5	0.7 ± 0.5	0.6 ± 0.5	0.7 ± 0.4	1 ± 0.5	1.2 ± 0.5
HONO-PD	2.9 ± 1.9	1.9 ± 1.3	1.3 ± 0.7	1 ± 0.3	0.9 ± 0.3	0.9 ± 0.3	0.9 ± 0.3	1.1 ± 0.4	1.4 ± 0.3	1.7 ± 0.3
HONO-SPD	6.9 ± 4.3	5.2 ± 3.8	3 ± 1.3	2.1 ± 0.7	1.8 ± 0.7	1.7 ± 0.6	1.8 ± 0.7	2 ± 0.5	2.7 ± 0.7	2.8 ± 0.8
NO-CD	43.9 ± 69.8	27.9 ± 40.8	14.9 ± 17.1	10.3 ± 7.8	7.3 ± 3	6 ± 4.5	6.4 ± 5.6	3.6 ± 3.4	2.6 ± 3.2	5.9 ± 7.7
NO-PD	49.3 ± 45.2	30 ± 26.2	21 ± 20.7	12.7 ± 14.7	9.4 ± 12.3	8.4 ± 9.5	5.7 ± 4.7	6.3 ± 6.8	9 ± 9	10 ± 10.3
NO-SPD	90.8 ± 73.4	79.3 ± 69.3	57.1 ± 52.3	34.8 ± 36.4	24.5 ± 28.7	19 ± 24.7	15 ± 18.8	11.8 ± 11	11.8 ± 7.9	22.4 ± 21
NO_2-CD	26.8 ± 15.7	22.7 ± 9.2	17.6 ± 7.1	17.1 ± 9	19.6 ± 9.6	21 ± 10.7	20.5 ± 9	21.4 ± 9	26 ± 12.5	30 ± 13.7
NO_2-PD	30 ± 6.9	28.8 ± 7.7	27.4 ± 9.6	24.8 ± 9.4	22.5 ± 10.6	25 ± 9.9	25.7 ± 9.3	27.1 ± 9	35 ± 8.7	36.2 ± 9.2
NO_2-SPD	39.8 ± 7.8	41.5 ± 8.3	42.3 ± 10.1	39.5 ± 12.6	38.5 ± 14.3	38 ± 14.7	38 ± 13.9	42 ± 15.4	45 ± 11.5	47 ± 10.8
O_3-CD	15.9 ± 8.8	19.5 ± 9.7	22.6 ± 8.3	25.5 ± 8.5	28.1 ± 9.1	29 ± 10.8	28 ± 10.8	29 ± 10.2	23.6 ± 10	17 ± 8.9
O_3-PD	9.6 ± 6.1	12.8 ± 6.2	18.7 ± 8.3	24.1 ± 8.4	28.2 ± 9.7	27 ± 10.8	28 ± 10.4	26 ± 10.5	17.4 ± 8.6	15 ± 11.6
O_3-SPD	6.3 ± 2.4	8.7 ± 4.5	12.8 ± 8.5	19.4 ± 12.9	24.1 ± 14.7	28 ± 16.6	29 ± 17.6	25 ± 16.1	17 ± 11.1	10.6 ± 9.7
$HONO/NO_2$-CD	4.1 ± 2.3	3.1 ± 1.9	3.3 ± 1.9	3.3 ± 1.3	3.1 ± 1.3	3.1 ± 1.3	2.9 ± 1.4	3.1 ± 1.4	3.9 ± 1.4	4.5 ± 2.2
$HONO/NO_2$-PD	9.4 ± 5.6	6.2 ± 3	4.7 ± 1.5	4.2 ± 1.2	4.7 ± 2.2	3.9 ± 0.7	3.7 ± 0.4	4.1 ± 1.2	4.3 ± 0.9	5 ± 1.5
$HONO/NO_2$-SPD	18.9 ± 13.7	13.7 ± 12	7.3 ± 3.5	5.6 ± 2.6	4.9 ± 2.1	4.8 ± 2.4	4.9 ± 1.6	5 ± 1	6.3 ± 1.8	6.2 ± 1.5
$HONO/NO_x$-CD	2.9 ± 2.1	2.2 ± 1.5	2.4 ± 1.5	2.5 ± 1.1	2.5 ± 1	2.6 ± 0.9	2.5 ± 0.9	2.8 ± 1	3.7 ± 1.1	4.1 ± 1.9
$HONO/NO_x$-PD	4.8 ± 2.4	3.8 ± 1.3	3.5 ± 1.2	3.5 ± 1.5	4 ± 2.1	3.4 ± 0.9	3.3 ± 0.5	3.7 ± 1.2	3.8 ± 0.7	4.3 ± 1.5
$HONO/NO_x$-SPD	8.2 ± 5.8	6.9 ± 5.7	4.3 ± 2	4 ± 2	3.8 ± 1.6	3.9 ± 1.9	4.3 ± 1.6	4.5 ± 1.2	5.5 ± 1.5	4.9 ± 1.3

Table S2-3 The error bars of Fig. 4. (The units of all species except $HONO/NO_2$ and $HONO/NO_x$ are ppbv. The units of $HONO/NO_2$ and $HONO/NO_x$ are %.)

	Local Time (hh:mm)			
Species-period	20:00	21:00	22:00	23:00
HONO-CD	1.3 ± 0.6	1.6 ± 0.9	2 ± 0.9	2.1 ± 0.9
HONO-PD	1.7 ± 0.7	1.8 ± 0.8	2 ± 0.9	2.1 ± 0.9
HONO-SPD	3.1 ± 0.9	3.2 ± 0.9	3.7 ± 0.8	4.6 ± 1.2
NO-CD	11.1 ± 16.9	14.5 ± 22.5	35.5 ± 68.9	50.8 ± 99.2
NO-PD	15 ± 14.1	15.3 ± 14.7	27.4 ± 28.5	33.9 ± 28.9
NO-SPD	29.4 ± 24.2	37.3 ± 26.6	38.5 ± 23.1	51.4 ± 31.4
NO_2-CD	31 ± 13.8	30.3 ± 14.5	31.6 ± 13.6	31 ± 14.3
NO_2-PD	37.3 ± 10.5	38.5 ± 13.9	38.3 ± 13.5	37.1 ± 13.2
NO_2-SPD	44.5 ± 11	43.5 ± 11.5	43.5 ± 11.1	42.1 ± 13.1
O_3-CD	13.3 ± 10.1	14 ± 11	12.2 ± 8.7	12.7 ± 8.8
O_3-PD	13.7 ± 10.3	10.9 ± 8.5	10.9 ± 7.7	12.2 ± 10.4
O_3-SPD	9.9 ± 8.6	10.8 ± 9.2	9.7 ± 8.7	9.6 ± 9.6
$HONO/NO_2$-CD	4.6 ± 2.2	5.7 ± 2.6	6.5 ± 2.6	6.8 ± 2.7
$HONO/NO_2$-PD	4.7 ± 1.9	4.6 ± 1.2	4.9 ± 0.8	5.3 ± 0.8
$HONO/NO_2$-SPD	7 ± 1.5	7.5 ± 1.4	8.9 ± 2.3	9.4 ± 2.4
$HONO/NO_x$-CD	4 ± 1.9	4.8 ± 2.2	4.9 ± 2.8	5 ± 3
$HONO/NO_x$-PD	3.9 ± 2.1	3.9 ± 1.3	3.8 ± 1	3.8 ± 0.9
$HONO/NO_x$-SPD	5.1 ± 1.5	5.2 ± 2	5.8 ± 2	5 ± 1.4

Table S3-1 The error bars of Fig. 5. (The units of all species except P_{OH+NO}^{net} are ppbv. The unit of P_{OH+NO}^{net} is ppbv/h.)

	Local Time (hh:mm)									
Species-period	19:00	20:00	21:00	22:00	23:00	00:00	01:00	02:00	03:00	04:00
P_{OH+NO}^{net}-CD	0.04 ± 0.06	0.08 ± 0.12	0.11 ± 0.17	0.33 ± 0.54	0.47 ± 0.79	0.12 ± 0.13	0.07 ± 0.08	0.03 ± 0.03	0.01 ± 0.1	0.02 ± 0.1
HONO-CD	1.18 ± 0.48	1.32 ± 0.62	1.62 ± 0.9	2.02 ± 0.94	2.09 ± 0.9	1.67 ± 1.34	1.43 ± 0.63	1.26 ± 0.44	1.2 ± 0.3	1.2 ± 0.22
NO-CD	5.4 ± 6.5	10.2 ± 14.4	13.3 ± 19.2	38.2 ± 62.2	54.9 ± 89.7	15 ± 14.8	8.8 ± 8.6	3.7 ± 4.2	1.5 ± 2.3	2.5 ± 2.6
P_{OH+NO}^{net}-HD	0.07 ± 0.07	0.1 ± 0.1	0.1 ± 0.1	0.19 ± 0.2	0.23 ± 0.2	0.4 ± 0.34	0.44 ± 0.4	0.34 ± 0.35	0.3 ± 0.34	0.3 ± 0.34
HONO-HD	1.7 ± 0.27	1.71 ± 0.68	1.82 ± 0.78	1.98 ± 0.89	2.06 ± 0.93	3.21 ± 1.54	3.05 ± 1.27	3.01 ± 1.08	3.3 ± 1.17	3.5 ± 1.34
NO-HD	8.5 ± 8.4	12.2 ± 11.5	12.5 ± 12	22.4 ± 23.3	27.7 ± 23.6	46.8 ± 39.5	51.2 ± 45.6	40.5 ± 40	35.9 ± 39	38 ± 39.7
P_{OH+NO}^{net}-SHD	0.15 ± 0.15	0.2 ± 0.17	0.25 ± 0.18	0.26 ± 0.16	0.35 ± 0.23	0.55 ± 0.75	0.7 ± 0.85	0.9 ± 0.96	0.9 ± 1.0	0.8 ± 0.86
HONO-SHD	2.8 ± 0.8	3.1 ± 0.9	3.2 ± 0.9	3.7 ± 0.8	4.6 ± 1.2	3.7 ± 0.9	4 ± 0.8	4.2 ± 0.6	4.4 ± 0.8	4.6 ± 1
NO-SHD	18 ± 17	24 ± 20	30 ± 21	31 ± 19	42 ± 25	64 ± 84	81 ± 96	104 ± 108	105 ± 110	90 ± 97

Table S3-2 The error bars of Fig. 5. (The units of all species except P_{OH+NO}^{net} are ppbv. The unit of P_{OH+NO}^{net} is ppbv/h.)

	Local Time (hh:mm)	
Species-period	05:00	06:00
P_{OH+NO}^{net}-CD	0.12 ± 0.18	0.17 ± 0.22
HONO-CD	1.25 ± 0.21	1.36 ± 0.35
NO-CD	13.7 ± 20.9	19.5 ± 25.1
P_{OH+NO}^{net}-HD	0.32 ± 0.22	0.28 ± 0.25
HONO-HD	3.5 ± 1.16	3.56 ± 1.09
NO-HD	38 ± 25.2	33.8 ± 28.5
P_{OH+NO}^{net}-SHD	0.82 ± 0.87	0.7 ± 0.68
HONO-SHD	4.6 ± 1.2	4.6 ± 1.5
NO-SHD	95.6 ± 99	81.8 ± 77.1

Table S4-1 The error bars of Fig. 8. (The units of all species except $HONO_{correct}/NO_2$ are ppbv. The unit of $HONO_{correct}/NO_2$ is %.)

	Local Time (hh:mm)									
Species-period	19:00	20:00	21:00	22:00	23:00	00:00	01:00	02:00	03:00	04:00
$HONO_{correct}$-CD	1.0 ± 0.4	1.1 ± 0.6	1.4 ± 0.8	1.6 ± 0.7	1.6 ± 0.6	1.4 ± 1.4	1.2 ± 0.7	1.1 ± 0.5	1.1 ± 0.4	1.1 ± 0.2
NO_2-CD	30 ± 15	31 ± 15	30 ± 15	34 ± 15	34 ± 15	25 ± 9	24 ± 8	22 ± 8	20 ± 8	20 ± 8
$HONO_{correct}/NO_2$-CD	3.7 ± 2.2	3.9 ± 2.2	4.9 ± 2.6	5.5 ± 2.7	5.7 ± 2.9	11 ± 18.2	8.9 ± 12	8.6 ± 10.8	8.5 ± 9.7	7.7 ± 7.4
$HONO_{correct}$-HD	1.4 ± 0.3	1.4 ± 0.7	1.5 ± 0.7	1.6 ± 0.8	1.7 ± 0.8	2.7 ± 1.3	2.5 ± 1	2.5 ± 0.8	2.9 ± 0.9	3.1 ± 1.1
NO2-HD	36 ± 9	37 ± 10	39 ± 14	38 ± 13	37 ± 13	41 ± 10	41 ± 11	40 ± 11	38 ± 7	37 ± 5
$HONO_{correct}/NO_2$-HD	4.2 ± 1.5	3.8 ± 2	3.8 ± 1.2	4 ± 0.8	4.4 ± 0.7	6.7 ± 3.1	6.5 ± 2.8	6.7 ± 2.8	7.8 ± 3.1	8.7 ± 3.8
$HONO_{correct}$-SHD	2.4 ± 0.6	2.6 ± 0.7	2.7 ± 0.7	3.2 ± 0.7	4.1 ± 1.3	3.1 ± 0.8	3.3 ± 0.6	3.4 ± 0.7	3.6 ± 1	3.9 ± 1.1
NO_2-SHD	47 ± 11	44 ± 11	43 ± 11	44 ± 11	42 ± 13	45 ± 9	43 ± 9	43 ± 9	42 ± 8	42 ± 8
$HONO_{correct}/NO_2$-SHD	5.4 ± 1.4	6.1 ± 1.4	6.5 ± 1.4	7.8 ± 2.2	14.4 ± 16.7	7 ± 1.9	7.8 ± 1.6	8.1 ± 2.2	8.8 ± 2.8	9.3 ± 2.9

Table S4-2 The error bars of Fig. 8. (The units of all species except $HONO_{correct}/NO_2$ are ppbv. The unit of $HONO_{correct}/NO_2$ is %.)

	Local Time (hh:mm)	
Species-period	05:00	06:00
$HONO_{correct}$-CD	1.0 ± 0.4	1.1 ± 0.6
NO_2-CD	30 ± 15	31 ± 15
$HONO_{correct}/NO_2$-CD	3.7 ± 2.2	3.9 ± 2.2
$HONO_{correct}$-HD	1.4 ± 0.3	1.4 ± 0.7
NO_2-HD	36 ± 9	37 ± 10
$HONO_{correct}/NO_2$-HD	4.2 ± 1.5	3.8 ± 2
$HONO_{correct}$-SHD	2.4 ± 0.6	2.6 ± 0.7
NO_2-SHD	47 ± 11	44 ± 11
$HONO_{correct}/NO_2$-SHD	5.4 ± 1.4	6.1 ± 1.4

Reference

Cui, L., Li, R., Zhang, Y., Meng, Y., Fu, H., and Chen, J.: An observational study of nitrous acid (HONO) in Shanghai, China: The aerosol impact on HONO formation during the haze episodes, Sci. Total Environ., 630, 1057-1070, https://doi.org/10.1016/j.scitotenv.2018.02.063, 2018.

Duan, J., Qin, M., Ouyang, B., Fang, W., Li, X., Lu, K., Tang, K., Liang, S., Meng, F., Hu, Z., Xie, P., Liu, W., and Häsler, R.: Development of an incoherent broadband cavity-enhanced absorption spectrometer for in situ measurements of HONO and NO_2, Atmos. Meas. Tech., 11, 4531-4543, https://doi.org/10.5194/amt-11-4531-2018, 2018.

Elshorbany, Y. F., Steil, B., Brühl, C., and Lelieveld, J.: Impact of HONO on global atmospheric chemistry calculated with an empirical parameterization in the EMAC model, Atmos. Chem. Phys., 12, 9977-10000, https://doi.org/10.5194/acp-12-9977-2012, 2012.

Harrison, R. M., Peak, J. D., and Collins, G. M.: Tropospheric cycle of nitrous acid, J. Geophys. Res., 101, 14429-14439, https://doi.org/10.1029/96jd00341, 1996.

Harrison, R. M., and Collins, G. M.: Measurements of Reaction Coefficients of NO2 and HONO on Aerosol Particles, J. Atmos. Chem., 30, 397-406, https://doi.org/10.1023/A:1006094304069, 1998.

Heland, J., Kleffmann, J., Kurtenbach, R., and Wiesen, P.: A new instrument to measure gaseous nitrous acid (HONO) in the atmosphere, Environ. Sci. Technol., 35, 3207-3212, https://doi.org/10.1021/es000303t, 2001.

Hirokawa, J., Kato, T., and Mafuné, F.: In Situ Measurements of Atmospheric Nitrous Acid by Chemical Ionization Mass Spectrometry Using Chloride Ion Transfer Reactions, Anal. Chem., 81, 8380-8386, https://doi.org/10.1021/ac901117b, 2009.

Kleffmann, J., Becker, K. H., Lackhoff, M., and Wiesen, P.: Heterogeneous conversion of NO2 on carbonaceous surfaces, PCCP, 1, 5443-5450, https://doi.org/10.1039/a905545b, 1999.

Lelieveld, J., Gromov, S., Pozzer, A., and Taraborrelli, D.: Global tropospheric hydroxyl distribution, budget and reactivity, Atmos. Chem. Phys., 16, 12477-12493, https://doi.org/10.5194/acp-16-12477-2016, 2016.

Li, X., Brauers, T., Häseler, R., Bohn, B., Fuchs, H., Hofzumahaus, A., Holland, F., Lou, S., Lu, K. D., Rohrer, F., Hu, M., Zeng, L. M., Zhang, Y. H., Garland, R. M., Su, H., Nowak, A., Wiedensohler, A., Takegawa, N., Shao, M., and Wahner, A.: Exploring the atmospheric chemistry of nitrous acid (HONO) at a rural site in Southern China, Atmos. Chem. Phys., 12, 1497-1513, https://doi.org/10.5194/acp-12-1497-2012, 2012.

Lu, X., Wang, Y., Li, J., Shen, L., and Fung, J. C. H.: Evidence of heterogeneous HONO formation from aerosols and the regional photochemical impact of this HONO source, Environ. Res. Lett., 13, https://doi.org/10.1088/1748-9326/aae492, 2018.

Markovic, M. Z., VandenBoer, T. C., and Murphy, J. G.: Characterization and optimization of an online system for the simultaneous measurement of atmospheric water-soluble constituents in the gas and particle phases, J. Environ. Monit., 14, 1872-1884, https://doi.org/10.1039/c2em00004k, 2012.

Michoud, V., Colomb, A., Borbon, A., Miet, K., Beekmann, M., Camredon, M., Aumont, B., Perrier, S., Zapf, P., Siour, G., Ait-Helal, W., Afif, C., Kukui, A., Furger, M., Dupont, J. C., Haeffelin, M., and Doussin, J. F.: Study of the unknown HONO daytime source at a European suburban site during the MEGAPOLI summer and winter field campaigns, Atmos. Chem. Phys., 14, 2805-2822, https://doi.org/10.5194/acp-14-2805-2014, 2014.

Min, K. E., Washenfelder, R. A., Dubé, W. P., Langford, A. O., Edwards, P. M., Zarzana, K. J., Stutz, J., Lu, K., Rohrer, F., Zhang, Y., and Brown, S. S.: A broadband cavity enhanced absorption spectrometer for aircraft measurements of glyoxal, methylglyoxal, nitrous acid, nitrogen dioxide, and water vapor, Atmos. Meas. Tech., 9, 423-440, https://doi.org/10.5194/amt-9-423-2016, 2016.

Roberts, J. M., Veres, P., Warneke, C., Neuman, J. A., Washenfelder, R. A., Brown, S. S., Baasandorj, M., Burkholder, J. B., Burling, I. R., Johnson, T. J., Yokelson, R. J., and de Gouw, J.: Measurement of HONO, HNCO, and other inorganic acids by negative-ion proton-transfer chemical-ionization mass spectrometry (NI-PT-CIMS): application to biomass burning emissions, Atmos. Meas. Tech., 3, 981-990, https://doi.org/10.5194/amt-3-981-2010, 2010.

Rohrer, F., and Berresheim, H.: Strong correlation between levels of tropospheric hydroxyl radicals and solar ultraviolet radiation, Nature, 442, 184-187, https://doi.org/10.1038/nature04924, 2006.

Sailor, D. J.: Simulated Urban Climate Response to Modifications in Surface Albedo and Vegetative Cover, J. Appl. Meteorol., 34, 1694-1704, https://doi.org/10.1175/1520-0450-34.7.1694, 1995.

Spataro, F., Ianniello, A., Esposito, G., Allegrini, I., Zhu, T., and Hu, M.: Occurrence of atmospheric nitrous acid in the urban area of Beijing (China), Sci. Total Environ., 447, 210-224, https://doi.org/10.1016/j.scitotenv.2012.12.065, 2013.

Stutz, J.: Nitrous acid formation in the urban atmosphere: Gradient measurements of NO_2 and HONO over grass in Milan, Italy, J. Geophys. Res., 107, https://doi.org/10.1029/2001jd000390, 2002.

Su, H., Cheng, Y. F., Shao, M., Gao, D. F., Yu, Z. Y., Zeng, L. M., Slanina, J., Zhang, Y. H., and Wiedensohler, A.: Nitrous acid (HONO) and its daytime sources at a rural site during the 2004 PRIDE-PRD experiment in China, J. Geophys. Res., 113, D14312-14321, https://doi.org/10.1029/2007jd009060, 2008.

Tan, Z., Rohrer, F., Lu, K., Ma, X., Bohn, B., Broch, S., Dong, H., Fuchs, H., Gkatzelis, G. I., Hofzumahaus, A., Holland, F., Li, X., Liu, Y., Liu, Y., Novelli, A., Shao, M., Wang, H., Wu, Y., Zeng, L., Hu, M., Kiendler-Scharr, A., Wahner, A., and Zhang, Y.: Wintertime photochemistry in Beijing: observations of RO_x radical concentrations in the North China Plain during the BEST-ONE campaign, Atmos. Chem. Phys., 18, 12391-12411, https://doi.org/10.5194/acp-18-12391-2018, 2018.

Tian, Y., Xue, Q., Xiao, Z., Chen, K., and Feng, Y.: PMF-GAS Methods to Estimate Contributions of Sources and Oxygen for $PM_{2.5}$, Based on Highly Time-Resolved $PM_{2.5}$

Species and Gas Data, Aerosol Air Qual. Res., 18, 2956-2966, https://doi.org/10.4209/aaqr.2018.07.0244, 2018.

Wang, S., Yin, S., Zhang, R., Yang, L., Zhao, Q., Zhang, L., Yan, Q., Jiang, N., and Tang, X.: Insight into the formation of secondary inorganic aerosol based on high-time-resolution data during haze episodes and snowfall periods in Zhengzhou, China, Sci. Total Environ., 660, 47-56, https://doi.org/10.1016/j.scitotenv.2018.12.465, 2019.

Winer, A. M., and Biermann, H. W.: Long pathlength differential optical absorption spectroscopy (DOAS) measurements of gaseous HONO, NO_2 and HCNO in the California South Coast Air Basin, Res. Chem. Intermed., 20, 423-445, https://doi.org/10.1163/156856794X00405, 1994.

Zhang, B., and Tao, F.-M.: Direct homogeneous nucleation of NO2, H2O, and NH3 for the production of ammonium nitrate particles and HONO gas, Chem. Phys. Lett., 489, 143-147, https://doi.org/10.1016/j.cplett.2010.02.059, 2010.

Zhang, W., Tong, S., Ge, M., An, J., Shi, Z., Hou, S., Xia, K., Qu, Y., Zhang, H., Chu, B., Sun, Y., and He, H.: Variations and sources of nitrous acid (HONO) during a severe pollution episode in Beijing in winter 2016, Sci. Total Environ., 648, 253-262, https://doi.org/10.1016/j.scitotenv.2018.08.133, 2019.

Characteristics, sources, and reactions of nitrous acid during winter at an urban site in the Central Plains Economic Region in China

Qi Hao, Nan Jiang*, Ruiqin Zhang, Liuming Yang, and Shengli Li

Key Laboratory of Environmental Chemistry and Low Carbon Technologies of Henan Province, Research Institute of Environmental Science, College of Chemistry, School of Ecology and Environment, Zhengzhou University, Zhengzhou 450001, China

Abstract

Nitrous acid (HONO) in the core city of the Central Plains Economic Region was measured using an ambient ion monitor from January 9 to 31, 2019. Measurement time intervals were classified into the following periods in accordance with the daily mean values of $PM_{2.5}$: clean days (CD), polluted days (PD), and severely polluted days (SPD). The HONO concentrations during CD, PD, and SPD were 1.2, 2.3, and 3.7 ppbv, respectively. The contribution of the homogeneous reaction, heterogeneous conversion, and direct emission to HONO sources varied under different pollution levels. The mean values of the net HONO production of the homogeneous reaction (P^{net}_{OH+NO}) in CD, PD, and SPD periods were 0.13, 0.26, and 0.56 ppbv h^{-1}, respectively. The average conversions of NO_2 (C_{HONO}) in CD, PD, and SPD periods were 0.72×10^{-2}, 0.64×10^{-2}, and 1.54×10^{-2} h^{-1}, respectively, indicating that the heterogeneous conversion of NO_2 was unimportant than the homogeneous reaction. Furthermore, the net production of the homogeneous reaction may have been the main factor for the increase in HONO under high-NO_X conditions (i.e., when the concentration of NO was higher than that of NO_2) at nighttime. Daytime HONO budget analysis showed that the mean values of the unknown source ($P_{unknown}$) during CD, PD, and SPD periods were 0.26, 0.40, and 1.83 ppbv h^{-1}, respectively. The values of P^{net}_{OH+NO}, C_{HONO}, and $P_{unknown}$ in the SPD period were comparatively larger than those in other periods, indicating that HONO participated in many reactions. The proportions of nighttime HONO sources also changed during the entire sampling period. Direct emission and a

heterogeneous reaction controlled HONO production in the first half of the night and provided a contribution larger than that of the homogeneous reaction. The proportion of homogenization gradually increased in the second half of the night due to the steady increase in NO concentration. The hourly level of HONO abatement pathways, except for OH + HONO, was at least 0.22 ppbv h^{-1} in the SPD period. The cumulative frequency distribution of the $HONO_{emission}$/HONO ratio (less than 20%) was approximately 77%, which suggested that direct emission was not important. The heterogeneous HONO production increased when the relative humidity (RH) increased, but it decreased when RH increased further. The average HONO/NO_X ratio (4.9%) was more than twice the assumed globally averaged value (2.0%).

1. Introduction

Nitrous acid (HONO) is important in the photochemical cycle and can provide hydroxyl radicals (OH) (Harrison et al., 1996):

$HONO + h\nu \rightarrow \cdot OH + NO$ ($300\ nm < \lambda < 405\ nm$) (R1).

According to measurement and simulation studies (Alicke et al., 2002), the contribution of HONO to ·OH concentration can reach 25−50%, especially when the concentration of OH radicals produced by the photolysis of ozone, acetone, and formaldehyde is relatively low (two to three hours after sunrise) (Czader et al., 2012). HONO photolysis was the most important primary source of ·OH which contributed up to 46 % of the total primary production rate of radicals for daytime conditions (Tan et al., 2018). ·OH is an important oxidant in the atmosphere, and it can react with organic substances, control the oxidation capacity of the atmosphere, and accelerate the formation of secondary aerosols in the urban atmosphere (Sörgel et al., 2011). Therefore, the changes in the contribution of the homogeneous reaction, heterogeneous conversion, and direct emission during pollution can be observed by studying the formation mechanism of HONO.

Several instruments have been used to determine ambient HONO concentrations, and these include differential optical absorption spectrophotometer (DOAS)

(Elshorbany et al., 2012; Winer and Biermann, 1994), long path absorption photometer (LOPAP) (Heland et al., 2001), wet chemical derivatization technique-HPLC/UV-Vis detection (Michoud et al., 2014), stripping coil-UV/Vis absorption photometer (SC-AP) (Pinto et al., 2014), IBBCEAS (Duan et al., 2018; Min et al., 2016), CIMS (Hirokawa et al., 2009; Roberts et al., 2010), and ambient ion monitor (AIM) (VandenBoer et al., 2014). A result comparison of different instruments showed that SC-AP is compatible with two spectral measurement instruments, namely, LOPAP and DOAS (Pinto et al., 2014). Compared with HONO measured by SC-AP deployed onsite, HONO measured by AIM has a small error and is within the acceptable analytical uncertainty (VandenBoer et al., 2014). Previous studies have reported that HONO concentrations range from a few pptv in clean remote areas to several ppbv (0.1−2.1 ppbv) in air-polluted urban areas (Hou et al., 2016; Michoud et al., 2014).

The sources of HONO are direct emission and homogeneous and heterogeneous reactions (Acker et al., 2005; Grassian, 2001; Kurtenbach et al., 2001). HONO can be directly discharged into the atmosphere during vehicle operation and biomass combustion. Through a tunneling experiment, Kurtenbach et al. (2001) have discovered that motor vehicles emit a small amount of HONO, and the HONO/NO_X ratio of HONO combustion sources (aside from NO_X and other pollutants) is 0.1–0.8%. Another study showed that the homogeneous reaction of NO and OH radicals is the major source of HONO under increased NO concentrations (Spataro et al., 2013). Furthermore, HONO can react with the ·OH (Alicke, 2003; Vogel et al., 2003). Tong et al. (2015) used NO + OH and HONO + OH homogeneous reactions, to calculate the net generation rate of HONO homogeneous reactions at night, which are expressed as:

$NO + {\cdot}OH \rightarrow HONO$ (R2);

$HONO + {\cdot}OH \rightarrow NO_2 + H_2O$ (R3).

Such calculations have been applied in studies on homogeneous reactions and daytime budgets (Hou et al., 2016; Huang et al., 2017). These are studies of homogeneous reactions, and some researchers have begun to explore the mechanism of NO_2

heterogeneous reactions. Finlayson-Pitts et al. (2003) studied the mechanism of chemical adsorption of NO_2 and H ions on the adsorbed surface was revealed by using isotope-labeled water:

$$2NO_2 + H_2O \rightarrow HONO + HNO_3 \quad \text{(R4)}.$$

In China, most studies for HONO have concentrated on the Yangtze River Delta, Pearl River Delta, and Jing-Jin-Ji region. For example, Hao et al. (2006) reported that field measurement results, especially HONO/NO_2 and relative humidity (RH), have a significant correlation and proved that heterogeneous reactions are an important source of nighttime HONO. Although the specific chemical mechanisms of heterogeneous reactions remain unknown, the intensity of HONO formation by NO_2 can be expressed by the HONO conversion frequency (Alicke et al., 2002; Li et al., 2012). Su et al. (2008a) revealed the importance of the ·OH from HONO during daytime (9:00–15:00 local time) and found that many unknown sources which are closely related to the solar radiation leading to HONO formation. The unknown sources of HONO may include the NO_2 photolysis of sooty surface and adsorbed nitric acid and nitrate at UV wavelengths (Kleffmann et al., 1999). The homogeneous nucleation of NO_2, H_2O, and NH_3 is the HONO formation pathway (Zhang and Tao, 2010). In the meanwhile, HONO can deposit and react with amines in forming nitrosamines (Li et al., 2012) for sinking. The method of budget analysis needs to include the HONO sources and sinks. The researchers suggested that the method of budget analysis is crucial for obtaining the missing source. Spataro et al. (2013) measured the HONO level in Beijing's urban area and discussed the spatiotemporal changes, meteorological effects, and contributions of HONO from different sources. They used the measured HONO data to compare pollution periods in Beijing's urban and suburban areas. Tong et al. (2015) discovered that the pathway of the HONO formation mechanism, namely, direct emission, heterogeneous formation, and homogeneous reaction is the same, but the pathway is different in the two sites. A few studies (Cui et al., 2018; Hou et al., 2016) compared the characteristics and sources of HONO during severe-pollution and clean periods.

Although the definitions of the two periods are different, both can be used to analyze the diurnal variation, source, and daytime budget of HONO during the aggravation of pollution.

There is no study of HONO in the Central Plains Economic Region (CPER), with a total population of 0.18 billion by the end of 2011. CPER is the important region for food production and modern agriculture published by the Chinese government (http://www.gov.cn/zhengce/content/2011-10/07/content_8208.htm). The file described the different factors which affect atmospheric pollution, including the level of economic development, energy structure, industrial structure and geographical location (solar radiation) with the Yangtze River Delta, Pearl River Delta, and Jing-Jin-Ji region. As the core city of CPER, Zhengzhou characterized by severe PM (particulate matters) pollution (Jiang et al., 2018b), is selected in the study. In recent years, comprehensive PM research has been conducted on the chemical characteristics of PM in Zhengzhou (Li et al., 2019), source apportionment (Liu et al., 2019), health risks (Jiang et al., 2019), and emission source profiles (Jiang et al., 2018a). However, no study has been performed on the sources and characteristics of HONO in Zhengzhou. Moreover, no synthetic research on different pollution levels in the area is available. In the current study, AIM was used to sample and analyze HONO concentrations. The interactions between HONO and other factors, such as $PM_{2.5}$, during pollution, were assessed to understand the formation and removal of HONO and the influence on different pollution periods. The levels of $PM_{2.5}$ were divided into three periods to analyze the HONO sources, sinks, and reactions in different periods. Many papers (Huang et al., 2017; Tong et al., 2016) took $PM_{2.5}$ as the main control factor of HONO, and studied the differences of HONO sources and characteristics between clean and polluted periods. No homogeneous reaction, direct emission, heterogeneous reaction, and daytime budget analysis were conducted during the period of worsening pollution (namely HD period in this paper). Total NO_X emissions in cities with different leading factors of emissions have been declining year by year due to Chinese government emission control measures,

but some Chinese cities are still in high-NO_X areas (e.g. Beijing, Shanghai, Guangzhou and Zhengzhou.) (Kim et al., 2015; Liu et al., 2017). Under high-NO_X conditions, some papers (Cui et al., 2018; Hou et al., 2016) suggested that heterogeneous reaction was the main source of HONO and did not conduct a quantitative analysis of homogeneous reaction, especially in winter. So, we explore relevant studies of homogeneous reactions. In addition, the source contributions of HONO at night varied with the degree of pollution level were not explained. RH was also analyzed to provid a detailed understanding of HONO generation intensity under different RH conditions. Analysis of the sources of HONO at night provides strong support for conducting HONO budget analysis during daytime. To the best of the authors' knowledge, the formation characteristics of HONO at continuous and high time resolutions and different pollution levels have not been studied in Zhengzhou. This work can assist the governments of the CPER in formulating policy to decrease the level of HONO precursors, i.e., NO and NO_2, and HONO direct emission from the vehicle.

2. Experiment and methods

2.1. Sampling site and period

The sampling site is on the rooftop (sixth floor) of a building in Zhengzhou University (34°48' N, 113°31' E), which is located in the northwestern part of Zhengzhou, China. The observation height is about 20 m from the ground, and the observation platform is relatively open without any tall buildings around. The site is about 500 m from the western Fourth-Ring Expressway of Zhengzhou City and about 2 km from Lian Huo Expressway to the north. The measurement period was from January 9 to 31, 2019. Daily data were divided into two periods, namely, daytime (7:00–18:00 local time) and nighttime (19:00–6:00 the next day, LT).

2.2. Instruments

AIM (URG-9000D, Thermo, USA), an online ion chromatographic monitoring system for particle and gas components in the atmosphere, was used to measure HONO concentration continuously at a temporal resolution of 1 h. The atmospheric airflow

entered the $PM_{2.5}$ cyclone cutting head through the sample tube, and gas–solid separation was performed with a parallel plate denuder with a new synthetic polyamide membrane. The denuder had no moving parts and could be changed without stopping the sampler. HONO was absorbed by the denuder with an absorption liquid (5.5 mM H_2O_2). The chemicals that could be oxidized were absorbed by H_2O_2 on the porous membrane surface, but several gases (e.g., O_2 and N_2) were expelled by the air pump. The abundance of other gaseous acids and bases affected the efficiency of HONO collection by AIM due to the relation between Henry's law constant and pH. This measurement method and its details have been successfully evaluated in many field studies (Markovic et al., 2012; Tian et al., 2018; Wang et al., 2019), and shown in the supplement. In addition, a QXZ1.0 automatic weather station (Yigu Technologies, China) was used for synchronous observation of meteorological parameters, including temperature (T), RH, wind direction (WD), and wind speed (WS). A temporal resolution of the model analyzer (TE [used for measuring O_3], 48i [used for measuring CO], 42i [used for measuring NO, NO_X, and NO_2], and TEOM 1405 $PM_{2.5}$ monitor [used for measuring $PM_{2.5}$], Thermo Electron, USA) is 1 h. Detailed information can be found in the work of (Wang et al., 2019). Measurement technique, detection limit, and accuracy of measured species are shown in **Table S1**.

During the sampling period, all instruments were subjected to strict quality control to avoid possible contamination. The instrument accessories and sampling process were periodically replaced and calibrated, respectively. The instrument parts and consumables were changed before the observation process, and the sampling flow was calibrated to reduce the negative effect of accessories. Before this measurement period, the membrane of the denuder has been replaced and standard anion and cation solutions have been prepared on Jan. 3rd. The standard curve should be drawn to ensure the appropriateness of the correlation coefficient ($\geqslant$ 0.999) and the accuracy of the sample retention time and response value. The minimum detection limit of AIM was 0.004 ppbv. Other detailed information can be found in the work of (Wang et al., 2019).

3. Results and Discussion

3.1. Temporal variations of meteorological parameters and pollutants

The daily changes in meteorological parameters and $PM_{2.5}$ are shown in **Fig. 1**. In accordance with the daily average concentration level of $PM_{2.5}$, the analysis and measurement process was divided into three periods (clean days [CD], polluted days [PD], and severely polluted days [SPD]). The days wherein the daily averages of $PM_{2.5}$ were lower than the daily average of second grade in China National Ambient Air Quality Standards (CNAAQS) (75 μg m^{-3}) represented CD (January 9, 16, 17, 21, 22, 23, 26, and 31), with RH ranging from 5 to 79% and WS ranging from 0 to 4.2 m s^{-1}. The days wherein the daily averages of $PM_{2.5}$ were between 75 and 115 μg m^{-3} represented PD (January 10, 15, 18, 20, 25, 27, and 28), with RH ranging from 17 to 86% and WS ranging from 0 to 4.6 m s^{-1}. The days wherein the daily averages of $PM_{2.5}$ were higher than 115 μg m^{-3} represented SPD (January 11, 12, 13, 14, 19, 24, 29 and 30), with RH ranging from 30 to 96% and WS ranging from 0 to 3.5 m s^{-1}. Northwest or east wind was observed in most of the observation periods, except for January 21–22. WD was north, the maximum WS reached 4 m/s, the $PM_{2.5}$ concentration decreased rapidly, and the effect of pollutant removal was evident. **Table 1** lists the data statistics of HONO, $PM_{2.5}$, NO_2, NO, NO_X, HONO/NO_2, HONO/NO_X, O_3, CO, T, RH, WS, and WD during the measurement period together with their mean value ± standard deviation. The meteorological parameters in **Table 1** show that the average RH in CD, PD, and SPD periods was 33, 49, and 68%, respectively. In SPD, RH was high and WD was low (mean value of 0.4 m s^{-1}).

In accordance with the data on trace gases, the average HONO values in CD, PD, and SPD were 1.1, 2.3, and 3.7 ppbv, respectively. The mean values of NO_2 were 25, 33, and 42 ppbv (46, 63, and 78 μg m^{-3} lower than the first grade in CNAAQS [80 μg m^{-3}]), respectively. The mean values of CO were 1, 1, and 2 ppmv (1, 2, and 2 mg m^{-3} lower than the first grade in CNAAQS [4 mg m^{-3}]), respectively. **Fig. 2** shows the concentration changes in HONO and gas species throughout the measurement period.

The variations of the average HONO, $PM_{2.5}$, NO_2, and CO in the three periods were similar. The mean values of all pollutant concentrations except O_3 in the SPD period were the largest, and those in the CD period were the smallest. The highest mean value of O_3 occurred in the CD period, similar to previous observations (Hou et al., 2016; Huang et al., 2017; Zhang et al., 2019).

The HONO concentrations ranged from 0.2 to 14.8 ppbv and had an average of 2.5 ppbv, which is higher than the average values of 0.6 (Rappenglück et al., 2013), 1.5 (Hou et al., 2016), and 1.0 ppbv (Huang et al., 2017) in previous urban studies. The diurnal variations of HONO during the measurement were similar in the three periods, as shown in **Fig. 3** and **Fig. 4**. The diurnal variations of HONO, NO, NO_2, O_3, $HONO/NO_2$, and $HONO/NO_X$ are illustrated in **Fig. 4**. The error bars of **Fig. 4** were placed separately in the tables of the supplement (**Table S2**). After sunset, the HONO concentrations in CD, PD, and SPD began to accumulate due to the attenuation of solar radiation and the stabilization of the boundary layer (Cui et al., 2018). The maximum values of 1.7, 4.1, and 6.9 ppbv were reached in the morning (08:00–10:00 LT) in CD, PD, and SPD, respectively. After 10:00 LT, the HONO concentration decreased because of the increased solubility and rapid photolysis, remaining at a low level before sunset (14:00–16:00 LT). The NO concentration decreased rapidly in the forenoon, and remained low in the afternoon. After sunset, the concentrations of NO and NO_2 began to increase and remained at a higher level than the daytime. Furthermore, the diurnal variation of NO in the CD period was similar to that of NO_2. The peak was reached at around 09:00 LT due to vehicle emission in the morning rush hours, and the lowest value was observed at around 16:00 LT. After 18:00 LT, the boundary layer height decreased in the evening rush hours, resulting in an increase in NO and NO_2 concentrations (Hendrick et al., 2014). O_3 showed a diurnal cycle and had maximum values in CD, PD, and SPD periods in the afternoon. The $HONO/NO_2$ ratio is commonly used to estimate the formation of HONO in NO_2 transformation (Wang et al., 2013). Compared with HONO formation, NO_2 transformation is less affected by the

253 migration of atmospheric airmass during atmospheric migration (Li et al., 2012). The
254 $HONO/NO_2$ ratio in the CD period began to increase after sunset and reached its peak
255 at night. Then, it decreased in the morning as a result of the enhancement of NO_2
256 emission and photolysis of HONO. However, the mean value of $HONO/NO_2$ in PD and
257 SPD periods gradually increased from nighttime and eventually reached the maximum
258 values of 14.3 and 18.9% at 09:00 and 10:00 LT, respectively. The average $HONO/NO_X$
259 ratio (4.9%) was more than twice the assumed globally averaged value (2.0%)
260 (Elshorbany et al., 2014). This result indicates that the strength of the heterogeneous
261 reaction increased slightly with the exacerbation of pollution. The $HONO/NO_2$ ratio
262 showed a diurnal cycle with a low level in the afternoon and a high level after sunset
263 due to the heterogeneous reaction of NO_2 on the ground and aerosol surface (Su et al.,
264 2008b). For comparison, the daytime and nighttime HONO, $HONO/NO_2$, and
265 $HONO/NO_X$ mean values in other cities around the world are listed in **Table 2**. The
266 values of HONO, $HONO/NO_2$, and $HONO/NO_X$ in Zhengzhou are relatively higher
267 than those in other parts of the world. The reason for this phenomenon is that
268 Zhengzhou is a high-NO_X area which provides HONO with abundant precursors (NO_2
269 and NO) in winter (Kim et al., 2015).

270 ## 3.2. Nocturnal HONO sources and formation

271 ### 3.2.1. Homogeneous reaction of NO and OH

272 The homogeneous reaction of NO and OH (R2 and R3) is the main pathway of
273 HONO formation in the gas phase. Spataro et al. (2013) found that the formation
274 mechanism leads to an increase in HONO in high-pollution areas with an increase in
275 NO at night. P_{OH+NO}^{net} can be understood as the net hourly HONO production amount
276 of homogeneous reaction and is calculated as

277 $$P_{OH+NO}^{net} = k_{OH+NO}[OH][NO] - k_{OH+HONO}[OH][HONO] \quad (1).$$

278 At T = 298 K and P = 101 kPa, the rate constants of k_{OH+NO} and $k_{OH+HONO}$ are
279 9.8×10^{-12} and 6.0×10^{-12} molecule cm^{-3}, respectively (Atkinson et al., 2004; Sander et
280 al., 2003). [OH] is the concentration of ·OH that was not measured during the campaign.

Therefore, Tan et al. (2018) found that by the field measurement, the average concentration of ·OH in Beijing at nighttime was about 2.5×10^5 molecule cm^{-3}. Moreover, the same ·OH concentration was also used to calculate the homogeneous reaction of HONO in the recent researches of Beijing (Zhang et al., 2019), Shanghai (Cui et al., 2018), and Xi'an (Huang et al., 2017). And, nighttime OH concentration increased as the latitude decreases ranged 3 to 6×10^5 molecule cm^{-3} (Lelieveld et al., 2016). Zhengzhou has a lower latitude than Beijing, so the concentration of OH used in this study is 2.5×10^5 molecule cm^{-3}. P^{net}_{OH+NO} primarily depends on the concentrations of NO and HONO because the reaction rates of k_{OH+NO} and $k_{OH+HONO}$ are close. **Fig. 5** shows the nocturnal variations of P^{net}_{OH+NO}, NO, and HONO during CD, PD, and SPD periods. The error bars of **Fig. 5** were placed separately in the tables of the supplement (**Table S3**). When the NO levels were high, the variations of P^{net}_{OH+NO} followed those of NO during the three periods (Atkinson et al., 2004). The mean value of P^{net}_{OH+NO} was 0.33 ppbv h^{-1}, and the specific values in CD, PD, and SPD periods were 0.13, 0.26, and 0.56 ppbv h^{-1}, respectively. We assumed ± 50% ·OH values to estimate the uncertainty of P^{net}_{OH+NO}. The ·OH values of 1.25×10^5 and 3.75×10^5 molecule cm^{-3} were calculated the P^{net}_{OH+NO} values of 0.16 and 0.49 ppbv h^{-1}.

P^{net}_{OH+NO} varied from 0.01 to 0.47 ppbv h^{-1} during the CD period. The mean value of P^{net}_{OH+NO} increased before midnight, decreased after midnight, and increased slightly at 3 am. In the PD period, P^{net}_{OH+NO} ranged from 0.07 to 0.44 ppbv h^{-1}. The situation was similar to that in the CD period, except that the value remained almost constant. In addition, the contribution of HONO from homogeneous reaction during the SPD period was larger than those in the CD and PD periods, and the level of P^{net}_{OH+NO}, with an average value of 0.56 ppbv h^{-1}, was lower than the value in a previous study (2.18 ppbv h^{-1} in Beijing) (Tong et al., 2015). From 19:00 LT to 03:00 LT, the mean value of P^{net}_{OH+NO} increased from 0.15 to 0.9 ppbv h^{-1}. HONO increased from 2.84 to 4.59 ppbv and subsequently decreased to 4.43 ppbv. By integrating P^{net}_{OH+NO} during the eight hours, the homogeneous reaction can provide an accumulated HONO formation of at

least 3.36 ppbv (i.e., 0.15 + 0.20 + 0.25 + 0.25 + 0.35 + 0.56 + 0.7 + 0.9 ppbv). However, the mean accumulation value of measured HONO in this nighttime period was merely 1.59 ppbv. With the increase in pollution level, the HONO accumulation period at nighttime increased. This result indicates that first, the homogeneous reaction of OH + NO is sufficient to augment HONO in the first half of the night, although NO_2 transformation and other sources may still exist. When the concentration of NO is relatively high, the net production generated by OH + NO may be the leading factor for the increase in HONO at night (Tong et al., 2015). Second, the hourly level of HONO abatement pathways, except OH + HONO, should be at least 0.22 ppbv h^{-1} (i.e., 3.36 – 1.59 ppbv)/8 h). This phenomenon may arise because the dry deposition on ground surfaces can be the main HONO removal pathway at night, similar to a previous study (Li et al., 2012).

3.2.2. Direct emission

At present, no HONO emission inventory or emission factor database for Zhengzhou is available. As a result, estimating any HONO from direct emission is difficult. In the current study, directly emitted HONO could have been generated by vehicle exhaust and biomass combustion because the site is close to the western Fourth-Ring Expressway of Zhengzhou City and about Lian Huo Expressway to the north. Hence, only night data (17:00–06:00 LT) were considered to avoid the problem of instant photolysis of directly emitted HONO. In a previous study, the HONO/NO_X ratio from tunnel measurement was set to 0.65% to estimate an upper limit of HONO emitted by traffic near the site (Kurtenbach et al., 2001). The minimum value of HONO/NO_X in the SPD period in the current work was 1.5%, which is slightly higher than the value measured in the abovementioned study. Directly emitted HONO at night was not transformed immediately. The HONO concentrations corrected by direct emissions are given as

$$[HONO]_{correct} = [HONO] - [HONO]_{emission} = [HONO] - 0.0065 \times [NO_X] \quad (2),$$

where $[HONO]_{emission}$, $[NO_X]$, and 0.0065 are direct emission HONO concentration,

337 NO_X concentration, and HONO/NO_2 direct emission ratio, respectively. The direct
338 emission contribution was estimated by comparing the direct emission HONO with the
339 observed HONO. The ranges of $HONO_{emission}$/HONO in CD, PD, and SPD periods were
340 2–52%, 6–34%, and 2–41%, respectively, and the mean values were 17, 16, and 16%,
341 respectively. The frequency distribution of the $HONO_{emission}$/HONO ratio at nighttime
342 is shown in **Fig. 6**. For this upper limit estimation, the frequency distribution of
343 $HONO_{emission}$/HONO (less than 20%) was approximately 77%. Hence, direct emission
344 may not be the main reason for the high growth of HONO levels. Compared with the
345 direct emission of other sites, that of the measurement site accounted for a lower
346 proportion possibly because the site is relatively far from the highway on the campus.

347 **3.2.3. Heterogeneous conversion of NO_2 to HONO**

348 NO_2 is an important precursor for HONO formation. In addition, recent
349 field measurements in many urban locations have shown that a positive
350 correlation exists between HONO and NO_2 (Cui et al., 2018; Hao et al.,
351 2006; Huang et al., 2017; Zhang et al., 2019), suggesting they have a
352 common source. Moreover, Acker et al. (2005) reported that different
353 meteorological conditions may lead to significant differences in the
354 relationship between the source and receptor, and these differences lead to
355 various types of correlation. During the measurement period, the
356 HONO/NO_2 ratio varied between 1.3 and 59.0%, with an average of 7.6%,
357 which is slightly higher than the 6.2% average in a previous study (Cui et
358 al., 2018). The HONO/NO_2 ratio calculated in this work is much larger than
359 that calculated for direct emission (< 1%) (Kurtenbach et al., 2001), suggesting
360 that heterogeneous reactions may be a more important pathway for HONO
361 production than direct emissions. With regard to the heterogeneous
362 conversion of NO_2, several studies (An et al., 2012; Shen and Zhang, 2013)
363 have reported that the surface of soot particles is the medium of NO_2
364 conversion. The contribution of soot surface to HONO production is usually

much lower than expected because the uptake efficiency of NO_2 decreases with the prolonged reaction time caused by surface deactivation. The aerosol surface is an important medium for the heterogeneous transformation from NO_2 to HONO (Liu et al., 2014). The mass concentration of aerosols was used as an alternative to identify the influence of aerosols in this study because the surface density of aerosols could not be obtained.

The correlations between $PM_{2.5}$ and $HONO/NO_2$ ratio in CD, PD, and SPD periods are shown in **Fig. 7**. With the exacerbation of the $PM_{2.5}$ level, the average value of $HONO/NO_2$ gradually increased, indicating that the aerosol surface occupied an important position in the heterogeneous transformation. A comparison of $HONO/NO_2$ and HONO with $PM_{2.5}$ showed that the correlation between $HONO/NO_2$ and $PM_{2.5}$ ($R^2 = 0.23$) was weaker than that between HONO and $PM_{2.5}$ ($R^2 = 0.55$) in the entire period. The main source of HONO could not have been the transformation of NO_2. Notably, the HONO correlation in the PD period was significantly stronger than that in the two other periods. This result proves that HONO-related reactions occurred more frequently during this period. The fair correlation between HONO and $PM_{2.5}$ may pinpoint the mainly anthropogenic origins of these two pollutants with the high direct or indirect contribution of combustion sources. The reason for the increased HONO during the heavy pollution period could be by the comparatively high loading and large particle surface (Cui et al., 2018). Similar phenomena have been observed in a correlation study on CO and HONO wherein CO was used as a tracer for traffic-induced emissions and tested by considering the correlation between HONO and CO over an identical time interval (Qin et al., 2009). The correlation coefficient between HONO and CO was relatively moderate ($R^2 = 0.43$), indicating that HONO and CO could come from the same source of emissions. Generally speaking, CO and

NO are mainly related to combustion processes such as vehicle emissions, fossil fuel and biomass combustion (Tong et al., 2016). Thus, fossil fuel and biomass combustion may contribute to HONO production, but they can not be measured directly.

The absorbed water influenced the heterogeneous formation (Stutz et al., 2004). The influence of RH on the heterogeneous conversion is shown in **Fig. 7(d)**. When RH was less, the $HONO/NO_2$ ratio slowly increased. When RH was increased, the $HONO/NO_2$ ratio began to increase rapidly with RH. The $HONO/NO_2$ ratio decreased when RH reached a certain high level. Similar variation patterns have been obtained in previous studies (Huang et al., 2017; Qin et al., 2009; Tong et al., 2015). Surface adsorbed water functions not only as sources but also as sinks of HONO by affecting the hydrolysis of NO_2 and the sedimentation of HONO to generate HONO (Ammann et al., 1998). When RH ranged at the middle level, the heterogeneous conversion of NO_2 to HONO was more significant than that of deposition. This phenomenon confirms that RH improved the conversion efficiency (Stutz et al., 2004). However, the surface reached saturation when RH reached a certain high level. The excess water restricted NO_2 transformation (Wojtal et al., 2011). The absorption and dissolution of HONO by the saturated surface water layer caused $HONO/NO_2$ ratio to decrease drastically.

The correlation between $HONO_{correct}$ and NO_2 at nighttime is shown in **Fig. S1**. $HONO_{correct}$ was used in the calculation to exclude the influence of direct emission on NO_2 conversion. The nocturnal variations of $HONO_{correct}$, NO_2, and $HONO_{correct}/NO_2$ ratios in the CD, PD, and SPD periods are presented in **Fig. 8**. The error bars of **Fig. 8** were placed separately in the tables of the supplement (**Table S4**). In general, the $HONO_{correct}/NO_2$ ratio reached its maximum at or before midnight but decreased after midnight. In the PD and

SPD periods, HONO was generated by heterogeneous reaction (R4), and NO_2 decreased after midnight. The production of HONO was equal to its loss (mainly night deposition), and HONO concentration reached a relatively s In the current study, directly emitted HONO state (Stutz, 2002). The weak correlation between nighttime $HONO/NO_2$ and $PM_{2.5}$ can be reasonably explained by the stable $HONO_{correct}/NO_2$ ratio after midnight (Qin et al., 2009). A previous study (Xu et al., 2015) found that a low $HONO_{correct}$ in the first half of the night (19:00–00:00 LT) indicates an important contribution of automobile exhaust emissions, and a low $HONO_{correct}$ in the second half of the night means heterogeneous reactions dominate. Therefore, the heterogeneous reaction conversion rate of HONO was calculated in the current study by using the data of $HONO_{correct}$.

The conversion rate of HONO (C_{HONO}) is usually used as an indicator to test the efficiency of NO_2 heterogeneous reactions. Total $HONO_{correct}$ was assumed to be generated by the heterogeneous transformation of NO_2. The formula for the conversion rate of NO_2 (C_{HONO}) is as follows (Su et al., 2008a; Xu et al., 2015):

$$C_{HONO} = \frac{([HONO_{correct}]_{t2} - [HONO_{correct}]_{t1}}{(t2 - t1)\,[NO_2]} \quad (3),$$

where $[NO_2]$ is the average concentration of NO_2 within the t2–t1 time interval (1 h). In this study, the averaged conversion rate of NO_2 was 1.02×10^{-2} h^{-1}. The mean values of C_{HONO} in the CD, PD, and SPD periods were 0.72×10^{-2}, 0.64×10^{-2}, and 1.54×10^{-2} h^{-1}, respectively. The averaged conversion rates in this study were 0.58×10^{-2} and 1.46×10^{-2} h^{-1} higher than those of Beijing I (polluted) and II (heavily polluted) periods, respectively. The increase in the conversion rate demonstrates that NO_2 had high reaction efficiency through the process from NO_2 to HONO in the aggravation of pollution, which could have led to the high utilization efficiency of the aerosol surface. The exact uptake coefficients of NO_2 on ground and aerosol surfaces

are variable and should be different (Harrison and Collins, 1998). The present analysis simplified this process by treating the ground and aerosol surfaces the same. The uptake coefficient is mainly dependent on the surface characteristics, e.g. surface type and moisture (Lu et al., 2018).

3.3. Daytime HONO budget

The expression of $dHONO/dt$ represents the observed variations of hourly HONO concentrations, for which we can use $\Delta HONO/\Delta dt$ instead:

$$dHONO/dt = sources - sinks$$

$$= (P_{unknown} + P_{OH+NO} + P_{emi} + P_{het}) - (L_{OH+HONO} + L_{photo}) \quad (4),$$

$$P_{OH+NO} = k_{OH+NO}\,[OH]\,[NO] \quad (5),$$

$$L_{OH+HONO} = k_{OH+HONO}\,[OH]\,[HONO] \quad (6).$$

The $dHONO/dt$ calculated from the measurements was small and evenly distributed around zero (Li et al., 2012). $P_{unknown}$ is the production rate by an unknown daytime HONO source. P_{OH+NO} is the rate of reaction of NO and OH. P_{emi} represents the direct emission rate of HONO from combustion processes. By studying the source and reduction, the daytime HONO budget was analyzed with Eq. (4) (Su et al., 2008b). The heterogeneous transformation mechanism was assumed to be the same for day and night. Therefore, the daytime heterogeneous productivity ($P_{het} = C_{HONO} \times [NO_2]$) was calculated with the nighttime mean values of C_{HONO} in different periods. $L_{OH+HONO}$ is the rate of the reaction between OH and HONO (R3). The calculation formulas of P_{OH+NO} and $L_{OH+HONO}$ have been provided in **Section 3.2.1**. Upon sunlight irradiation, ·OH and NO were formed as R1. L_{photo} represents the photolysis loss rate of HONO ($L_{photo} = J_{HONO} \times [HONO]$). The photolysis frequency and ·OH concentration could not be directly measured in this study. Therefore, the tropospheric ultraviolet and visible (TUV) transfer model of the National Center for Atmospheric Research (http://cprm.acom.ucar.edu/Models/TUV/

Interactive_TUV/) (Hou et al., 2016) was used to calculate the J_{HONO} value. The J_{HONO} values obtained this way were assumed in clear sky days without clouds. O_3 column and the surface albedo. O_3 column density measured by the Ozone Monitoring Instrument (OMI, data available at https://ozonewatch.gsfc.nasa.gov/data/omi/Y2019/). The O_3 column density ranges from 292 to 306 DU during the entire period. The experimental site being situated in an urban region, the surface albedo is considered as 0.13 (Sailor, 1995). The ground elevation and the measurement altitude are 168 and 188 m respectively. The concentration of OH radicals was calculated with the formulas of NO_2, O_3, and J_{O^1D} in the supplement (Rohrer and Berresheim, 2006). Aerosol effects were considered by using aerosol optical thickness (AOD), single scattering albedo (SSA), and Angstrom exponent as inputs in the TUV model. Typical AOD, SSA, and Angstrom exponent values of 1.32, 0.9, and 1.3, respectively, were adopted for the PD and SPD periods. In the CD period, the respective values were 0.66, 0.89, and 1.07 (Che et al., 2015; Cui et al., 2018; Hou et al., 2016). We wanted to study that under the same output conditions from the TUV model in the PD and SPD periods, the impact of different pollution levels changed on the daytime budget. Hence, the average profiles of J_{HONO} and J_{O^1D} concentrations in the CD, PD, and SPD periods are shown in **Fig. 9**. The mean values of J_{HONO} and ·OH concentration at noon in the CD, PD, and SPD periods were 5.93×10^{-4}, 3.79×10^{-4}, and 3.79×10^{-4} molecule cm^{-3} and 4.10×10^{6}, 2.93×10^{6}, and 3.76×10^{6} molecule cm^{-3}, respectively. The results of the calculated OH radicals ranged from $(0.58-11.49)\times10^{6}$ molecule cm^{-3}, and the mean value was 3.57×10^{6} molecule cm^{-3} at noon in Zhengzhou.

Each production and loss rate of daytime HONO during CD, PD, and SPD periods is illustrated in **Fig. 9** together with dHONO/dt. $P_{unknown}$ was at a high level before midday. $P_{unknown}$ approached 0 ppbv h^{-1} after midday. In the CD, PD, and SPD periods, the mean values of $P_{unknown}$ were 0.26, 0.40,

and 1.83 ppbv h^{-1}, respectively; the mean values of P_{OH+NO} were 1.14, 2.07, and 4.03 ppbv h^{-1}, respectively; the mean values of P_{emi} were 0.17, 0.30, and 0.43 ppbv h^{-1}, respectively; and the mean values of P_{het} were 0.14, 0.18, and 0.55 ppbv h^{-1}, respectively. The midday time $P_{unknown}$ (1.83 ppbv h^{-1}) calculated in Zhengzhou during the winter haze pollution period was close to the result obtained from Beijing's urban area (Hou et al., 2016) (1.85 ppbv h^{-1}). The $P_{unknown}$ contribution to daytime HONO sources in CD, PD, and SPD periods accounted for 15, 14, and 28% of the HONO production rate ($P_{unknown}$ + P_{OH+NO} + P_{emi} + P_{het}), respectively. Previous studies (Spataro et al., 2013; Yang et al., 2014) have shown that meteorological conditions, such as solar radiation and WS, can affect unknown sources. The low $P_{unknown}$ contribution of daytime HONO concentration may be related to the low solar radiation and low wind speed during severe pollution. The concentration of NO has a great influence on P_{OH+NO}, so the homogeneous reaction is still an important pathway of HONO production during the daytime. In addition to the photolysis of HONO and the homogeneous reaction of HONO and OH, one or more important sinks might exist to control the variation between the sources and sinks of the daytime HONO during complex contamination. However, further research is needed to analyze the unknown sources of daytime HONO.

4. Conclusions

Ambient HONO measurement using AIM with other atmospheric pollutants and meteorological parameters was conducted in the CPER. The HONO concentrations during the entire measurement varied from 0.2 to 14.8 ppbv, with an average of 2.5 ppbv. The HONO concentrations in the CD, PD, and SPD periods were 1.1, 2.3, and 3.7 ppbv, respectively, and the HONO/NO_2 ratios were 4.7, 7.1, and 9.4%, respectively. HONO concentration was a combined action of direct emission and heterogeneous reaction, and the contributions of the two were higher than that of homogeneous reaction in the first half of the night. However, the proportion of homogenization gradually increased in the second half of the night due to the steady increase in NO

concentration. The hourly level of other HONO abatement pathways aside from OH + HONO should be at least 0.22 ppbv h^{-1} in the SPD period. The sum of the frequency distributions of the $HONO_{emission}$/HONO ratio (less than 20%) was approximately 77%, indicating that the direct emission of HONO was not the main source of the observed HONO level at night. The mean values of $HONO_{emission}$/HONO in the CD, PD, and SPD periods were 17, 16, and 16%, respectively. This phenomenon means that the policy of restricting motor vehicles published by the local government in January 2019 had a good effect on decreasing HONO emissions. In addition, when RH increased at the middle level, the heterogeneous HONO production increased, but it decreased when RH increased further due to the effect of surface water. The contribution of the three sources varied with different pollution levels. The mean values of C_{HONO} in the CD, PD, and SPD periods were 0.72×10^{-2}, 0.64×10^{-2}, and 1.54×10^{-2} h^{-1}, respectively. At nighttime in the SPD period, the heterogeneous conversion of NO_2 appeared to be unimportant. Furthermore, the net production generated by homogeneous reaction may be the leading factor for the increase in HONO under high-NO_X conditions (i.e., the concentration of NO was relatively higher than that of NO_2) at nighttime. The mean value of P^{net}_{OH+NO} in the CD, PD, and SPD periods were 0.13, 0.26, and 0.56 ppbv h^{-1}, respectively. Daytime HONO budget analysis showed that the mean values of $P_{unknown}$ in the CD, PD, and SPD periods were 0.26, 0.40, and 1.83 ppbv h^{-1}, respectively. Although the values of P_{OH+NO} had high uncertainty because of the variation of NO concentrations, P_{OH+NO} contributed the most to HONO production during the daytime. After the analysis, C_{HONO}, P^{net}_{OH+NO}, and $P_{unknown}$ in the SPD period were larger than those in the other periods, indicating that HONO participated in many reactions.

Acknowledgments

The study was supported by the financial support from the National Natural Science Foundation of China (51808510, 51778587), National Key Research and Development Program of China (2017YFC0212400), Natural Science Foundation of Henan Province of China

561 (162300410255).

Reference

Acker, K., Möller, D., Auel, R., Wieprecht, W., and Kalaß, D.: Concentrations of nitrous acid, nitric acid, nitrite and nitrate in the gas and aerosol phase at a site in the emission zone during ESCOMPTE 2001 experiment, Atmos. Res., 74, 507-524, https://doi.org/10.1016/j.atmosres.2004.04.009, 2005.

Alicke, B., Platt, U., and Stutz, J.: Impact of nitrous acid photolysis on the total hydroxyl radical budget during the Limitation of Oxidant Production/Pianura Padana Produzione di Ozono study in Milan, J. Geophys. Res., https://doi.org/10.1029/2000jd000075, 2002.

Alicke, B.: OH formation by HONO photolysis during the BERLIOZ experiment, J. Geophys. Res., 108, https://doi.org/10.1029/2001jd000579, 2003.

Ammann, M., Kalberer, M., Jost, D. T., Tobler, L., Rössler, E., Piguet, D., Gäggeler, H. W., and Baltensperger, U.: Heterogeneous production of nitrous acid on soot in polluted air masses, Nature, 395, 157-160, https://doi.org/10.1038/25965, 1998.

An, J., Li, Y., Chen, Y., Li, J., Qu, Y., and Tang, Y.: Enhancements of major aerosol components due to additional HONO sources in the North China Plain and implications for visibility and haze, Adv. Atoms. Sci., 30, 57-66, https://doi.org/10.1007/s00376-012-2016-9, 2012.

Atkinson, R., Baulch, D. L., Cox, R. A., Crowley, J. N., Hampson, R. F., Hynes, R. G., Jenkin, M. E., Rossi, M. J., and Troe, J.: Evaluated kinetic and photochemical data for atmospheric chemistry: Volume I - gas phase reactions of O_x, HO_x, NO_x and SO_x species, Atmos. Chem. Phys., 4, 1461-1738, https://doi.org/10.5194/acp-4-1461-2004, 2004.

Che, H., Xia, X., Zhu, J., Wang, H., Wang, Y., Sun, J., Zhang, X., and Shi, G.: Aerosol optical properties under the condition of heavy haze over an urban site of Beijing, China, Environ. Sci. Pollut. Res., 22, 1043-1053, https://doi.org/10.1007/s11356-014-3415-5, 2015.

589 Cui, L., Li, R., Zhang, Y., Meng, Y., Fu, H., and Chen, J.: An observational study of
590 nitrous acid (HONO) in Shanghai, China: The aerosol impact on HONO formation
591 during the haze episodes, Sci. Total Environ., 630, 1057-1070,
592 https://doi.org/10.1016/j.scitotenv.2018.02.063, 2018.
593 Czader, B. H., Rappenglück, B., Percell, P., Byun, D. W., Ngan, F., and Kim, S.:
594 Modeling nitrous acid and its impact on ozone and hydroxyl radical during the
595 Texas Air Quality Study 2006, Atmos. Chem. Phys., 12, 6939-6951,
596 https://doi.org/10.5194/acp-12-6939-2012, 2012.
597 Duan, J., Qin, M., Ouyang, B., Fang, W., Li, X., Lu, K., Tang, K., Liang, S., Meng, F.,
598 Hu, Z., Xie, P., Liu, W., and Häsler, R.: Development of an incoherent broadband
599 cavity-enhanced absorption spectrometer for in situ measurements of HONO and
600 NO_2, Atmos. Meas. Tech., 11, 4531-4543, https://doi.org/10.5194/amt-11-4531-
601 2018, 2018.
602 Elshorbany, Y. F., Steil, B., Brühl, C., and Lelieveld, J.: Impact of HONO on global
603 atmospheric chemistry calculated with an empirical parameterization in the EMAC
604 model, Atmos. Chem. Phys., 12, 9977-10000, https://doi.org/10.5194/acp-12-9977-
605 2012, 2012.
606 Elshorbany, Y. F., Crutzen, P. J., Steil, B., Pozzer, A., Tost, H., and Lelieveld, J.:
607 Global and regional impacts of HONO on the chemical composition of clouds and
608 aerosols, Atmos. Chem. Phys., 14, 1167-1184, https://doi.org/10.5194/acp-14-1167-
609 2014, 2014.
610 Finlayson-Pitts, B. J., Wingen, L. M., Sumner, A. L., Syomin, D., and Ramazan, K.
611 A.: The heterogeneous hydrolysis of NO2 in laboratory systems and in outdoor and
612 indoor atmospheres: An integrated mechanism, PCCP, 5, 223-242,
613 https://doi.org/10.1039/b208564j, 2003.
614 Grassian, V. H.: Heterogeneous uptake and reaction of nitrogen oxides and volatile
615 organic compounds on the surface of atmospheric particles including oxides,
616 carbonates, soot and mineral dust: Implications for the chemical balance of the

troposphere, Int. Rev. Phys. Chem., 20, 467-548, https://doi.org/10.1080/01442350110051968, 2001.

Hao, N., Zhou, B., Chen, D., and Chen, L.: Observations of nitrous acid and its relative humidity dependence in Shanghai, J. Environ. Sci.-China, 18, 910-915, https://doi.org/10.1016/s1001-0742(06)60013-2, 2006.

Harrison, R. M., Peak, J. D., and Collins, G. M.: Tropospheric cycle of nitrous acid, J. Geophys. Res., 101, 14429-14439, https://doi.org/10.1029/96jd00341, 1996.

Harrison, R. M., and Collins, G. M.: Measurements of Reaction Coefficients of NO2 and HONO on Aerosol Particles, J. Atmos. Chem., 30, 397-406, https://doi.org/10.1023/A:1006094304069, 1998.

Heland, J., Kleffmann, J., Kurtenbach, R., and Wiesen, P.: A new instrument to measure gaseous nitrous acid (HONO) in the atmosphere, Environ. Sci. Technol., 35, 3207-3212, https://doi.org/10.1021/es000303t, 2001.

Hendrick, F., Müller, J. F., Clémer, K., Wang, P., De Mazière, M., Fayt, C., Gielen, C., Hermans, C., Ma, J. Z., Pinardi, G., Stavrakou, T., Vlemmix, T., and Van Roozendael, M.: Four years of ground-based MAX-DOAS observations of HONO and NO_2 in the Beijing area, Atmos. Chem. Phys., 14, 765-781, https://doi.org/10.5194/acp-14-765-2014, 2014.

Hirokawa, J., Kato, T., and Mafuné, F.: In Situ Measurements of Atmospheric Nitrous Acid by Chemical Ionization Mass Spectrometry Using Chloride Ion Transfer Reactions, Anal. Chem., 81, 8380-8386, https://doi.org/10.1021/ac901117b, 2009.

Hou, S., Tong, S., Ge, M., and An, J.: Comparison of atmospheric nitrous acid during severe haze and clean periods in Beijing, China, Atmos. Environ., 124, 199-206, https://doi.org/10.1016/j.atmosenv.2015.06.023, 2016.

Huang, R. J., Yang, L., Cao, J., Wang, Q., Tie, X., Ho, K. F., Shen, Z., Zhang, R., Li, G., Zhu, C., Zhang, N., Dai, W., Zhou, J., Liu, S., Chen, Y., Chen, J., and O'Dowd, C. D.: Concentration and sources of atmospheric nitrous acid (HONO) at an urban

site in Western China, Sci. Total Environ., 593-594, 165-172, https://doi.org/10.1016/j.scitotenv.2017.02.166, 2017.

Jiang, N., Dong, Z., Xu, Y., Yu, F., Yin, S., Zhang, R., and Tang, X.: Characterization of PM_{10} and $PM_{2.5}$ Source Profiles of Fugitive Dust in Zhengzhou, China, Aerosol Air Qual. Res., 18, 314-329, https://doi.org/10.4209/aaqr.2017.04.0132, 2018a.

Jiang, N., Wang, K., Yu, X., Su, F., Yin, S., Li, Q., and Zhang, R.: Chemical characteristics and source apportionment by two receptor models of size-segregated aerosols in an emerging megacity in China, Aerosol Air Qual. Res., 18, 1375–1390, https://doi.org/10.4209/aaqr.2017.10.0413, 2018b.

Jiang, N., Liu, X., Wang, S., Yu, X., Yin, S., Duan, S., Shenbo, W., Zhang, R., and Li, S.: Pollution characterization, source identification, and health risks of atmospheric-particle-bound heavy metals in PM_{10} and $PM_{2.5}$ at multiple sites in an emerging megacity in the Central Region of China, Aerosol Air Qual. Res., 19, 247-271, https://doi.org/10.4209/aaqr.2018.07.0275, 2019.

Kim, D.-R., Lee, J.-B., Keun Song, C., Kim, S.-Y., Ma, Y.-l., Lee, K.-M., Cha, J.-S., and Lee, S.-D.: Temporal and spatial distribution of tropospheric NO_2 over Northeast Asia using OMI data during the years 2005–2010, Atmos. Pollut. Res., 6, 768-776, https://doi.org/10.5094/apr.2015.085, 2015.

Kleffmann, J., Becker, K. H., Lackhoff, M., and Wiesen, P.: Heterogeneous conversion of NO2 on carbonaceous surfaces, PCCP, 1, 5443-5450, https://doi.org/10.1039/a905545b, 1999.

Kurtenbach, R., Becker, K. H., Gomes, J. A. G., Kleffmann, J., Lorzer, J. C., Spittler, M., Wiesen, P., Ackermann, R., Geyer, A., and Platt, U.: Investigations of emissions and heterogeneous formation of HONO in a road traffic tunnel, Atmos. Environ., 35, 3385-3394, https://doi.org/10.1016/s1352-2310(01)00138-8, 2001.

Lelieveld, J., Gromov, S., Pozzer, A., and Taraborrelli, D.: Global tropospheric hydroxyl distribution, budget and reactivity, Atmos. Chem. Phys., 16, 12477-12493, https://doi.org/10.5194/acp-16-12477-2016, 2016.

672 Li, Q., Jiang, N., Yu, X., Dong, Z., Duan, S., Zhang, L., and Zhang, R.: Sources and
673 spatial distribution of PM2.5-bound polycyclic aromatic hydrocarbons in
674 Zhengzhou in 2016, Atmos. Res., 216, 65–75,
675 https://doi.org/10.1016/j.atmosres.2018.09.011, 2019.
676 Li, X., Brauers, T., Häseler, R., Bohn, B., Fuchs, H., Hofzumahaus, A., Holland, F.,
677 Lou, S., Lu, K. D., Rohrer, F., Hu, M., Zeng, L. M., Zhang, Y. H., Garland, R. M.,
678 Su, H., Nowak, A., Wiedensohler, A., Takegawa, N., Shao, M., and Wahner, A.:
679 Exploring the atmospheric chemistry of nitrous acid (HONO) at a rural site in
680 Southern China, Atmos. Chem. Phys., 12, 1497-1513, https://doi.org/10.5194/acp-
681 12-1497-2012, 2012.
682 Liu, F., Beirle, S., Zhang, Q., van der, A. R., Zheng, B., Tong, D., and He, K.: NOx
683 emission trends over Chinese cities estimated from OMI observations during 2005
684 to 2015, Atmos Chem Phys, 17, 9261-9275, https://doi.org/10.5194/acp-17-9261-
685 2017, 2017.
686 Liu, X., Jiang, N., Yu, X., Zhang, R., Li, S., Li, Q., and Kang, P.: Chemical
687 characteristics, sources apportionment, and risk assessment of PM2.5 in different
688 functional areas of an emerging megacity in China, Aerosol Air Qual. Res., 19,
689 2222-2238, https://doi.org/10.4209/aaqr.2019.02.0076, 2019.
690 Liu, Z., Wang, Y., Costabile, F., Amoroso, A., Zhao, C., Huey, L. G., Stickel, R., Liao,
691 J., and Zhu, T.: Evidence of aerosols as a media for rapid daytime HONO
692 production over China, Environ. Sci. Technol., 48, 14386-14391,
693 https://doi.org/10.1021/es504163z, 2014.
694 Lu, X., Wang, Y., Li, J., Shen, L., and Fung, J. C. H.: Evidence of heterogeneous
695 HONO formation from aerosols and the regional photochemical impact of this
696 HONO source, Environ. Res. Lett., 13, https://doi.org/10.1088/1748-9326/aae492,
697 2018.
698 Markovic, M. Z., VandenBoer, T. C., and Murphy, J. G.: Characterization and
699 optimization of an online system for the simultaneous measurement of atmospheric

water-soluble constituents in the gas and particle phases, J. Environ. Monit., 14, 1872-1884, https://doi.org/10.1039/c2em00004k, 2012.

Michoud, V., Colomb, A., Borbon, A., Miet, K., Beekmann, M., Camredon, M., Aumont, B., Perrier, S., Zapf, P., Siour, G., Ait-Helal, W., Afif, C., Kukui, A., Furger, M., Dupont, J. C., Haeffelin, M., and Doussin, J. F.: Study of the unknown HONO daytime source at a European suburban site during the MEGAPOLI summer and winter field campaigns, Atmos. Chem. Phys., 14, 2805-2822, https://doi.org/10.5194/acp-14-2805-2014, 2014.

Min, K. E., Washenfelder, R. A., Dubé, W. P., Langford, A. O., Edwards, P. M., Zarzana, K. J., Stutz, J., Lu, K., Rohrer, F., Zhang, Y., and Brown, S. S.: A broadband cavity enhanced absorption spectrometer for aircraft measurements of glyoxal, methylglyoxal, nitrous acid, nitrogen dioxide, and water vapor, Atmos. Meas. Tech., 9, 423-440, https://doi.org/10.5194/amt-9-423-2016, 2016.

Pinto, J. P., Dibb, J., Lee, B. H., Rappenglück, B., Wood, E. C., Levy, M., Zhang, R. Y., Lefer, B., Ren, X. R., Stutz, J., Tsai, C., Ackermann, L., Golovko, J., Herndon, S. C., Oakes, M., Meng, Q. Y., Munger, J. W., Zahniser, M., and Zheng, J.: Intercomparison of field measurements of nitrous acid (HONO) during the SHARP campaign, J. Geophys. Res.-Atmos., 119, 5583-5601, https://doi.org/10.1002/2013jd020287, 2014.

Qin, M., Xie, P., Su, H., Gu, J., Peng, F., Li, S., Zeng, L., Liu, J., Liu, W., and Zhang, Y.: An observational study of the HONO–NO_2 coupling at an urban site in Guangzhou City, South China, Atmos. Environ., 43, 5731-5742, https://doi.org/10.1016/j.atmosenv.2009.08.017, 2009.

Rappenglück, B., Lubertino, G., Alvarez, S., Golovko, J., Czader, B., and Ackermann, L.: Radical precursors and related species from traffic as observed and modeled at an urban highway junction, J. Air Waste Manage. Assoc., 63, 1270-1286, https://doi.org/10.1080/10962247.2013.822438, 2013.

727 Roberts, J. M., Veres, P., Warneke, C., Neuman, J. A., Washenfelder, R. A., Brown, S.
728 S., Baasandorj, M., Burkholder, J. B., Burling, I. R., Johnson, T. J., Yokelson, R. J.,
729 and de Gouw, J.: Measurement of HONO, HNCO, and other inorganic acids by
730 negative-ion proton-transfer chemical-ionization mass spectrometry (NI-PT-
731 CIMS): application to biomass burning emissions, Atmos. Meas. Tech., 3, 981-990,
732 https://doi.org/10.5194/amt-3-981-2010, 2010.
733 Rohrer, F., and Berresheim, H.: Strong correlation between levels of tropospheric
734 hydroxyl radicals and solar ultraviolet radiation, Nature, 442, 184-187,
735 https://doi.org/10.1038/nature04924, 2006.
736 Sailor, D. J.: Simulated Urban Climate Response to Modifications in Surface Albedo
737 and Vegetative Cover, J. Appl. Meteorol., 34, 1694-1704,
738 https://doi.org/10.1175/1520-0450-34.7.1694, 1995.
739 Sander, S., Friedl, R., Golden, D., Kurylo, M., Huie, R., Orkin, V., Moortgat, G.,
740 Ravishankara, A. R., Kolb, C., Molina, M., and Finlayson-Pitts, B.: Chemical
741 Kinetics and Photochemical Data for Use in Atmospheric Studies; JPL Publication
742 02-25, 2003.
743 Shen, L. J., and Zhang, Z. F.: Heterogeneous reactions of NO_2 on the surface of black
744 carbon, Prog. Chem., 25, 28-35, 2013.
745 Sörgel, M., Regelin, E., Bozem, H., Diesch, J. M., Drewnick, F., Fischer, H., Harder,
746 H., Held, A., Hosaynali-Beygi, Z., Martinez, M., and Zetzsch, C.: Quantification of
747 the unknown HONO daytime source and its relation to NO_2, Atmos. Chem. Phys.,
748 11, 10433-10447, https://doi.org/10.5194/acp-11-10433-2011, 2011.
749 Spataro, F., Ianniello, A., Esposito, G., Allegrini, I., Zhu, T., and Hu, M.: Occurrence
750 of atmospheric nitrous acid in the urban area of Beijing (China), Sci. Total
751 Environ., 447, 210-224, https://doi.org/10.1016/j.scitotenv.2012.12.065, 2013.
752 Stutz, J.: Nitrous acid formation in the urban atmosphere: Gradient measurements of
753 NO_2 and HONO over grass in Milan, Italy, J. Geophys. Res., 107,
754 https://doi.org/10.1029/2001jd000390, 2002.

Stutz, J., Alicke, B., Ackermann, R., Geyer, A., Wang, S., White, A. B., Williams, E. J., Spicer, C. W., and Fast, J. D.: Relative humidity dependence of HONO chemistry in urban areas, J. Geophys. Res., 109, 03307-03319, https://doi.org/10.1029/2003jd004135, 2004.

Su, H., Cheng, Y. F., Cheng, P., Zhang, Y. H., Dong, S., Zeng, L. M., Wang, X., Slanina, J., Shao, M., and Wiedensohler, A.: Observation of nighttime nitrous acid (HONO) formation at a non-urban site during PRIDE-PRD2004 in China, Atmos. Environ., 42, 6219-6232, https://doi.org/10.1016/j.atmosenv.2008.04.006, 2008a.

Su, H., Cheng, Y. F., Shao, M., Gao, D. F., Yu, Z. Y., Zeng, L. M., Slanina, J., Zhang, Y. H., and Wiedensohler, A.: Nitrous acid (HONO) and its daytime sources at a rural site during the 2004 PRIDE-PRD experiment in China, J. Geophys. Res., 113, D14312-14321, https://doi.org/10.1029/2007jd009060, 2008b.

Tan, Z., Rohrer, F., Lu, K., Ma, X., Bohn, B., Broch, S., Dong, H., Fuchs, H., Gkatzelis, G. I., Hofzumahaus, A., Holland, F., Li, X., Liu, Y., Liu, Y., Novelli, A., Shao, M., Wang, H., Wu, Y., Zeng, L., Hu, M., Kiendler-Scharr, A., Wahner, A., and Zhang, Y.: Wintertime photochemistry in Beijing: observations of RO_x radical concentrations in the North China Plain during the BEST-ONE campaign, Atmos. Chem. Phys., 18, 12391-12411, https://doi.org/10.5194/acp-18-12391-2018, 2018.

Tian, Y., Xue, Q., Xiao, Z., Chen, K., and Feng, Y.: PMF-GAS Methods to Estimate Contributions of Sources and Oxygen for $PM_{2.5}$, Based on Highly Time-Resolved $PM_{2.5}$ Species and Gas Data, Aerosol Air Qual. Res., 18, 2956-2966, https://doi.org/10.4209/aaqr.2018.07.0244, 2018.

Tong, S., Hou, S., Zhang, Y., Chu, B., Liu, Y., He, H., Zhao, P., and Ge, M.: Comparisons of measured nitrous acid (HONO) concentrations in a pollution period at urban and suburban Beijing, in autumn of 2014, Sci. China Chem., 58, 1393-1402, https://doi.org/10.1007/s11426-015-5454-2, 2015.

Tong, S., Hou, S., Zhang, Y., Chu, B., Liu, Y., He, H., Zhao, P., and Ge, M.: Exploring the nitrous acid (HONO) formation mechanism in winter Beijing: direct emissions

783 and heterogeneous production in urban and suburban areas, Faraday Discuss., 189,
784 213-230, https://doi.org/10.1039/c5fd00163c, 2016.
785 VandenBoer, T. C., Markovic, M. Z., Sanders, J. E., Ren, X., Pusede, S. E., Browne,
786 E. C., Cohen, R. C., Zhang, L., Thomas, J., Brune, W. H., and Murphy, J. G.:
787 Evidence for a nitrous acid (HONO) reservoir at the ground surface in Bakersfield,
788 CA, during CalNex 2010, J. Geophys. Res.-Atmos., 119, 9093-9106,
789 https://doi.org/10.1002/2013jd020971, 2014.
790 Vogel, B., Vogel, H., Kleffmann, J., and Kurtenbach, R.: Measured and simulated
791 vertical profiles of nitrous acid—Part II. Model simulations and indications for a
792 photolytic source, Atmos. Environ., 37, 2957-2966, https://doi.org/10.1016/s1352-
793 2310(03)00243-7, 2003.
794 Wang, S., Zhou, R., Zhao, H., Wang, Z., Chen, L., and Zhou, B.: Long-term
795 observation of atmospheric nitrous acid (HONO) and its implication to local NO_2
796 levels in Shanghai, China, Atmos. Environ., 77, 718-724,
797 https://doi.org/10.1016/j.atmosenv.2013.05.071, 2013.
798 Wang, S., Yin, S., Zhang, R., Yang, L., Zhao, Q., Zhang, L., Yan, Q., Jiang, N., and
799 Tang, X.: Insight into the formation of secondary inorganic aerosol based on high-
800 time-resolution data during haze episodes and snowfall periods in Zhengzhou,
801 China, Sci. Total Environ., 660, 47-56,
802 https://doi.org/10.1016/j.scitotenv.2018.12.465, 2019.
803 Winer, A. M., and Biermann, H. W.: Long pathlength differential optical absorption
804 spectroscopy (DOAS) measurements of gaseous HONO, NO_2 and HCNO in the
805 California South Coast Air Basin, Res. Chem. Intermed., 20, 423-445,
806 https://doi.org/10.1163/156856794X00405, 1994.
807 Wojtal, P., Halla, J. D., and McLaren, R.: Pseudo steady states of HONO measured in
808 the nocturnal marine boundary layer: a conceptual model for HONO formation on
809 aqueous surfaces, Atmos. Chem. Phys., 11, 3243-3261, https://doi.org/10.5194/acp-
810 11-3243-2011, 2011.

Xu, Z., Wang, T., Wu, J., Xue, L., Chan, J., Zha, Q., Zhou, S., Louie, P. K. K., and Luk, C. W. Y.: Nitrous acid (HONO) in a polluted subtropical atmosphere: Seasonal variability, direct vehicle emissions and heterogeneous production at ground surface, Atmos. Environ., 106, 100-109, https://doi.org/10.1016/j.atmosenv.2015.01.061, 2015.

Yang, Q., Su, H., Li, X., Cheng, Y., Lu, K., Cheng, P., Gu, J., Guo, S., Hu, M., Zeng, L., Zhu, T., and Zhang, Y.: Daytime HONO formation in the suburban area of the megacity Beijing, China, Sci. China Chem., 57, 1032-1042, https://doi.org/10.1007/s11426-013-5044-0, 2014.

Zhang, B., and Tao, F.-M.: Direct homogeneous nucleation of NO2, H2O, and NH3 for the production of ammonium nitrate particles and HONO gas, Chem. Phys. Lett., 489, 143-147, https://doi.org/10.1016/j.cplett.2010.02.059, 2010.

Zhang, W., Tong, S., Ge, M., An, J., Shi, Z., Hou, S., Xia, K., Qu, Y., Zhang, H., Chu, B., Sun, Y., and He, H.: Variations and sources of nitrous acid (HONO) during a severe pollution episode in Beijing in winter 2016, Sci. Total Environ., 648, 253-262, https://doi.org/10.1016/j.scitotenv.2018.08.133, 2019.

Figure Captions:

Fig. 1. Temporal trends of hourly average T, RH, WD, WS, and $PM_{2.5}$ during the measurement. (The shaded areas: white for the CD period; gray for the PD period; red for the SPD period.)

Fig. 2. Temporal variations of hourly average HONO, NO, NO_2, O_3, and CO during the measurement. (The shaded areas: white for the CD period; gray for the PD period; red for the SPD period.)

Fig. 3. Diurnal variations of HONO during the measurement.

Fig. 4. Diurnal variations of HONO, NO, NO_2, O_3, HONO/NO_2, and HONO/NO_X. The blue points and lines represented the CD period; the black points and lines represented the PD period; the red points and lines represented the SPD period.

Fig. 5. Nocturnal variations of $\mathbf{P_{OH+NO}^{net}}$, HONO and NO during CD, PD and SPD periods.

Fig. 6. Percentage distribution of the nighttime $HONO_{emission}$/HONO. (The dotted line represents the average of $HONO_{emission}$/HONO.)

Fig. 7. Nighttime correlation studies between $PM_{2.5}$ and HONO/NO_2, $PM_{2.5}$ and HONO, CO and HONO, RH and HONO/NO_2 during the entire measurement period, CD, PD, and SPD periods. The blue represented the full measurement period; the light blue represented CD period; the black represented PD period; the red represented SPD period.

Fig. 8. Nocturnal variations of $HONO_{correct}$, NO_2, and $HONO_{correct}/NO_2$ in CD, PD and SPD periods.

Fig. 9. The average profiles of J_{HONO} and J_{O^1D} concentrations during the daytime, and production and loss rate of the daytime HONO in CD, PD and SPD periods.

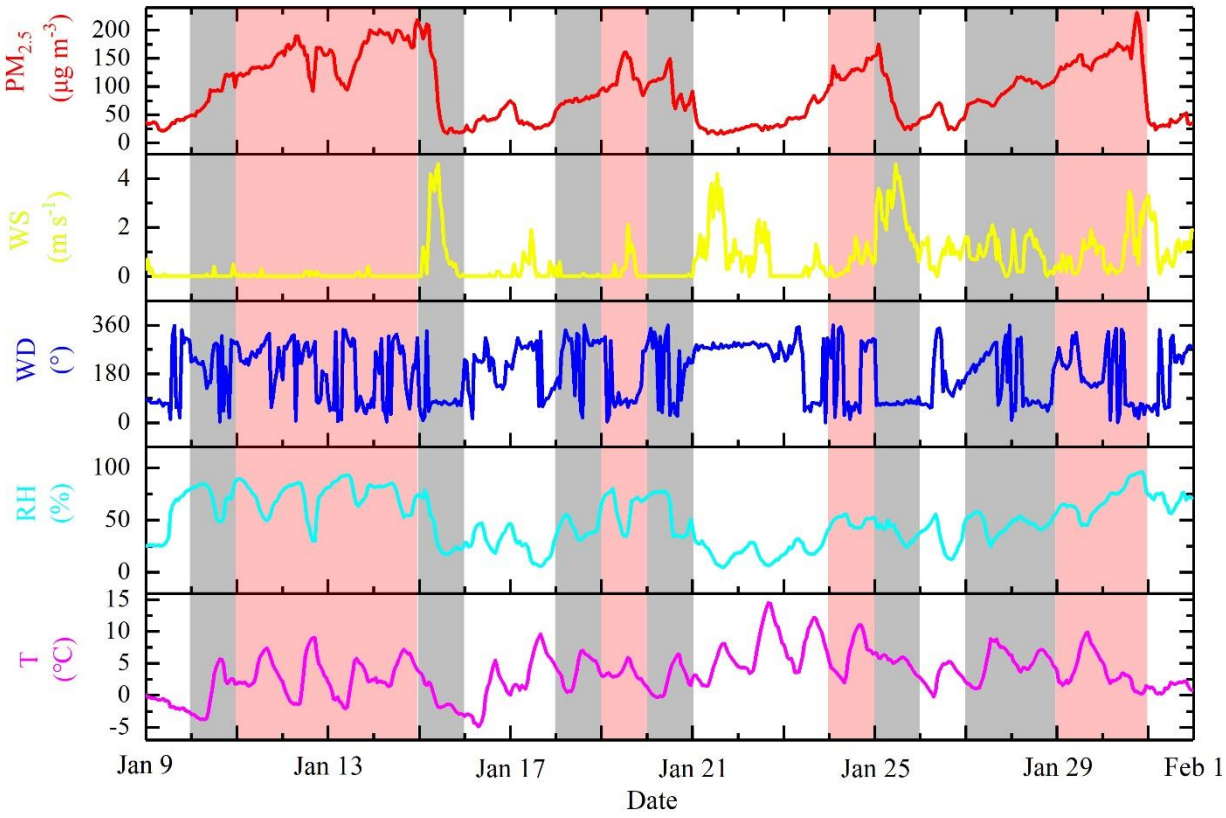

Fig. 1. Temporal trends of hourly average T, RH, WD, WS, and $PM_{2.5}$ during the measurement. (The shaded areas: white for the CD period; gray for the PD period; red for the SPD period.)

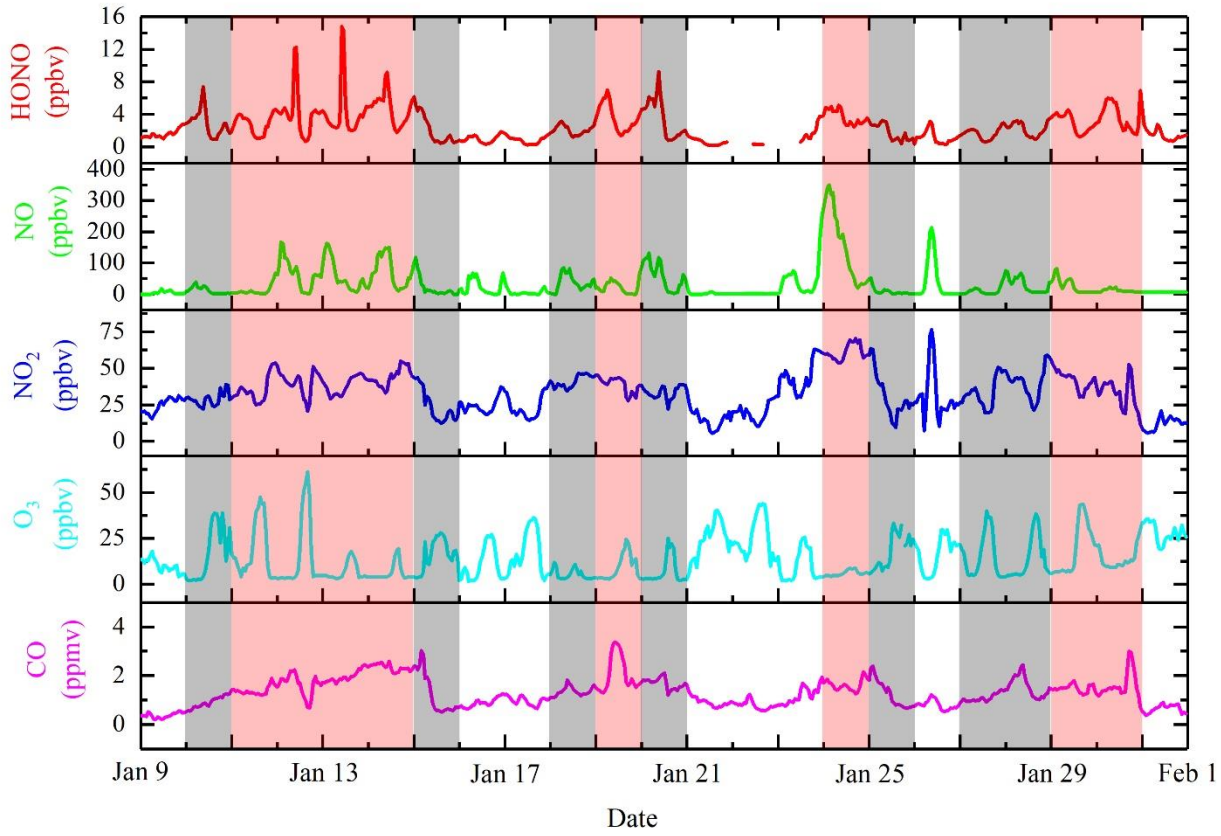

Fig. 2. Temporal variations of hourly average HONO, NO, NO_2, O_3, and CO during the measurement. (The shaded areas: white for the CD period; gray for the PD period; red for the SPD period.)

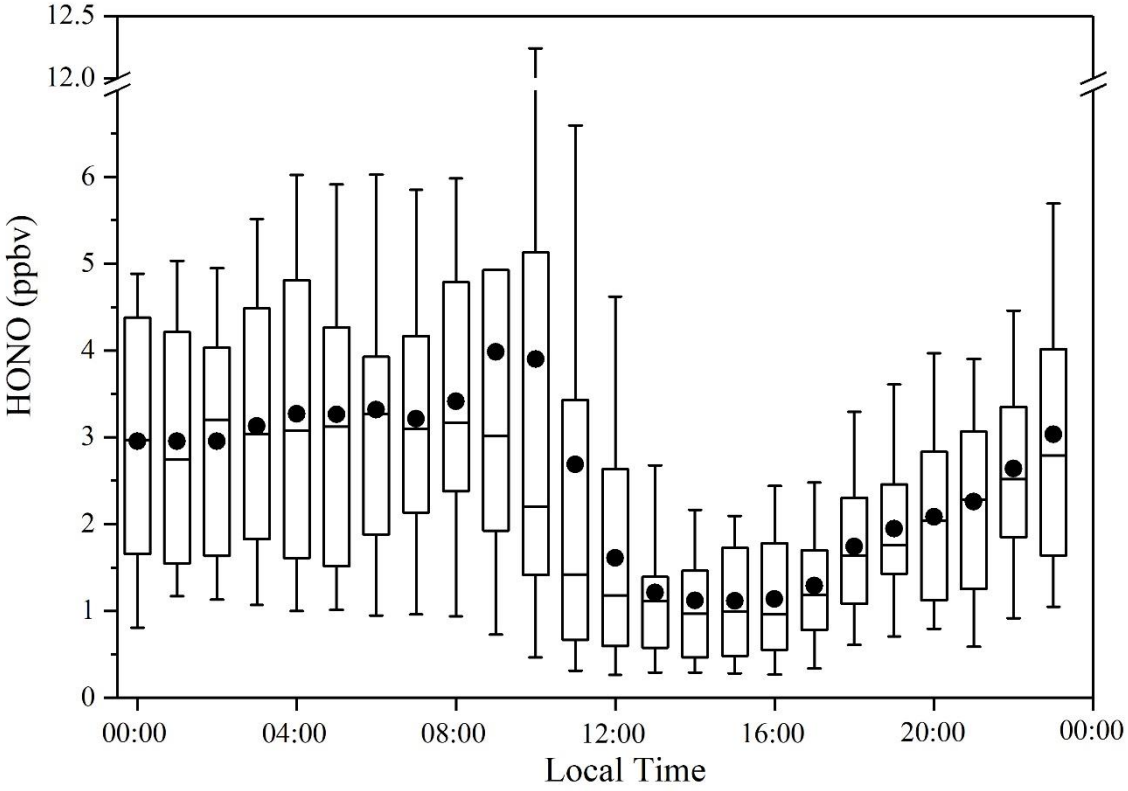

Fig. 3. Diurnal variations of HONO during the measurement.

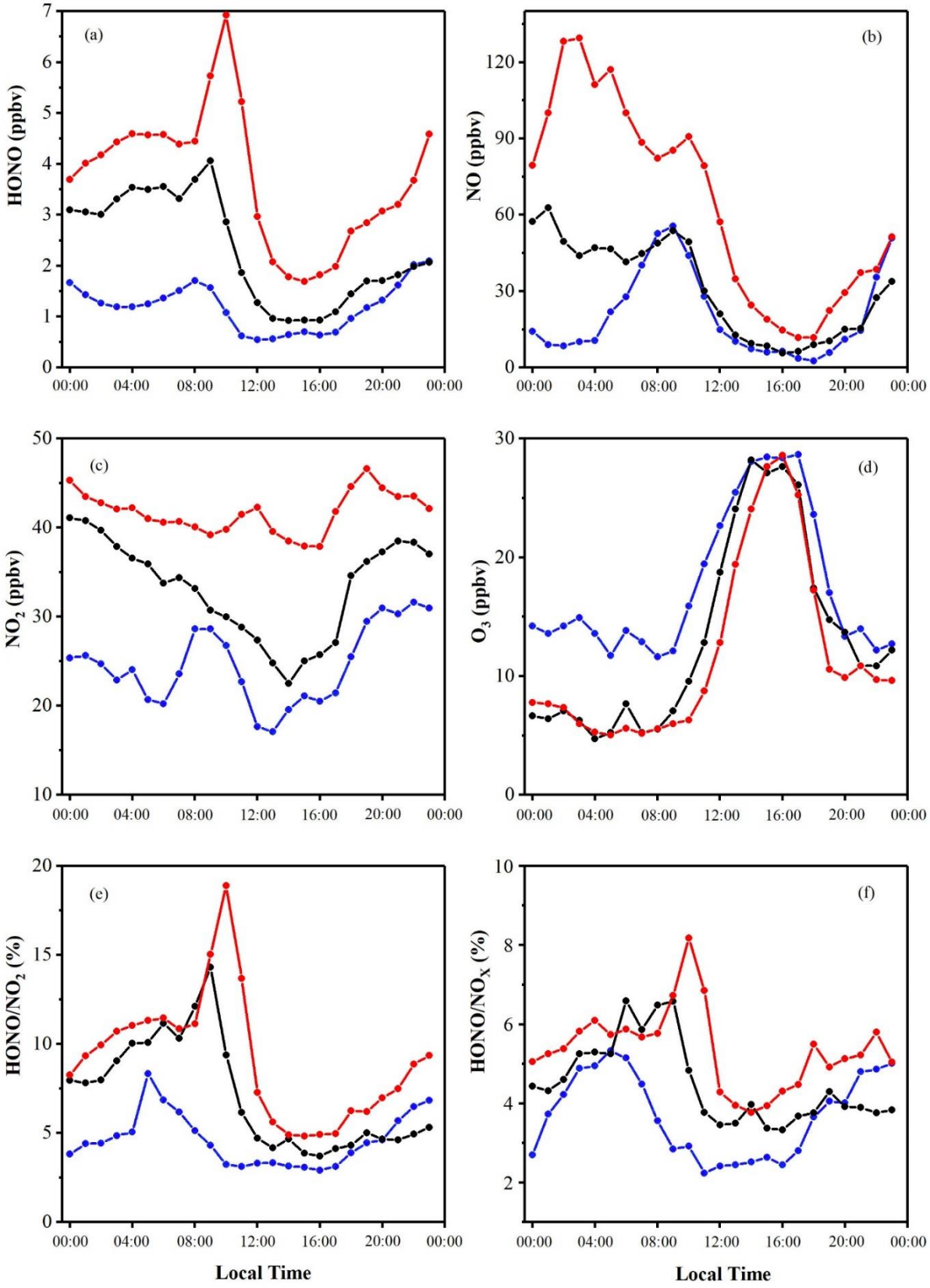

Fig. 4. Diurnal variations of HONO, NO, NO_2, O_3, HONO/NO_2, and HONO/NO_X. The blue points and lines represented the CD period; the black points and lines represented the PD period; the red points and lines represented the SPD period.

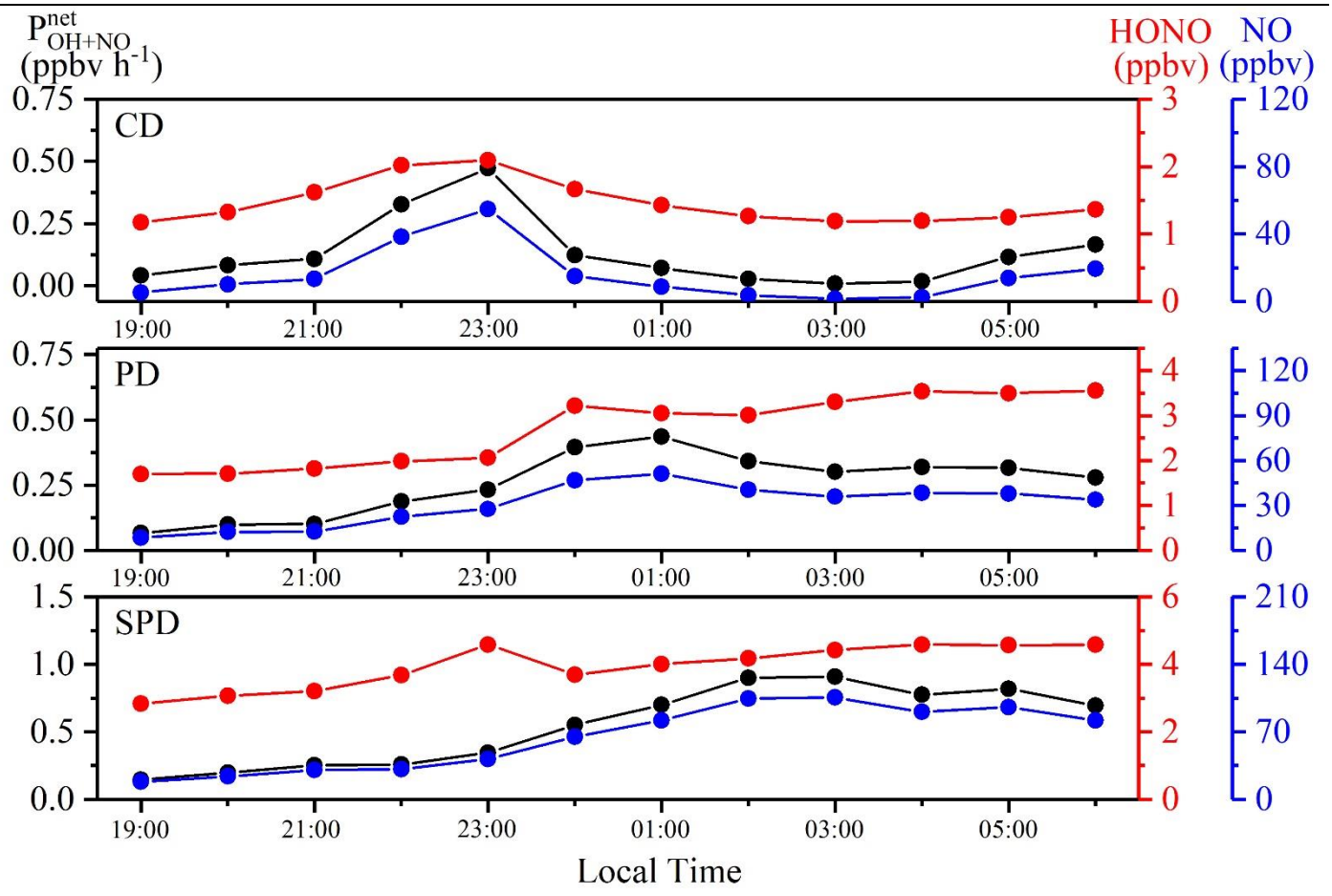

Fig. 5. Nocturnal variations of P^{net}_{OH+NO}, HONO and NO during CD, PD and SPD periods.

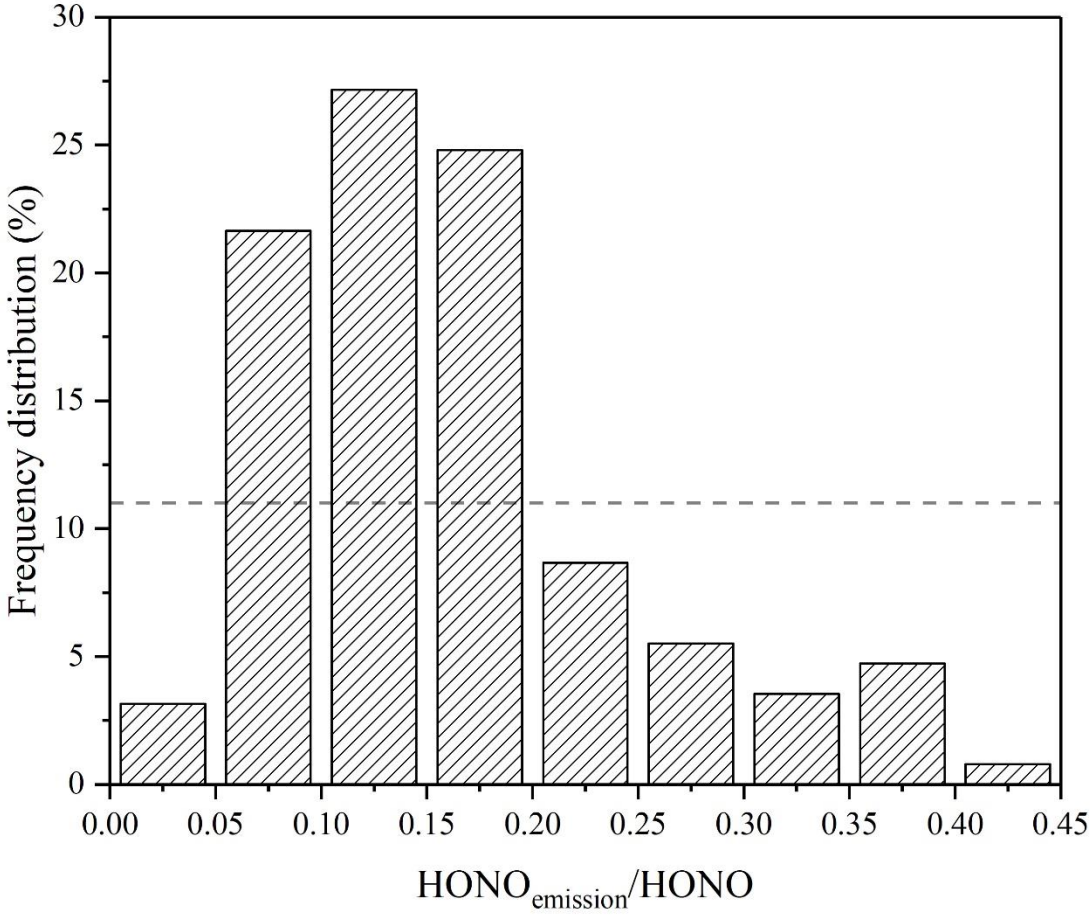

Fig. 6. Percentage distribution of the nighttime $HONO_{emission}/HONO$. (The dotted line represents the average of $HONO_{emission}/HONO$.)

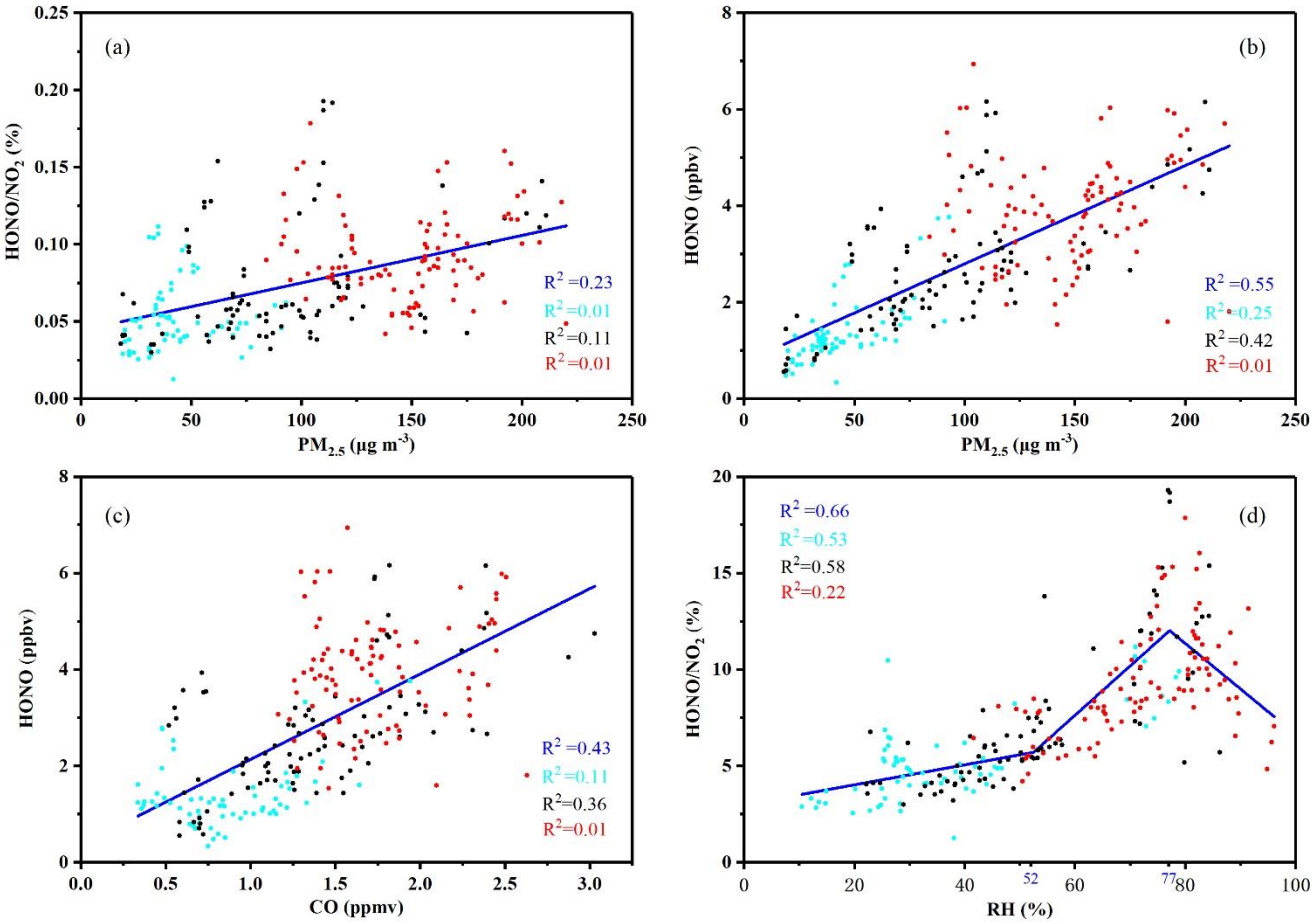

Fig. 7. Nighttime correlation studies between $PM_{2.5}$ and $HONO/NO_2$, $PM_{2.5}$ and HONO, CO and HONO, RH and $HONO/NO_2$ during the entire measurement period, CD, PD, and SPD periods. The blue represented the full measurement period; the light blue represented CD period; the black represented PD period; the red represented SPD period.

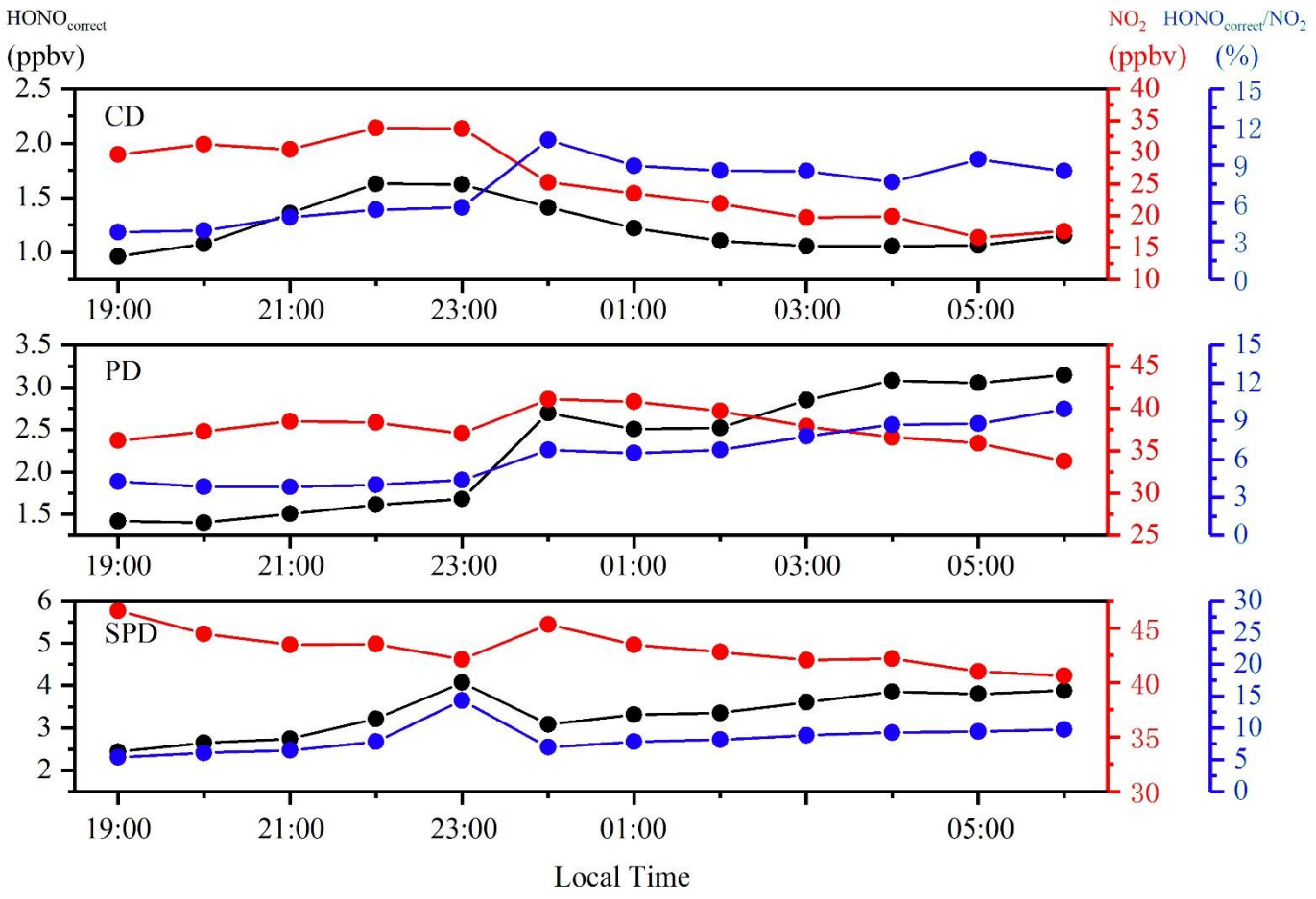

Fig. 8. Nocturnal variations of $HONO_{correct}$, NO_2, and $HONO_{correct}/NO_2$ in CD, PD and SPD periods.

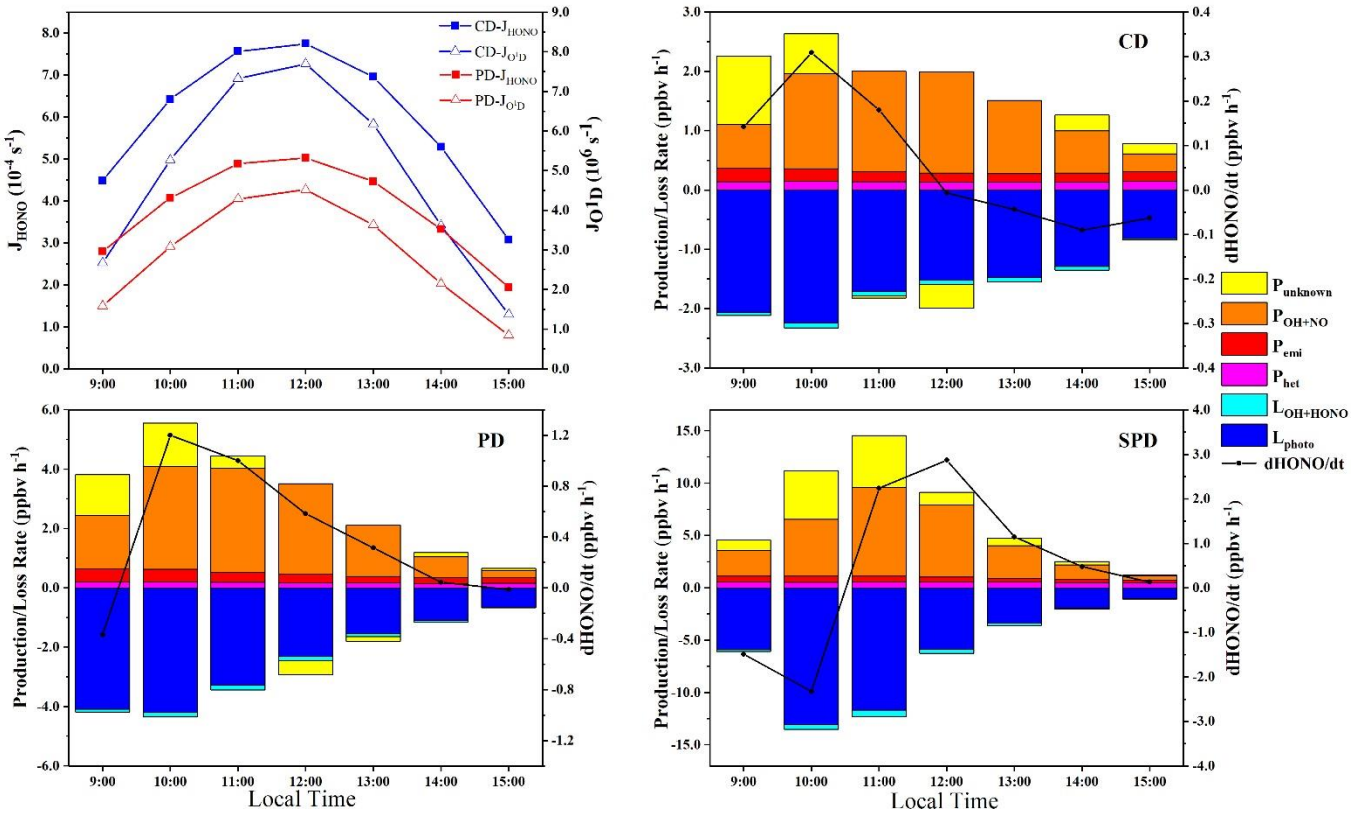

Fig. 9. The average profiles of J_{HONO} and J_{O^1D} concentrations during the daytime, and production and loss rate of the daytime HONO in CD, PD and SPD periods.

Table Captions:

Table 1. Data statistics of HONO, $PM_{2.5}$, NO_2, NO, NO_X, HONO/NO_2, HONO/NO_X, O_3, CO, T, RH, and WS during the measurement period, mean value ± standard deviation.

Table 2. Comparisons of the daytime and nighttime HONO level, HONO/NO_2, and HONO/NO_X mean values in Zhengzhou and other sites around the world.

Table 1.

Data statistics of HONO, $PM_{2.5}$, NO_2, NO, NO_X, $HONO/NO_2$, $HONO/NO_X$, O_3, CO, T, RH, and WS during the measurement period, mean value ± standard deviation.

Trace gases	CD			PD			SPD			Total days
	Day	Night	All	Day	Night	All	Day	Night	All	
$PM_{2.5}$ ($\mu g\ m^{-3}$)	37 ± 15	41 ± 17	39 ± 16	80 ± 32	93 ± 46	87 ± 40	148 ± 29	147 ± 33	147 ± 31	91 ± 54
HONO (ppbv)	0.9 ± 0.7	1.4 ± 0.7	1.1 ± 0.7	1.9 ± 1.7	2.7 ± 1.3	2.3 ± 1.5	3.5 ± 2.7	4.0 ± 1.1	3.7 ± 2.1	2.5 ± 1.9
CO (ppmv)	1 ± 0.3	1 ± 0.3	1 ± 0.3	1± 0.4	1 ± 0.6	1 ± 0.5	2 ± 0.6	2 ± 0.4	2 ± 0.5	1 ± 0.6
NO (ppbv)	18.4 ± 39.3	15 ± 34.3	16.7 ± 36.8	20.3 ± 26.2	30.7 ± 33.6	25.5 ± 30.4	40.8 ± 50.8	64.3 ± 82.1	52.5 ± 68.9	31.8 ± 51.4
NO_2 (ppbv)	23 ± 13	26 ± 13	25 ± 13	29 ± 9	38 ± 10	33 ± 11	40 ± 11	43 ± 10	42 ± 11	33 ± 14
O_3 (ppbv)	21.4 ± 11.5	13.8 ± 10.0	17.6 ± 11.4	17.4 ± 11.9	8.9 ± 8.1	13.1 ± 10.9	15.6 ± 14.2	7.9 ± 7.1	11.8 ± 11.8	14.2 ± 11.7
$HONO/NO_2$ (%)	4.2 ± 3.6	5.3 ± 2.2	4.7 ± 3.1	6.8 ± 5.8	7.4 ± 3.9	7.1 ± 4.9	9.0 ± 7.7	9.8 ± 5.8	9.4 ± 6.8	7.6 ± 6.4
$HONO/NO_X$ (%)	3.3 ± 2.7	6.0 ± 5.6	4.5 ± 4.5	4.4 ± 2.5	4.6 ± 1.7	4.5 ± 2.1	5.3 ± 3.4	5.8 ± 4.7	5.6 ± 4.1	4.9 ± 3.8
RH (%)	30 ± 21	36 ± 20	33 ± 21	44 ± 17	54 ± 18	49 ± 18	64 ± 18	73 ± 13	68 ± 16	50 ± 24
WS ($m\ s^{-1}$)	0.8 ± 1.0	0.5 ± 0.7	0.7 ± 0.9	1.1 ± 1.4	0.6 ± 0.9	0.9 ± 1.2	0.4 ± 0.7	0.3 ± 0.6	0.4 ± 0.7	0.6 ± 0.9
T (°C)	4.3 ± 4.6	2.7 ± 3.6	3.5 ± 4.2	3.7 ± 3.3	2.6 ± 3.1	3.1 ± 3.2	4.6 ± 3.2	2.9 ± 2.1	3.8 ± 2.8	3.5 ± 3.5

Table 2.

Comparisons of the daytime and nighttime HONO level, $HONO/NO_2$, and $HONO/NO_X$ mean values in Zhengzhou and other sites around the world.

Date (Site)	Instrument	HONO (ppbv)			$HONO/NO_2$ (%)		$HONO/NO_X$ (%)		Reference
		Day	Night	N/D	Day	Night	Day	Night	
Oct.–Nov. 2014 (Beijing, urban)	LOPAP (long path absorption photometer)	0.9	1.8	2.0	2.6	4.6	1.7	2.2	Tong et al., 2015
Feb.–Mar. 2014 (Beijing, urban)	LOPAP	1.8	2.1	1.2	3.8 (Severe haze)	4.3	2.5	2.5	Hou et al., 2016
		0.5	0.9	1.8	7.8 (Clean)	3.0	5.1	2.4	
Jul. 2006 (Guangzhou, rural)	LOPAP	0.2	0.9	4.5	1.0	2.5	4.3	4.5	Li et al., 2012
Jul. 2014–Aug. 2015 (Xi'an, urban)	LOPAP	0.5	1.6	3.2	3.3	6.2			Huang et al., 2017
Aug. 2010–Jun. 2012 (Shanghai, urban)	Active DOAS	0.8	1.1	1.4	4.2	4.5			Wang et al., 2013
Jul. 2009 (Paris, urban)	wet chemical derivatization technique-HPLC/UV-VIS detection	0.1	0.2	2.0	3.3	2.5			Michoud et al., 2014
Jan. 2019	AIM	2.2	2.8	1.3	6.8	8.5	4.4	5.5	This study